AD

US ARMY MATERIEL COMMAND

TECHNICAL REPORT BRL-TR-2699

AD-A164 150

MEASUREMENT OF INTERIOR BALLISTIC PERFORMANCE USING FM/FM RADIO TELEMETRY TECHNIQUES

James W. Evans

December 1985

US ARMY BALLISTIC RESEARCH LABORATORY
ABERDEEN PROVING GROUND, MARYLAND

DISCLAIMER NOTICE

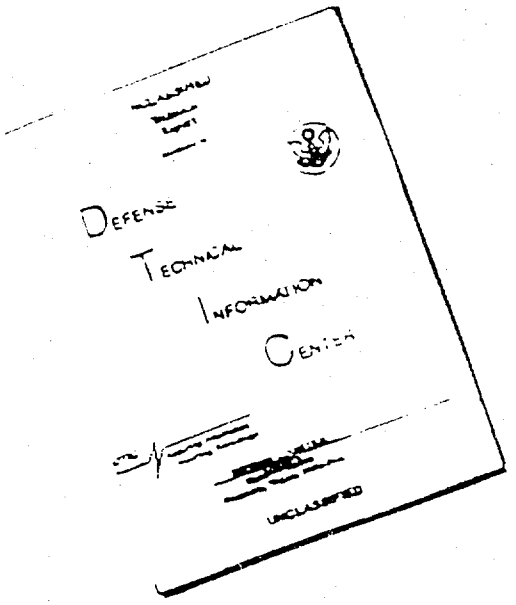

THIS DOCUMENT IS BEST QUALITY AVAILABLE. THE COPY FURNISHED TO DTIC CONTAINED A SIGNIFICANT NUMBER OF PAGES WHICH DO NOT REPRODUCE LEGIBLY.

Destroy this report when it is no longer needed.
Do not return it to the originator.

Additional copies of this report may be obtained from the National Technical Information Service, U. S. Department of Commerce, Springfield, Virginia 22161.

The findings in this report are not to be construed as an official Department of the Army position, unless so designated by other authorized documents.

The use of trade names or manufacturers' names in this report does not constitute indorsement of any commercial product.

SECURITY CLASSIFICATION OF THIS PAGE (When Data Entered)

REPORT DOCUMENTATION PAGE		READ INSTRUCTIONS BEFORE COMPLETING FORM
1. REPORT NUMBER Technical Report BRL-TR-2699	2. GOVT ACCESSION NO. AD-A164	3. RECIPIENT'S CATALOG NUMBER 150
4. TITLE (and Subtitle) Measurement of Interior Ballistic Performance Using FM/FM Radio Telemetry Techniques		5. TYPE OF REPORT & PERIOD COVERED Technical Report 6. PERFORMING ORG. REPORT NUMBER
7. AUTHOR(s) James W. Evans		8. CONTRACT OR GRANT NUMBER(s)
9. PERFORMING ORGANIZATION NAME AND ADDRESS US Army Ballistic Research Laboratory ATTN: SLCBR-IB Aberdeen Proving Ground, MD 21005-5066		10. PROGRAM ELEMENT, PROJECT, TASK AREA & WORK UNIT NUMBERS 1L162618AH80
11. CONTROLLING OFFICE NAME AND ADDRESS US Army Ballistic Research Laboratory ATTN: SLCBR-DD-T Aberdeen Proving Ground, MD 21005-5066		12. REPORT DATE December 1985 13. NUMBER OF PAGES 93
14. MONITORING AGENCY NAME & ADDRESS(if different from Controlling Office)		15. SECURITY CLASS. (of this report) Unclassified 15a. DECLASSIFICATION/DOWNGRADING SCHEDULE

16. DISTRIBUTION STATEMENT (of this Report)
Approved for Public Release; Distribution Unlimited.

17. DISTRIBUTION STATEMENT (of the abstract entered in Block 20, if different from Report)

18. SUPPLEMENTARY NOTES
Presented at the JANNAF 1983 Propulsion Meeting.

19. KEY WORDS (Continue on reverse side if necessary and identify by block number)
Interior Ballistics
Radio Telemetry
Pressure Measurements
Acceleration Measurements
Artillery
Soft Recovery

20. ABSTRACT (Continue on reverse side if necessary and identify by block number)
The continuous measurement of ballistic performance during the interior ballistic cycle of cannon launched projectiles is important to on-going research programs being conducted at the Ballistic Research Laboratory (BRL). These measurements, such as propelling gas pressure, projectile acceleration, and projectile-bore interactions, are necessary to evaluate existing weapon systems and validate newly formulated interior ballistic models. Of particular interest is the resistance to projectile motion and the behavior

DD FORM 1 JAN 73 1473 EDITION OF 1 NOV 65 IS OBSOLETE

UNCLASSIFIED
SECURITY CLASSIFICATION OF THIS PAGE (When Data Entered)

Abstract (cont):

of the projectile during the engraving process. The measurement of forces on projectiles and projectile-bore interactions requires that transducers be located on-board the projectile. In-bore measurements of ballistic performance are made at the BRL using an FM/FM, S-band telemeter.

Standard artillery projectiles are modified and instrumented with telemetry transmitting systems. These projectiles are test fired and data extracted via the real time telemetry link. The projectile systems are expendable free-flight rounds and those modified for recovery in the BRL Large Caliber Soft Recovery System (LCSRS). The instrumentation package for the recoverable rounds is configured so it can be removed from the projectile, recalibrated after exposure to the launch environment, and used on subsequent rounds.

The instrumentation on-board the projectile measures the base pressure, axial acceleration, strain, and on some projectiles, tangential acceleration. The axial acceleration is used to derive the interior ballistic trajectory. The base pressure and axial acceleration are used to derive the resistive pressure profile. The resistive pressure is defined as the sum of all frictional forces acting on the projectile divided by the cross-sectional area of the bore. It is calculated using the force balance equation applying Newton's Second Law. The resistive pressure, when plotted versus displacement, shows the forces during engraving and the down tube travel.

This report discusses the technique used to acquire the on-board data. It includes a description of the telemetry transmitting system, the telemetry receiving system, calibration procedures, and projectile modifications. Representative data acquired from test firings are presented from a number of instrumented projectiles both free-flight and into the LCSRS.

TABLE OF CONTENTS

TABLE OF CONTENTS (CONT'D)

LIST OF ILLUSTRATIONS

LIST OF ILLUSTRATIONS (CONT'D)

LIST OF ILLUSTRATIONS (CONT'D)

LIST OF ILLUSTRATIONS (CONT'D)

I. INTRODUCTION

The continuous measurements of ballistic performance during the interior ballistic cycle of cannon-launched projectiles is important to on-going research programs being conducted at the Ballistic Research Laboratory (BRL). These measurements, such as propelling gas pressure, projectile acceleration, and projectile-bore interactions, are necessary to evaluate existing weapon systems and validate newly formulated interior ballistic models. Of particular interest is the resistance to projectile motion and the behavior of the projectile during the engraving process.[1] The measurements of forces on projectiles and projectile-bore interactions require that transducers be located on-board the projectile. In-bore measurements are made at BRL using an S-Band telemeter as the data link.[2,3,4,5,6,7,8]

Standard FM/FM techniques and, when possible, commercially available components are used. Figure 1 is a block diagram of a typical transmitting

---

[1] E.B. Fisher, "Continued Development and Documentation of the Calspan Interior Ballistics Code," ARBRL-CR-00465, Calspan Corporation, Ballistic Research Laboratory, USA ARRADCOM, Aberdeen Proving Ground, MD, September 1981.

[2] J.W. Evans, "In-Bore Measurements of Projectile Acceleration and Base Pressure Using an S-Band Telemetry System," Proceedings of The International Telemetry Conference, Volume XI, October 1975.

[3] J.W. Evans, "In-Bore Measurements of Projectile Acceleration and Base Pressure Using an S-Band Telemetry System," Proceedings of the Fuze/ Munitions Environment Characterization Symposium II, October 1975.

[4] J.W. Evans, "In-Bore Measurements of Projectile Acceleration and Base Pressure Using an S-Band Telemetry System," Memorandum Report No. 2562, Ballistic Research Laboratories, Aberdeen Proving Ground, MD, December 1975.

[5] J.W. Evans, "Pressure and Acceleration Measurements In Large Caliber Cannons," Proceedings of the Tenth Transducer Workshop, June 1979.

[6] J.W. Evans, "Measurements On-Board A Projectile During The In-Tube Travel Using An FM/FM Telemeter," Proceedings of DEA-G-1060 Germany-United States Ballistic Research and Development, October 1980.

[7] J.W. Evans, "A Technique for Measuring Engraving and Bore Frictional Forces in Large Caliber Guns," Proceedings of the 1983 JANNAF Propulsion Meeting, CPIA Publication Number 370, February, 1983.

[8] J.W. Evans, C.R. Ruth, and E.V.Clarke, Jr., "Soft Recovery Tests of A 155-mm Cannon Launched Guided Projectile, Type T," ARBRL-MR-03107, Ballistic Research Laboratory, USA ARRADCOM, Aberdeen Proving Ground, MD, May 1981.

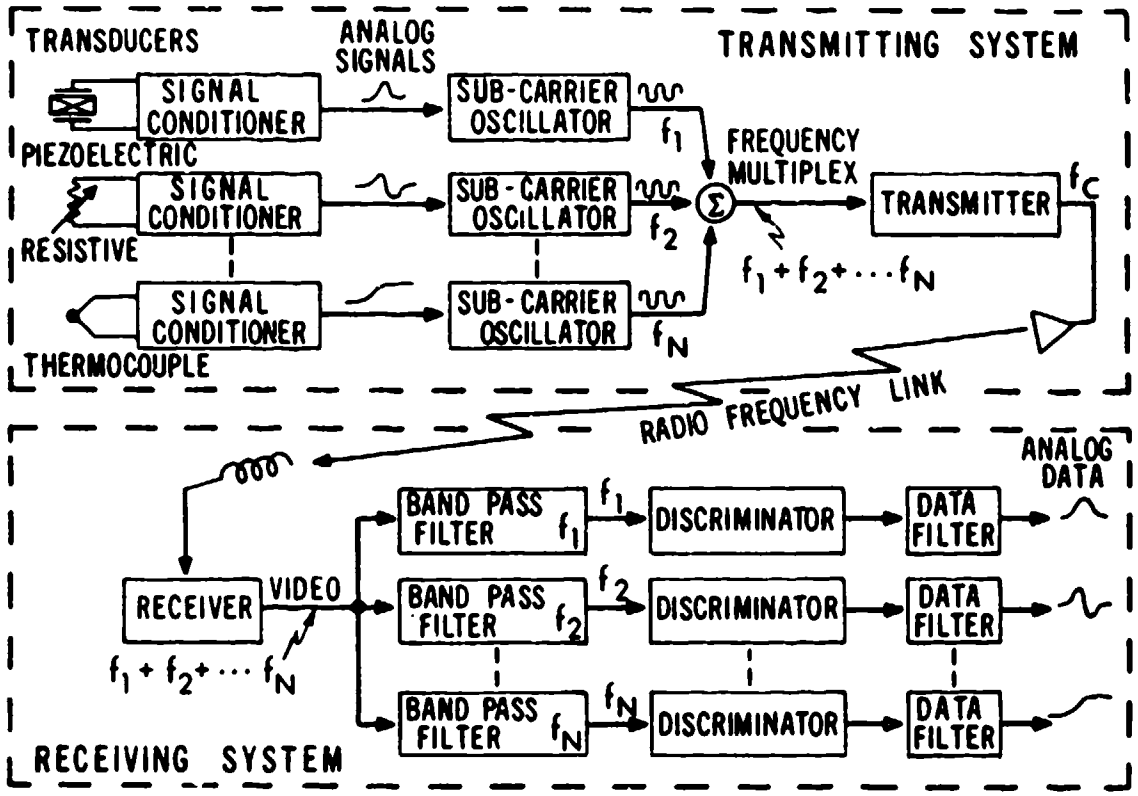

Figure 1. Standard FM/FM Telemetry System

and receiving system.[9] The transmitting system is on the projectile. The transducers and the associated signal conditioning frequency modulate the subcarrier oscillators. The subcarrier frequencies are summed and modulate the transmitter to form the FM/FM system. The real time data are transmitted, via the radio frequency link, to the receiving antenna. The receiver detects and discriminates the RF signal and outputs the video signal that is fed to parallel band-pass filters. This video signal is the same as the frequency multiplexed signal that originates from the subcarrier oscillators of the transmitting system. The band-pass filters select the desired subcarrier and present it to the discriminator used in the second detection process. The voltage analog signals for the various data channels are output through low-pass filters to a recording device.

Standard artillery projectiles are modified and instrumented with telemetry transmitting systems. In the past, free-flight projectiles have

---

[9] M.H. Nichols and L.L. Rauch, Radio Telemetry 2nd Edition, John Wiley and Sons, Inc., New York, NY, 1956.

been test fired and data successfully extracted via the real-time telemetry data link. The construction of telemetry transmitting systems is expensive and time-consuming. Therefore, it is desirable to recover the projectile so the instrumentation package can be reused. It is also desirable to recover the instrumentation so the transducers and transmitting system can be recalibrated after they have been exposed to the launch environment. With the design and construction of the BRL Large Caliber Soft Recovery System (LCSRS),[10] [11] [12] a useful test apparatus is available that permits reusing the instrumentation package.[8] [12] Therefore, artillery projectiles are modified for use with the LCSRS and instrumented with a telemetry transmitting system. They have been test fired, recovered, and the instrumentation reused on subsequent rounds.

This report discusses the technique used to acquire the on-board data. It includes a description of the telemetry transmitting system, the telemetry receiving system, calibration procedures, and projectile modifications. Representative data acquired from test firings are presented from a number of instrumented projectiles fired both free-flight and into the LCSRS.

II. TELEMETRY TRANSMITTING SYSTEM

A block diagram of a typical telemetry transmitting system is shown as Figure 2. This four channel system is configured to measure pressure and acceleration using piezoelectric transducers. Although only four channels are shown, several additional channels can be added as required. The subsystems used are commercially available and can be configured to make the desired measurement. Hardware for a 155-mm, M101 free flight projectile are shown as Figure 3. This system consists of a battery pack(B), the transmitter/antenna module(T), the electronics module(E), the accelerometer(A), and the pressure transducer(P). Also shown is the completely packaged transmitting system in a fuze housing. Each module is encapsulated in an epoxy and all the voids within the fuze housing are also filled. The individual subsystems, before interconnecting and packaging are shown as Figure 4.

---

[10] E.J. Halcin and J.A. Pratt, "Design of A Large Caliber Soft Recovery System for the Ballistic Research Laboratories," Contract Report No. 308, Honeywell Inc., Ballistic Research Laboratories, Aberdeen Proving Ground, MD, August 1976. (AD #B013626L)

[11] J.W. Evans, E.V. Clarke, Jr., and C.R. Ruth, "Large Caliber Projectile Soft Recovery," Proceedings of the 1979 JANNAF Propulsion Meeting, CPIA Publication Number 300, Volume I, March 1979.

[12] E.V. Clarke, Jr., C.R. Ruth, J.W. Evans, J.E. Bowen, J.R. Hewitt, and J.L. Stabile, "Large Caliber Projectile Soft Recovery," ARBRL-MR-03083, Ballistic Research Laboratory, USA ARRADCOM, Aberdeen Proving Ground, MD, February 1981.

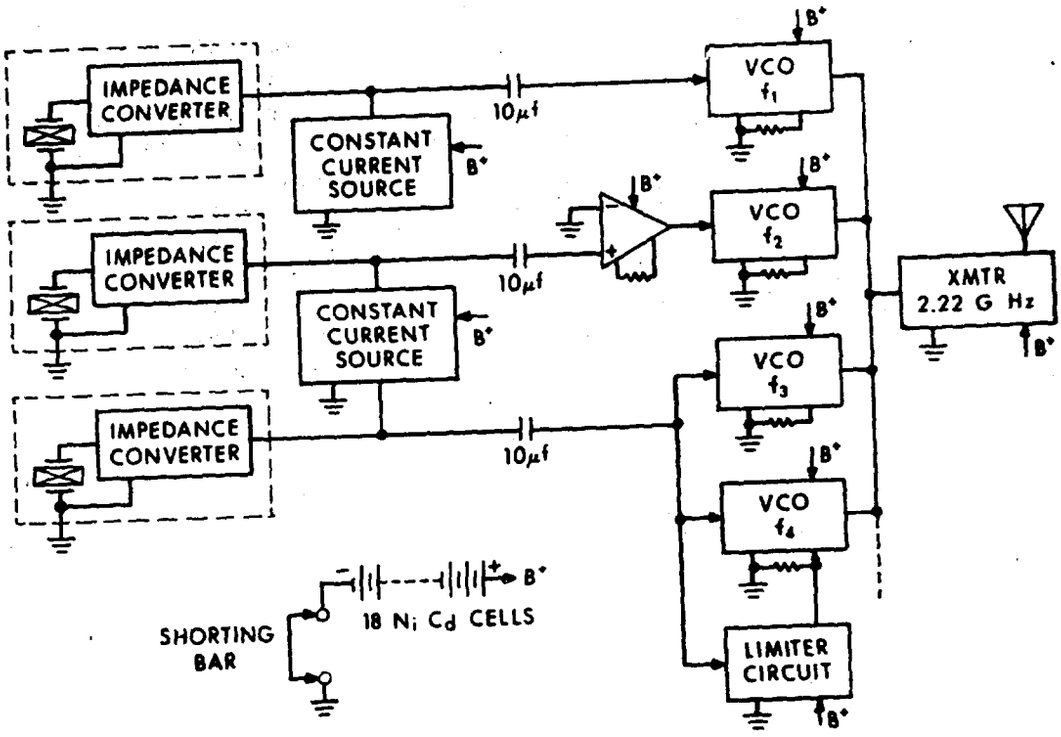

Figure 2. Telemetry Transmitting System, Block Diagram

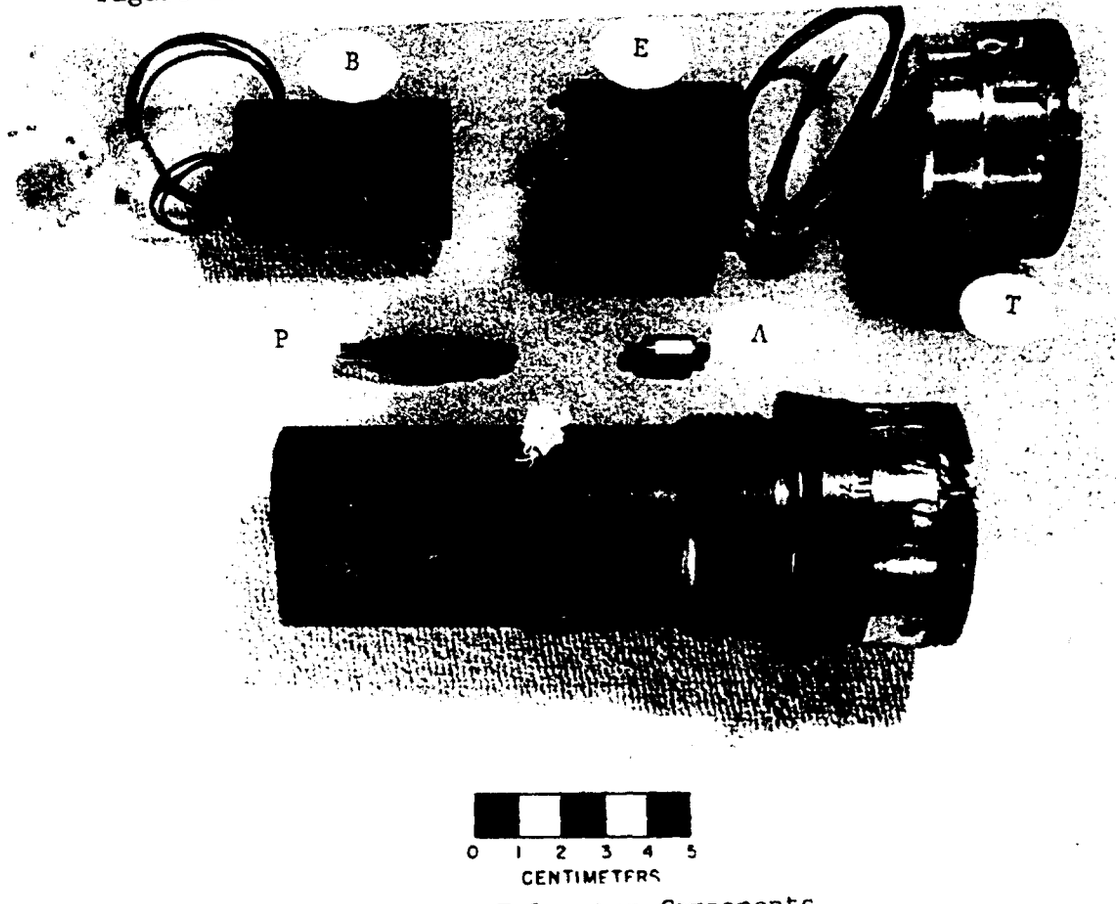

Figure 3. Telemetry Components

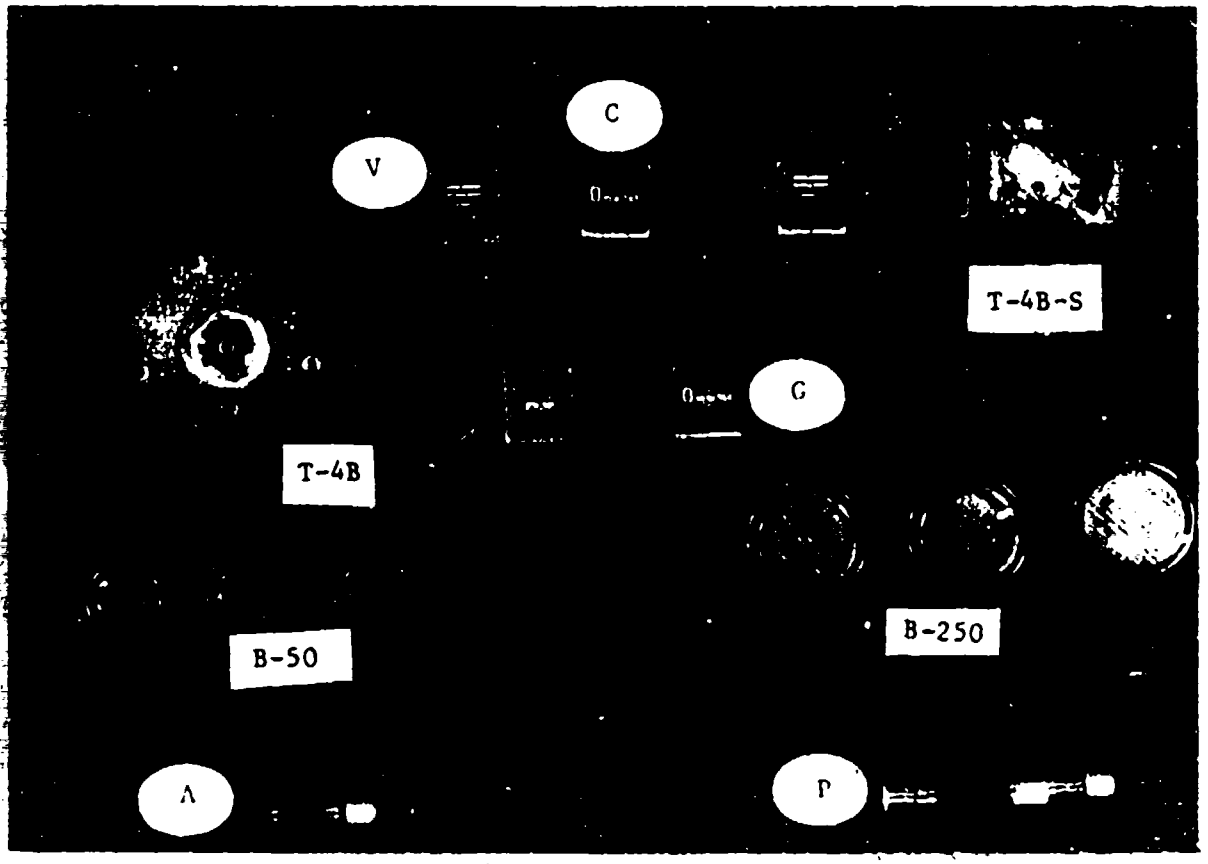

Figure 4. Telemetry Transmitting Subsystems

A. Piezoelectroc Transducers

The on-board pressure transducers (Figure 4, P) and accelerometers (Figure 4, A) used with the telemetry system are PCB Piezotronics, Inc. Models 109M[13] and 305M,[14] respectively. These transducers are selected because of their small power requirements and the small amount of circuitry required to interface them with the telemeter. Also the manufacturer, on request, will range the transducer to match the required voltage controlled oscillator (VCO) input voltage so gain or attenuation is not required.

---

[13] "Model 109A Pressure Transducer Instrumentation Manual," PCB Piezotronics, Inc., Buffalo, NY, 14255

[14] "Model 305M Accelerometer Instrumentation Manual," PCB Piezotronics, Inc., Buffalo, NY, 14255.

Both transducers are piezoelectric devices and each contain a P-Channel MOSFET source follower[15] within its housing. The source follower functions as an impedance converter and provides a nominal 100-ohm output impedance. A capacitor that shunts the piezoelectric element is used by the manufacturer to adjust the magnitude of the analog output. Full scale output for both units is five volts. Excitation required for the transducers is a two milliampere constant current source. This provides the bias voltage for the FET source with a nominal quiescent level of eleven volts. The analog signal is capacitive coupled to the VCO using a ten microfarad tantalum capacitor. A circuit diagram of the transducer is presented as Figure 5.

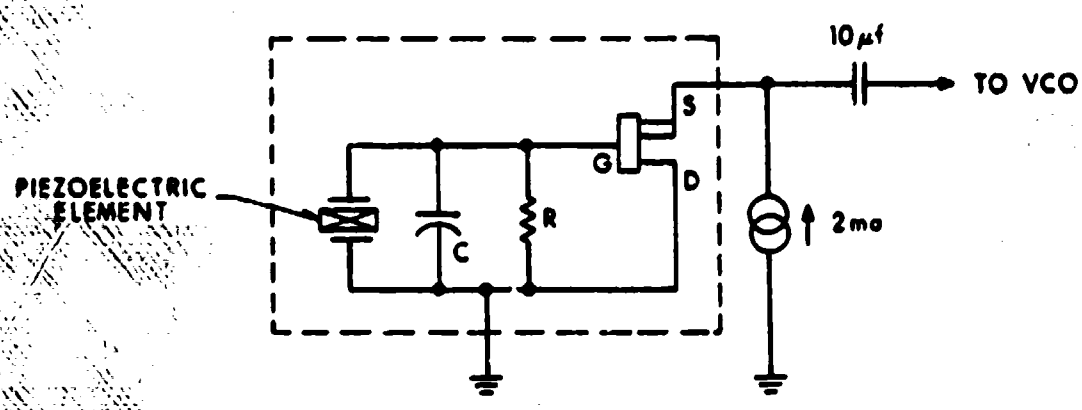

Figure 5. Piezoelectric Transducer, Circuit Diagram

The pressure transducer contains a very rigid, acceleration-compensated quartz element coupled to the source follower. This transducer is mounted in the projectile with its diaphragm exposed to the propelling gases via a short silicone grease column.

The accelerometer contains a seismic-mass-loaded quartz element coupled to the source follower. This transducer is mounted on the projectile long axis in the base structure of the projectile in tandem with and forward of the pressure transducer.

B. Constant Current Source

The constant current sources used to bias the transducers are designed and manufactured by Omnitek, Inc. Two similar thick-film, hybrid circuits are contained in a Omnitek standard, high "g" package (1.5cm X 1.3cm X 0.4cm). This subsystem (Model 22DL2A) requires a nominal 20 volts supply and is shown as C in Figure 4.

---

[15]PCB Piezotronics, Inc., General Guide To ICP Instrumentation, Pamphlet G-0001, Buffalo, NY.

C. Analog Amplifier

In the event that a transducer analog output voltage does not match the VCO requirements, an amplifier (Figure 2, Channel #2) is used to provide the necessary gain. The amplifiers used are Omnitek, Inc. Model 23L5-YE. These are differential amplifiers, here used in the single-ended mode, that have a variable gain, up to 500, contolled by an external resistor. They are thick-film, hybrid circuits packaged in a 1.3cm X 1.3cm X 0.8cm high "g" package (Figure 4, G).

D. Voltage Controlled Oscillator

The Omnitek, Inc. VCOs used have center frequencies that are separated by 64 kHz starting at 128 kHz. Each has a frequency deviation of ± 16 kHz that is a function of the input voltage. The input voltage range is typically zero to five volts or ± 2.5 volts, but can be tailored by the manufacturer to meet a specific requirement. The VCOs (Model 21C1-WEY) require a 20 volt power supply and are packaged in the standard high "g" package. The output of the VCOs have sufficient isolation so several can be connected together on a common bus. The VCO output amplitude is adjusted by an external resistor to provide the required modulation signal to the transmitter.

When a greater data frequency response is required, VCOs with a greater frequency deviation are used. Similar VCOs with a frequency deviation of ± 32 kHz are available. These units have center frequencies separated by 128 kHz starting at 384 kHz. VCOs with the two different frequency deviations may be used on the same transmitting system provided the required guard bands are not violated.

E. Limiter Circuit

In some cases it is desirable to modulate two VCOs, with different input voltage ranges, with the same transducer. This provides a high and low resolution channels. During the event, the high resolution channel is overdriven. The limiter circuit is used to insure that the VCO does not oscillate outside its prescribed frequency band and interfere with another data channel. The limiter circuit senses the VCO input voltage and when it exceeds the maximum permitted, it short circuits the VCO amplitude adjust resistor. This inhibits the VCO output and essentially turns off that data channel. The limiter circuit (Models 22DL1 & 22DL2) are designed and manufactured by Omnitek, Inc. Two separate circuits are contained in the standard, high "g" package.

F. Mixer Amplifier

In the event that the VCOs do not have sufficient output amplitude to directly drive the transmitter modulation, a mixer amplifier is used. The output of several VCOs can be connected to a common bus and to the input of the mixer amplifier. These amplifiers (Model 22M1A-E, manufactured by Omnitek, Inc.) have a fixed gain of 20 and are packaged in the standard, High "g" package.

G. Transmitter

The transmitters are manufactured by Microcom Corporation and have a nominal frequency of 2.22 GHz and output power of 20 milliwatts. Two models (Figure 4) are used. The Model T-4B-S has a semi-rigid coaxial cable for its RF output port while the Model T4B has a push connector concentric with the transmitter case. The selection of which type to use is determined by the antenna configuration. This basic transmitter is a free-running oscillator that has the capacity of 150 milliwatts output, but an attenuator is incorporated within its case to provide isolation between the transmitter and the antenna. This is done to minimize the frequency shift due to the varying voltage-standing-wave ratio as the projectile travels in the gun tube. The transmitter requires a 20-volt power supply at 50 milliamperes and has a nominal modulation sensitivity of 0.7 volts/MHz. The transmitters are frequency modulated by the frequency multiplexed signals from the VCOs. The amplitude of the individual VCO outputs are adjusted for the required peak carrier deviation.

Since data is acquired during the interior ballistic cycle, it is necessary to select a transmitter frequency that will propagate while in the gun tube, which is essentially a circular wave guide. From the theory of circular wave guides,[16] the cutoff frequency of the gun tube is determined by the relationship:

$$f = cp/\pi d \qquad (1)$$

where: f = cut-off frequency
c = speed of light
p = constant (1.84 for dominate mode propagation)
d = diameter of the gun tube

Any frequency below cutoff results in complete attenuation while in the tube and any frequency above cutoff will propagate. The 2.22 GHz transmitter selected will propagate from an 80-mm tube.

H. Antennas

The antennas used on the free-flight rounds are formed by a slot milled in a brass cylinder (Figure 3) that is attached to the front of the fuze housing. This configuration is selected since it presented a flat surface, on front of the projectile, to a microwave doppler radar that is used for independent projectile displacement measurements. The 1.6-mm-wide slot is a segment of a circle with an arc radius of 27.6 mm and a chord of 53.5 mm. The slot is filled with a fiberglass sheet that provides the

---

[16] L.A. Ware and H.R. Reed, Communication Circuits, 3rd Ed., John Wiley and Sons, Inc., New York, NY, 1958

required dielectric loading. The antenna is fed across the slot on the center of the arc by the T-4B-S transmitter RF coaxial cable. The outer conductor is soldered at the lower slot surface and the center conductor is soldered at the upper slot surface. One-hundred-ohm resistors are soldered across the slot, displaced by 20 degrees, on both sides of the feed coaxial cable to broad-band the antenna. A sketch of the configuration is shown as Figure 6. This arrangement matches the transmitter output impedance and the characteristic impedance of the semirigid coaxial cable.

Projectiles modified to be recovered in the LCSRS require they have a water scoop attached to the front of the projectile that is used in the recovery process. Since the water scoops are almost the diameter of the howitzer bore, it is necessary that the antenna be located within the water scoop. Also it is necessary that the antenna not interfere with the recovery process. Therefore, the radiating elements and feed cable of the antenna that protrude into the water path are housed in a phenolic fiberglass member. Upon impact with the water, this structure is designed to break away so it will not interfere with the water flow over the scoop surface. The T4B transmitter is mounted to the rear of the antenna lead port. The antenna (Figure 7) is contained in the phenolic member that is threaded at the base for mounting in the antenna-transmitter adapter. The base of the antenna-transmitter adapter houses the mating push-connector to the transmitter. A semirigid, coaxial cable, which passes through the long axis of the structure, is connected to fine wires that form the radiating elements. These elements are bent to conform to the outside of the phenolic member and run parallel to the long axis. A small 100-ohm resistor, connected across the dipole is used to broad-band the antenna. The structure, including the radiating elements and broad-banding resistor, is held in place using an epoxy. The antenna is matched to 50 ohms, the output impedance of the transmitter, by trimming the length of the radiating elements. This is accomplished using an RF bridge and comparing the antenna with a calibrated 50-ohm load. The antenna system is constructed as a single structure so it can be easily replaced after being destroyed in the LCSRS.

I. Strain Measurements

Strain measurements are made with foil-type, resistive, strain gages cemented to the area of interest. Typical measurements are made on the inner wall of the projectile under the rotating band. Both constant voltage excited bridges and constant current systems are used.

Figure 8 is the circuit diagram for a constant voltage excited bridge. The precision voltage regulator (μA723)[17] and associated discrete components maintain a constant voltage that excites the resistive bridges. The strain gages form two active arms of the bridge and are located 180 degrees apart on the projectile surface to compensate for the

---

[17] A. Adamian, "Voltage Regulator Handbook," Fairchild Camera and Instrument Corporation, Mountain View, CA, 1978.

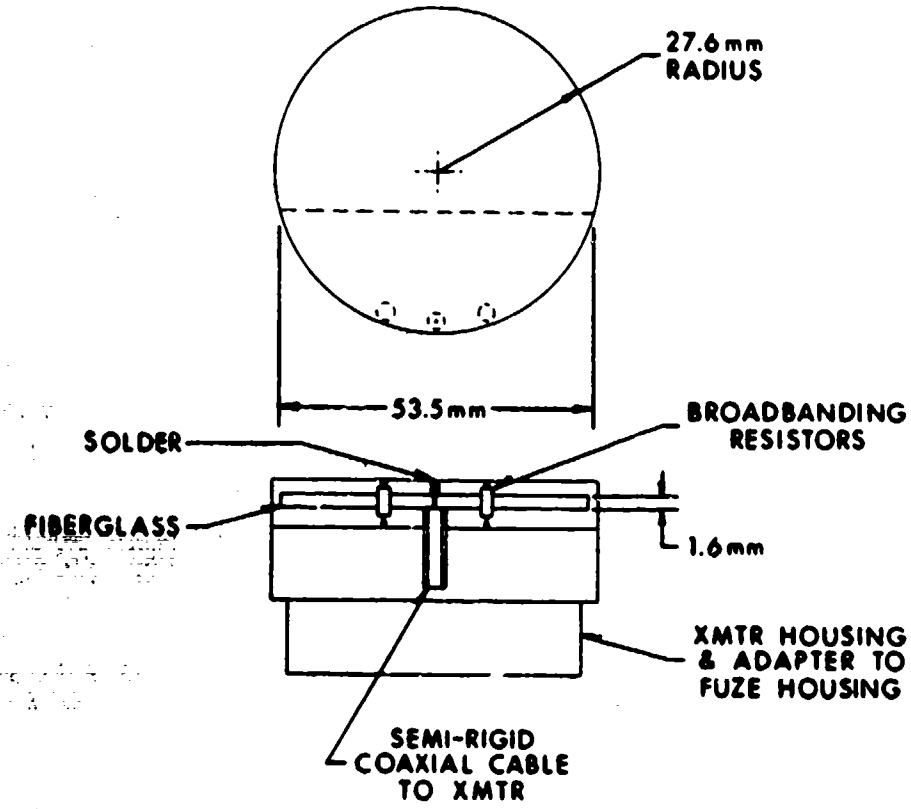

Figure 6. Slot Antenna

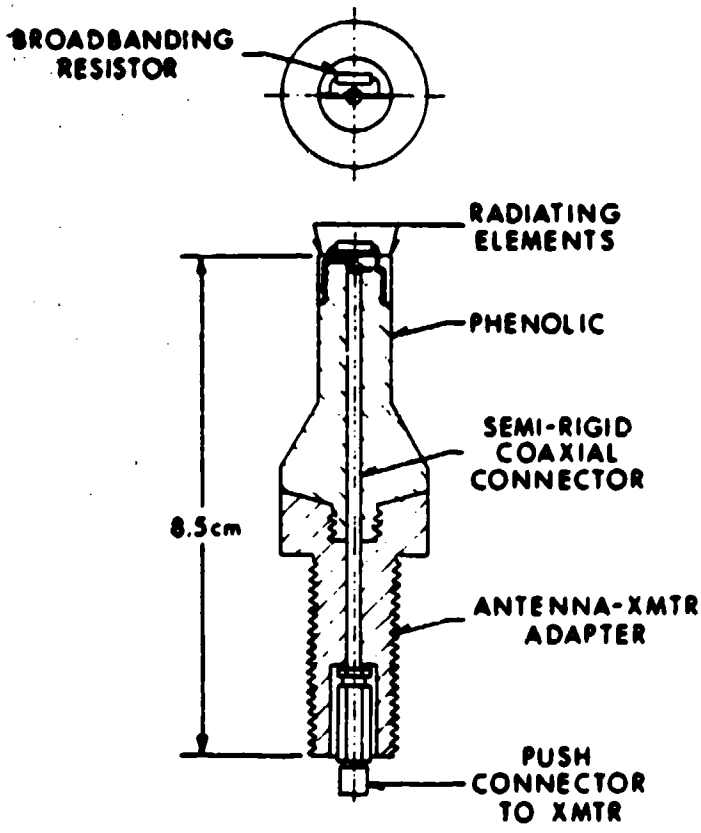

Figure 7. Dipole Antenna

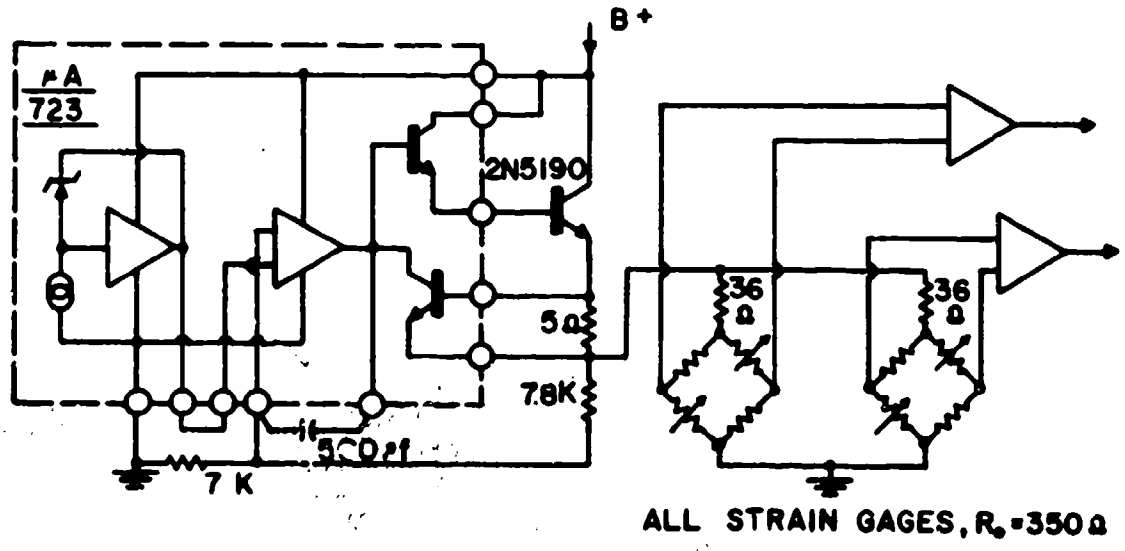

Figure 8. Strain Measuring System, Constant Voltage

bending moment of the projectile. The inactive arms of the bridge consists of similar strain gages isolated from mechanical strain. The use of the same type of bridge components minimize thermal drift. The differential, analog voltage output is amplified by an Omnitek amplifier to make it compatible with the VCOs.

The constant current system (Figure 9) uses an Omnitek constant current circuit. The gage is connected to one current source and the noninverting input of an Omnitek amplifier. A resistor connected to the other current source and the inverting input of the amplifier is used to adjust the quiescent output of the amplifier. This circuit is used when thermal drift is not critical since the gage and resistor have different temperature coefficients. The gain of the amplifier is adjusted to make the system compatible with the VCO.

J. Power Supply

The power supply for the transmitting system is configured using B-250 or B-50 nickel-cadmium cells. The B-250 cells have a current rating of 250 milliampere-hours and the B-50 have a 50 milliampere-hour rate, both at a 10-hour rate. The cells are connected together, by spot welded metal tabs, and encapsulated in an epoxy. Eighteen series connected B-250 cells provide a typical transmitting system with a 22-19 volt supply for greater than one hour. The B-50 cells are used when space restricts the use of the larger B-250 cells. Two paralleled stacks are required for operating the transmitting system for about one-half hour. These relative long operating periods permit system check-out and calibration using battery power.

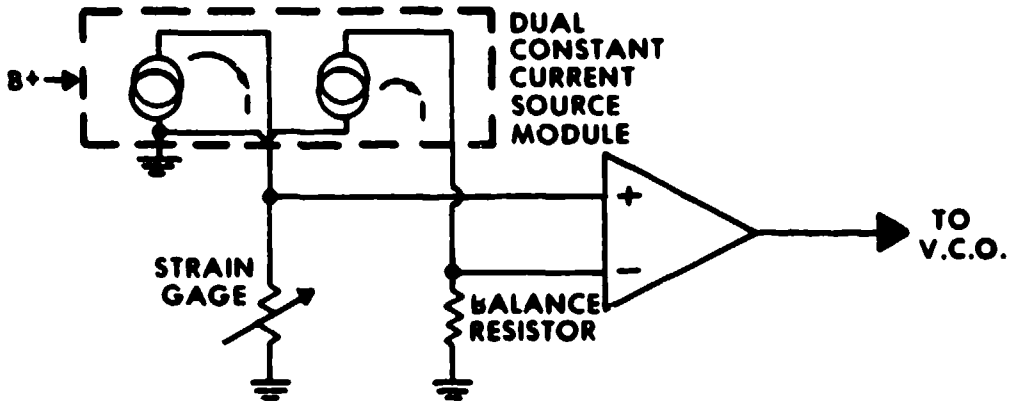

Figure 9. Strain Measuring System, Constant Current

This type power supply is selected since the nickel-cadmium cells can be recharged up to 1000 times. Recharging requires 140% of the milliampere-hours drained. The recharging constant current is 25 and 5 milliamperes for the B-250 and B-50 respectively.

The positive side of the battery pack is hard wired to the transmitting system and also to a test jack for monitoring and charging. The negative side is wired to a floating test jack. Since the common nodes of the transmitting subsystems are common to the projectile body, the battery negative test jack is shorted to the projectile body to turn the system on. A sketch of the shorting bar is presented as Figure 10.

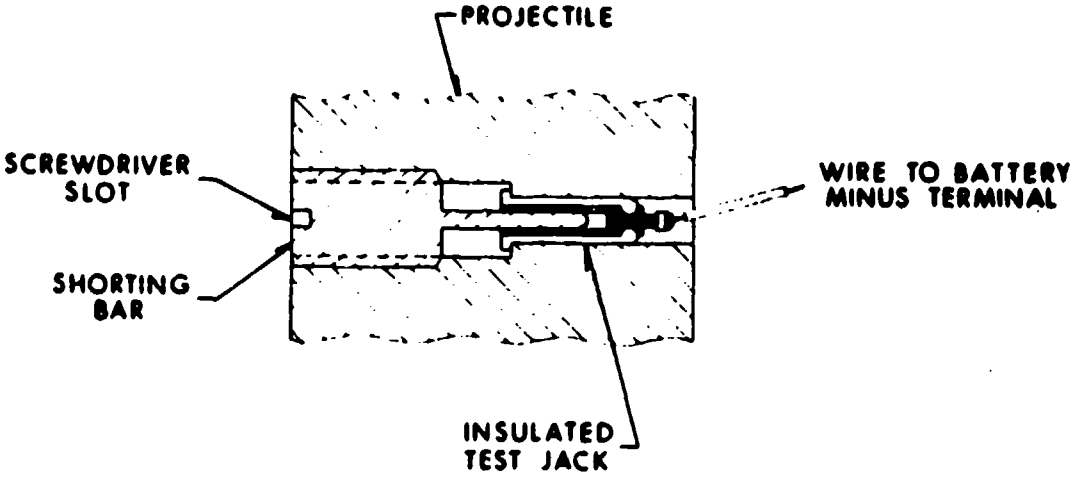

Figure 10. Shorting Bar

III. TELEMETRY RECEIVING SYSTEM

A block diagram of the telemetry receiving system is presented as Figure 11. Six data channels are shown, but only those applicable to a particular round are recorded. Additional channels are added if required.

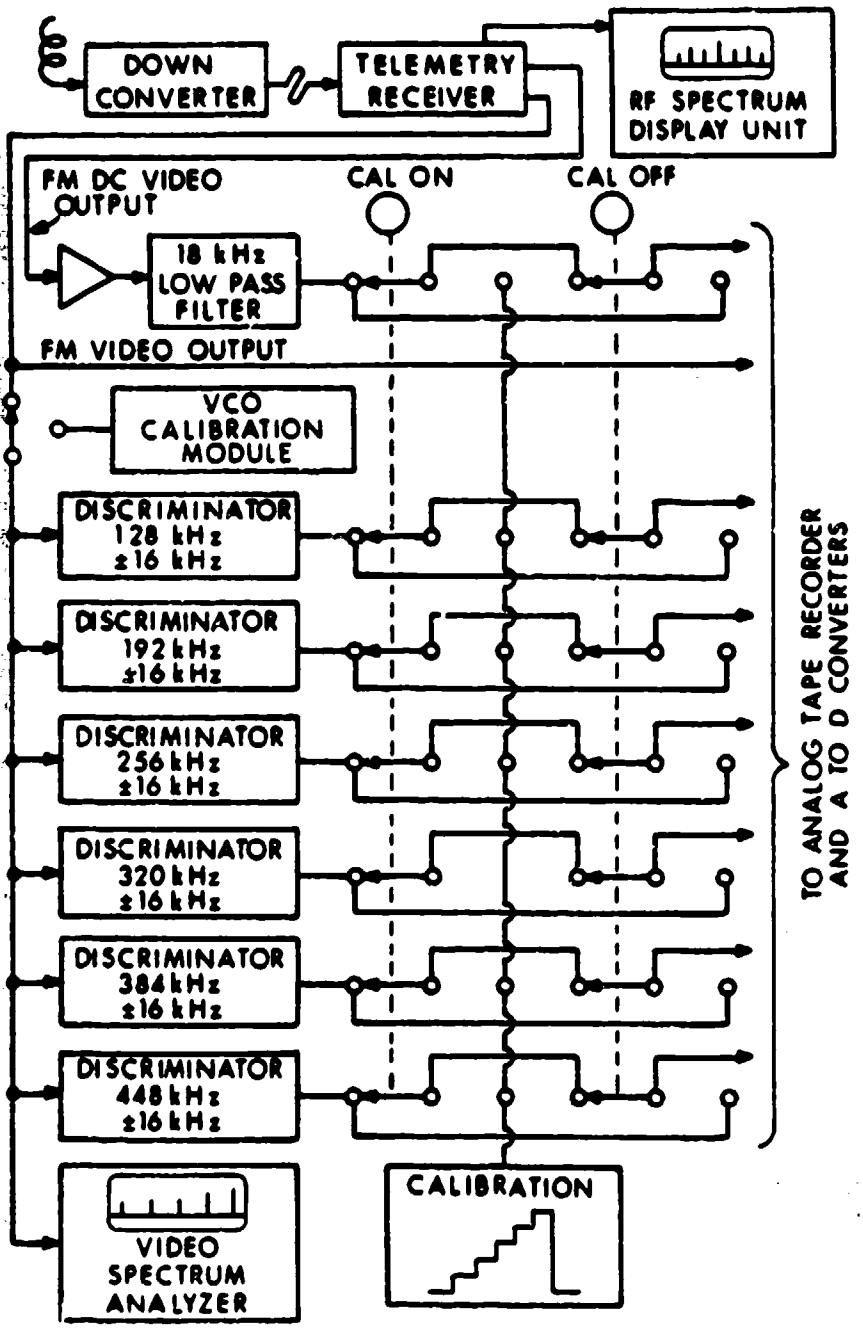

Figure 11. Telemetry Receiving System, Block Diagram

A. Radio Frequency Receiving System

The output signals transmitted from the projectile during the in-tube travel are received via a helical antenna (Andrew Corp., Model 55305) located forward and to the side of the muzzle. It was determined that precise positioning of the antenna is not critical, except that it be placed outside the area of extreme muzzle blast to prevent damage. Output signals from the antenna are fed into a down converter (NU-DEL Electronics, Model #MDC2223) that translates the nominal 2.22 GHz signal to a nominal 235 MHz signal. This is done to avoid the large attenuation at the 2.22 GHz frequency caused by the 30 metres of coaxial cable (RG-8/U) between the antenna and the receiver. Signal level input to the Astro Communications receiver (Model #TR104/Model TH100P Tuning Head) is then at minus 40 dbm. For most programs, the receiver intermediate frequency (IF) bandwidth is 3.3 MHz and the video bandwidth is 750 kHz. An output from the tuning head is fed to a spectrum display unit (Astro Communications, Model #103AP) and the video is fed to a Nelson Ross spectrum analyzer (Model # TA1013) as well as the bank of subcarrier discriminators. The spectra are used as an indicator while monitoring, adjusting, and calibrating the telemetry transmitting system.

The frequency modulated, direct coupled, video output signal of the receiver is used as an indicator of the transmitter frequency stability during the interior ballistic cycle. This signal is amplified and passed through an 18 kHz low pass filter to eliminate the subcarrier frequencies. This incidental FM is used to determine if the RF signal stayed within the IF bandwidth.

B. Data Discriminating System

The data discriminators used in the second detection process are EMR Data Systems Model #4130. Each discriminator assembly contains a channel selector module that has an input band width of 32 kHz and a center frequency that corresponds to one of the transmitting systems subcarriers. Also each discriminator assembly contains a low-pass, output filter module with a bandwidth of 8 kHz through which the analog data passes. Six discriminators are contained within a single chassis along with a calibration module. The video output from the receiver is fed to the channel selector modules via a common bus. The output from each discriminator channel is interrupted 350 milliseconds prior to the event to insert a voltage staircase calibration. This complies with an in-house data format for recording and reducing interior ballistic data.[18]

[18] C.L. Henry, R.L. Martz, and E.M. Wineholt, "An Improved Procedure For The Reduction of Interior Ballistic Data Recorded On Analog Tape," Memorandum Report No. 2374, Ballistic Research Laboratories, Aberdeen Proving Ground, MD, April 1974. (AD #919924L)

In the event the transmitting system is configured with VCOs with frequency deviations of $\pm$ 32 kHz, the channel selector modules must have input bandwidths to match. The output filter modules then have bandwidths of 16 kHz.

IV. TELEMETRY SYSTEM PARAMETERS

The telemetry system is designed to have equal transmission accuracy for each subcarrier channel. The discriminator output signal-to-noise ratio is a function of the varying receiver carrier-to-noise ratio as well as various parameters of the telemetry system. The general formula[19 20 21] used to estimate the noise performance of an FM/FM channel above receiver threshold is given as follows:

$$(S/N)_d = (S/N)_c \, (3/4)^{1/2} \, (B_c/B_{sc})^{1/2} \, (\Delta f_c/f_s) \, (\Delta f_s/B_{sc}) \qquad (2)$$

where:

$(S/N)_d$ = Discriminator Output Signal-To-Noise Ratio (RMS Voltage Ratio)

$(S/N)_c$ = Receiver Carrier-To-Noise Ratio (RMS Voltage Ratio)

B_c = Carrier Bandwidth (Receiver IF Bandwidth)

B_{sc} = Subcarrier Discriminator Bandwidth

Δf_c = Carrier Peak Deviation Due To The Particular Subcarrier Of Interest

f_s = Subcarrier Center Frequency

Δf_s = Subcarrier Peak Deviation

The receiver carrier-to-noise ratio for FM threshold is four (12 db) and the minimum acceptable discriminator signal-to-noise is 100 (1% data).

---

[19]Telemetry Working Group, Inter-Range Instrumentation Group, Range Commanders Council, Telemetry Standards, Document 106-71, White Sands Missile Range, NM 88002.

[20]W.J. Cruickshank, "A Feasibility Test of An "S" Band Telemetry System For Making In-bore Projectile Measurements," Memorandum Report No. 2335, Ballistic Research Laboratories, Aberdeen Proving Ground, MD, October 1973.

[21]W.J. Cruickshank, "Radio Telemetry Formula Applications, A Practical Users Guide," ARBRL-MR-03364, Ballistic Research Laboratory, Aberdeen Proving Ground, MD, August 1984.

Other parameters are determined as:

B_c = 3.3 MHz (normally used)

B_{sc} = 8 kHz (for VCO deviation of $\pm$ 16 kHz)
= 16 kHz (for VCO deviation of $\pm$ 32 kHz)

f_s = VCO Center Frequency

Δf_s = 16 kHz (for VCO deviation of $\pm$ 16 kHz)
= 32 kHz (for VCO deviation of $\pm$ 32 kHz)

The general formula is used to calculate the required carrier peak deviation due to the various subcarriers. The results of this calculation gives the following relationship:

$$\Delta f_c / f_s = \beta = 0.711 \quad ; \text{ for } B_{sc} = 8 \text{ kHz}$$

$$\Delta f_c / f_s = \beta = 1.005 \quad ; \text{ for } B_{sc} = 16 \text{ kHz}$$

where β is defined as the modulation index.[22]

Carrier peak deviations are adjusted to the required value by adjusting the output amplitude of the VCOs. The magnitude of the various carrier deviations are displayed on the video spectrum analyzer while operating the entire telemetry system. Relating the displayed magnitudes to the peak deviation requires calibration and adjustment of the receiving system. This is accomplished by replacing the telemetry transmitting system with an FM signal generator as depicted in Figure 12. The modulating frequency is varied to determine and adjust the frequency axis of the video spectrum analyzer. The amplitude of the modulating signal is varied while observing the video and RF spectra. The magnitude of the carrier and sidebands, displayed on the RF spectrum, vary when the amplitude of the modulating signal is varied. The magnitude of the carrier, first sidebands, second sidebands, etc., follow the Bessel Functions J_0, J_1, J_2, etc., respectively, with beta as the argument.[22] By selecting a modulating frequency and adjusting the modulating signal amplitude until the magnitude of the carrier or a set of sidebands go to zero, the peak deviation is established. For example, the first carrier drop-out occurs when β equals 2.405 (first root of J_0). By increasing the modulating signal amplitude from zero until first carrier drop-out, the peak carrier deviation can be calculated by $\beta = \Delta f_c / f_s$. The gain of the receiver video output and/or the gain of the video spectrum analyzer can be adjusted as desired to display and scale the peak carrier deviation. The telemetry system can then be observed and adjusted for the required peak deviation. A sketch of a typical video spectrum is shown as Figure 13.

---

[22] M. Schwartz, "Information Transmission, Modulation, and Noise," McGraw-Hill Book Company, Inc., New York, NY, 1959.

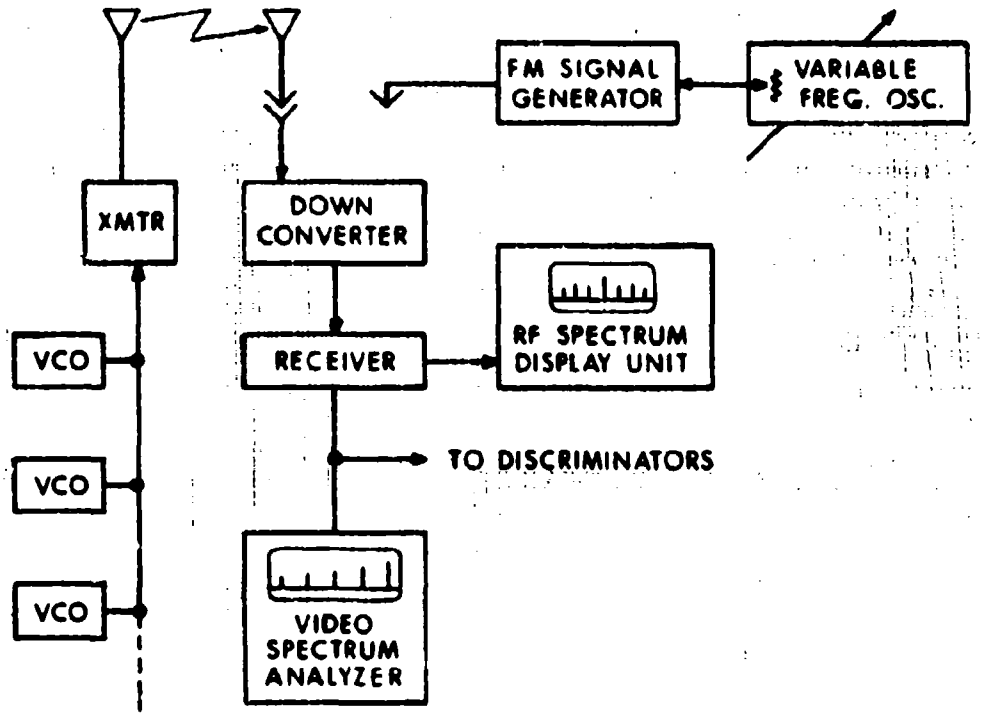

Figure 12. Frequency Modulation System, Block Diagram

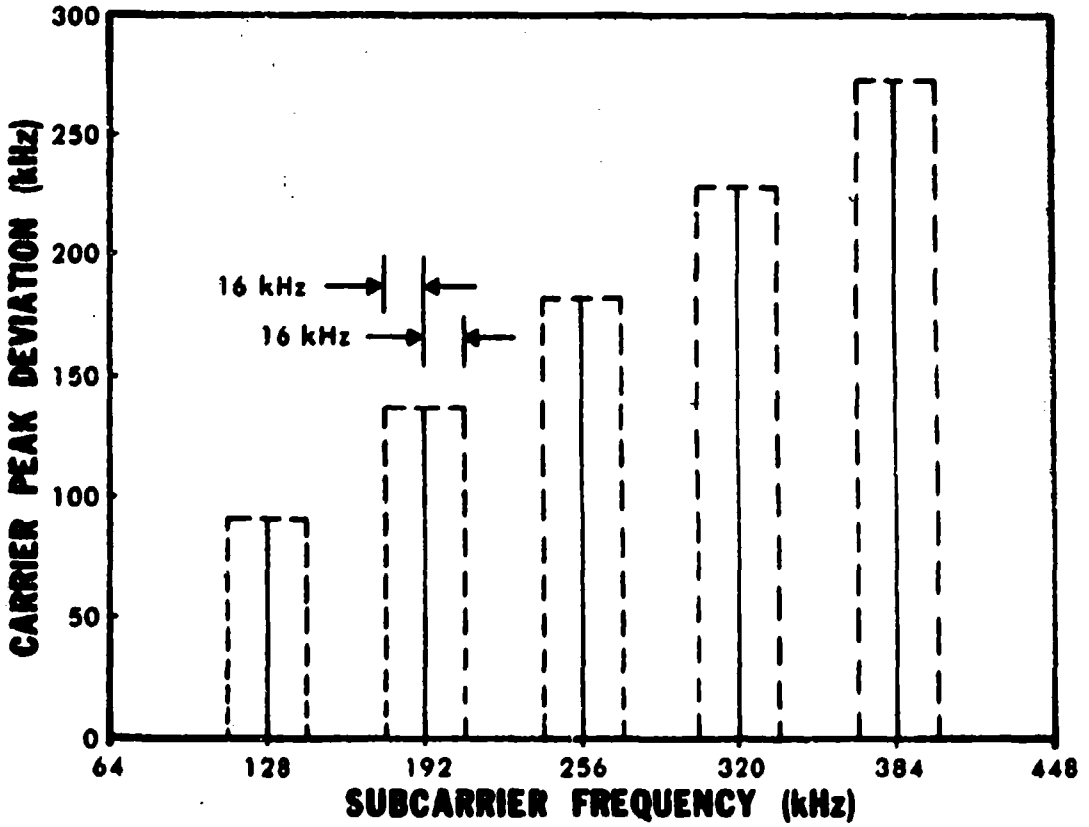

Figure 13. Typical Video Spectrum, $\beta = 0.711$

From FM transmission theory,[22] a modulation index of 0.711 produces two significant sidebands (significant sidebands are those with a magnitude at least one percent of the unmodulated carrier) and a carrier bandwidth (B_c) of four times the frequency of the modulating signal is recommended. With the carrier bandwidth normally used, subcarrier channels up to 768 kHz and this modulating index can be used. Should higher frequency channels be used, an adjustment to the normally used 750 kHz video bandwidth must be made. For the modulation index of 1.005, three significant sidebands are produced and a carrier bandwidth of six times the frequency of the modulating signal is recommended. This permits subcarrier channels up to 512 kHz and this modulating index to be used. If higher frequency channels are required, a wider bandwidth should be used along with the appropriate carrier peak deviations.

The total carrier peak deviation due to all the subcarriers cannot exceed the transmitter deviation limit or the receiver bandwidth. It is necessary to observe the data output of the various discriminator channels to determine distortions and cross-modulation products. In some instances it is necessary to decrease the carrier deviation using a trial and error method to optimize the system.

V. TELEMETRY SYSTEM CALIBRATION

The information transmitted by an FM/FM telemetry system is contained in the frequency of the subcarriers. Therefore, it is necessary to define the magnitude of the physical quantity being measured in terms of the output frequency of the VCOs. It is also necessary to correlate the discriminated outputs of the receiving system with the subcarrier frequencies. This, in effect, correlates the discriminated output with the physical quantities being measured.

A. Piezoelectric Channel Calibration, Transmitting System

The procedure for calibrating a pressure channel is shown in Figure 14. The pressure transducer is calibrated in a dead weight calibration facility. It is subject to several static pressure levels and the resulting output voltage is recorded. The set of points resulting from this calibration is used to determine the least square parabola with pressure as the dependent variable and output voltage as the independent variable. The VCO used in the pressure channel is calibrated by impressing a series of voltage levels on the input and measuring the resulting output frequency. This calibration is made while operating the telemetry transmitting and receiving systems and counting the output frequency at the appropriate channel selector filter. The measured frequencies are normalized to a change in frequency (Δf) where zero represents the VCO lower band-edge ($f_s - \Delta f_s$). The pressure-voltage relationship is used to calculate a corresponding pressure for the various voltage level inputs to the VCO. This forms a set of points of pressure and Δf that is used to determine the least square parabola with pressure at the dependent variable and Δf as the independent variable. This gives the desired relationship for pressure as a function of subcarrier frequency.

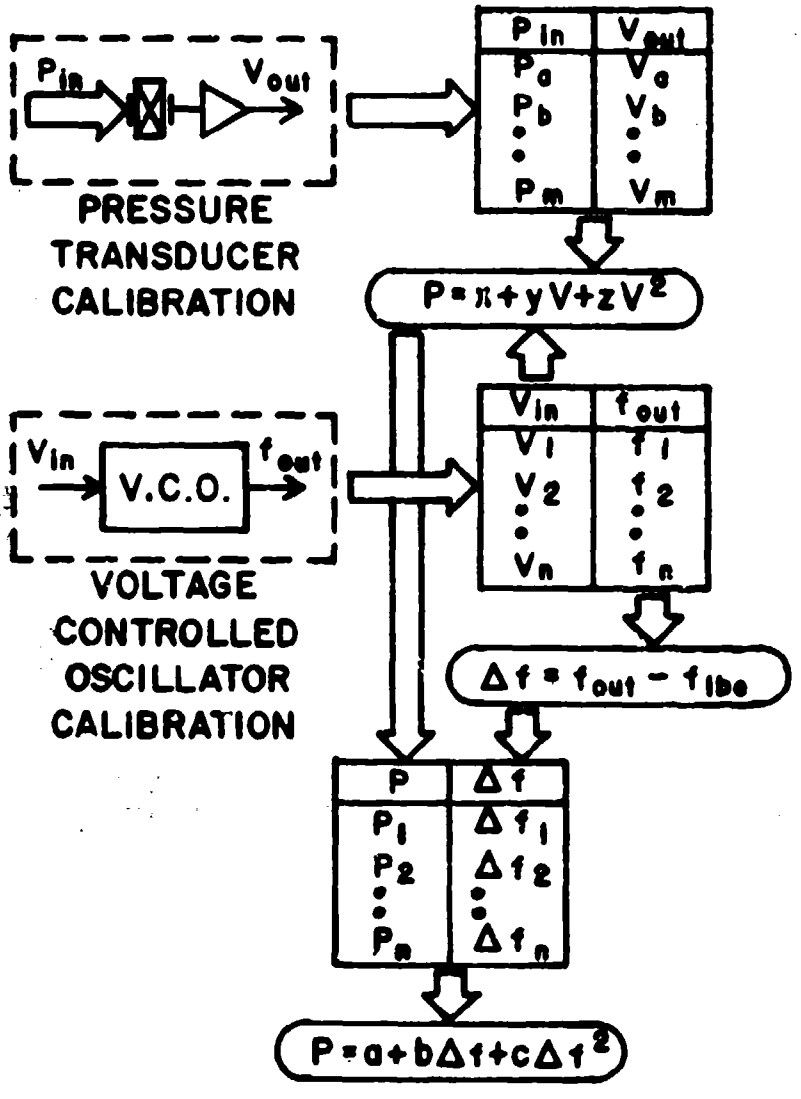

Figure 14. Pressure Channel Calibration

The procedure for calibrating an acceleration channel uses the manufacturer's linear calibration factor when an in-house accelerometer calibration facility is not available. The VCO used in the accelerometer data channel is calibrated and the frequency is normalized in a manner similar to the pressure channel (Figure 15). The acceleration-voltage relationship is used to calculate a corresponding acceleration for the various voltage level inputs to the VCO. The resulting set of points are used to determine the least square parabolic fit.

The numerical convolution of the results of the VCO and transducer calibrations is required since it is not practical to make a single calibration using the entire telemetry system. This is due to the physical locations of the two facilities. The form of the output of the convoluted calibration is required by the in-house data reduction process.[18] The

coefficients that are determined are input as the measurand calibration constants in the data reduction software.

The output impedance of the piezoelectric transducers is about 100 ohms and the input impedance of the VCOs is several hundred kilohms. Therefore, the loading factor is negligible and the VCO does not significantly alter the transducer output when they are interfaced. Convolution of the transducer calibration and the VCO transfer function is therefore a valid technique.

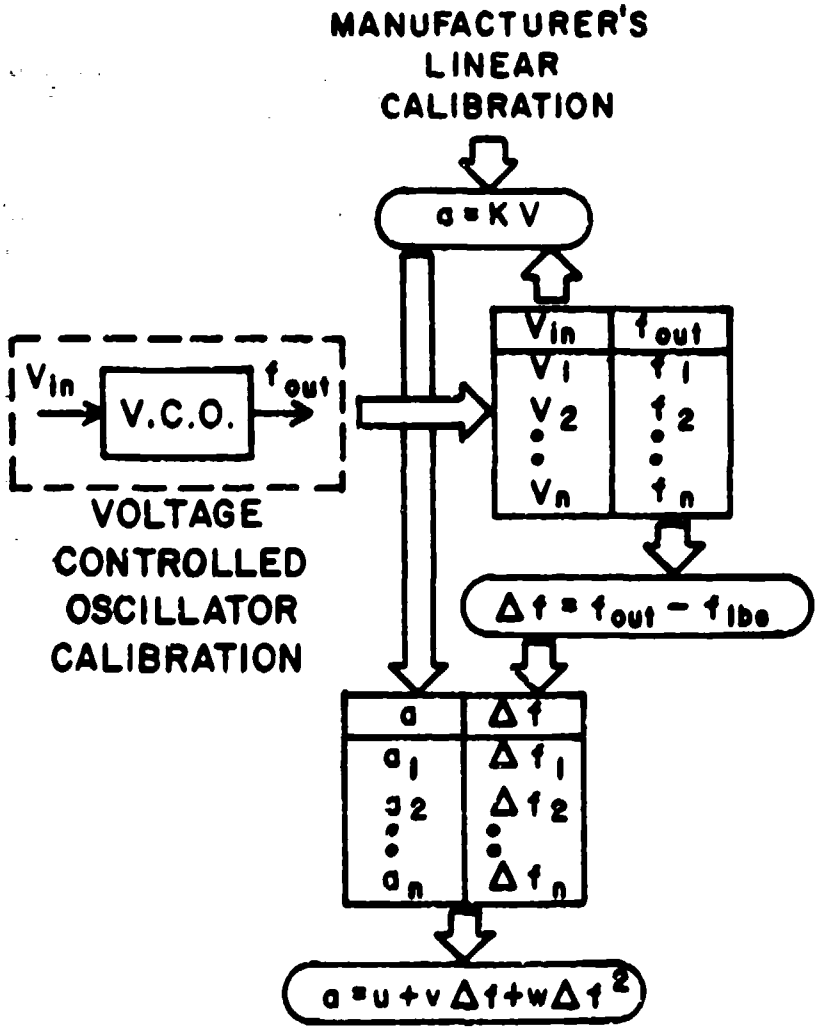

Figure 15. Acceleration Channel Calibration

B. Strain Channel Calibration, Transmitting System

The strain bridge channels are calibrated end-to-end by substituting precision decade resistors for the active arms of the bridge (Figure 16). First, the bridge is balanced with all strain gages connected. Then the

active arms are disconnected, one at a time, and the decade resistor is connected. After each substitution, the bridge is rebalanced to its original quiescent operating point. When both active arms have been replaced, the two substitution resistors are varied by the same resistive increments over the expected range. The VCO frequencies are recorded and normalized for each increment. The resistive increments are converted to strain increments using the manufacturer's gage factor. Then the least square parabolic fit is determined for the strain - Δf relationship.

C. Receiving System Calibration

The transmitting system calibration is correlated with the receiving system via the voltage staircase calibration (Figure 11). The magnitude

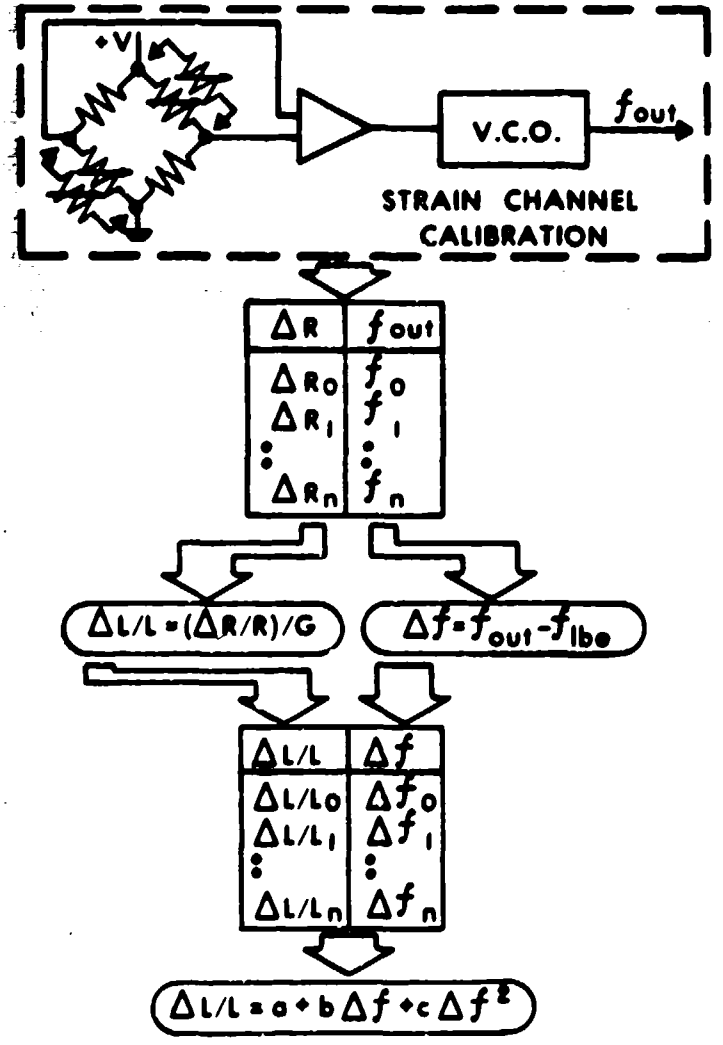

Figure 16. Strain Channel Calibration

and offset of the staircase are adjusted to be compatible with the recording device. The discriminator output voltage is correlated with the calibration staircase by adjusting its offset and output gain. The discriminator chassis contains a calibration module that can produce, using a crystal oscillator, the center, lower band-edge, and upper band-edge frequencies of each subcarrier. By manual selection, one calibration frequency at a time can be put on the video bus. A block diagram for one channel (Δf_s = 16 kHz) is presented as Figure 17. The lower band-edge ($f_s - \Delta f_s$) voltage is adjusted to coincide with the staircase baseline and the upper band-edge ($f_s + \Delta f_s$) voltage is adjusted to coincide with the

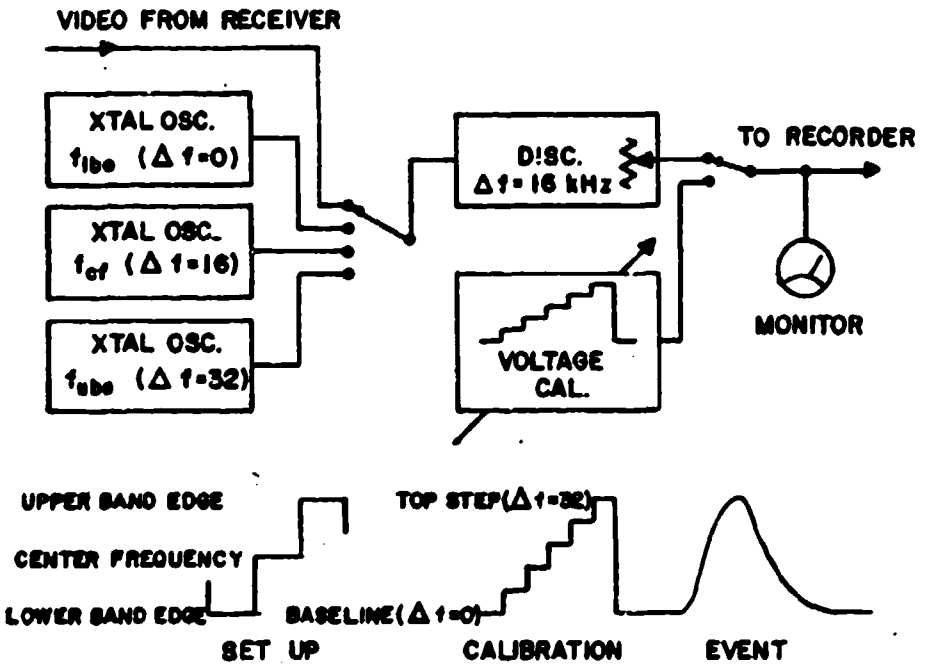

Figure 17. Receiving System Calibration

staircase top calibration step. These two extremes represent Δf equal to zero and 32 kHz (for Δf_s = 16 kHz) or 64 kHz (for Δf_s = 32 kHz) respectively in the transducer - VCO least square parabolic fit. This manual correlation of the staircase to the crystal frequencies is required since an automated calibration system is not available in-house. The recorded staircase and data from the event represent the VCO frequency excursion with the staircase steps defining the magnitude of the physical quantity being measured. The frequency excursion represented by the staircase top step is input for the system calibration in the data reduction software.

VI. RECORDING AND DATA REDUCTION

The analog data from the telemetry system, as well as hard-wire data, are recorded in real time by an analog-to-digital converter (A/DC) that is

a subsystem of the Ballistic Data Acquisition System (BALDAS). These data are simultaneously recorded on analog, FM, magnetic tape. Data recorded on analog tape can be played-back into the BALDAS for digitization. The BALDAS is a data acquisition and reduction system that operates under the control of a minicomputer (Digital Equipment Corp., PDP-11/45). Peripherals on the system include: magnetic cartridge disk drives, a magnetic tape drive, a printer/plotter (Versatec,Inc.,Model #1100A), an interactive terminal (Tektronic, Inc.,Model #4010) as well as the interfaces that drive the A/DC and other data acquistion hardware. A simplified block diagram of BALDAS is shown as Figure 18. Analog data digitized by the A/DC is strobed into the computer memory in real time. The sequence timer, setup under computer control, initiates hardware starts such as the gun firing pulse. The event timer records the elapsed time for hardware operation and times of arrival such as the firing pulse and velocity coil outputs. This is used to coordinate times with the digitized data. The analog tape controller automatically operates and monitors the analog tape recorder during the real time event and during playback of the recorded data into the A/DC. The computer sets up the acquisition hardware via the appropriate interfaces and monitors its function as required. The data acquisition is accomplished by operator initiation and interaction of the range operating personnel.

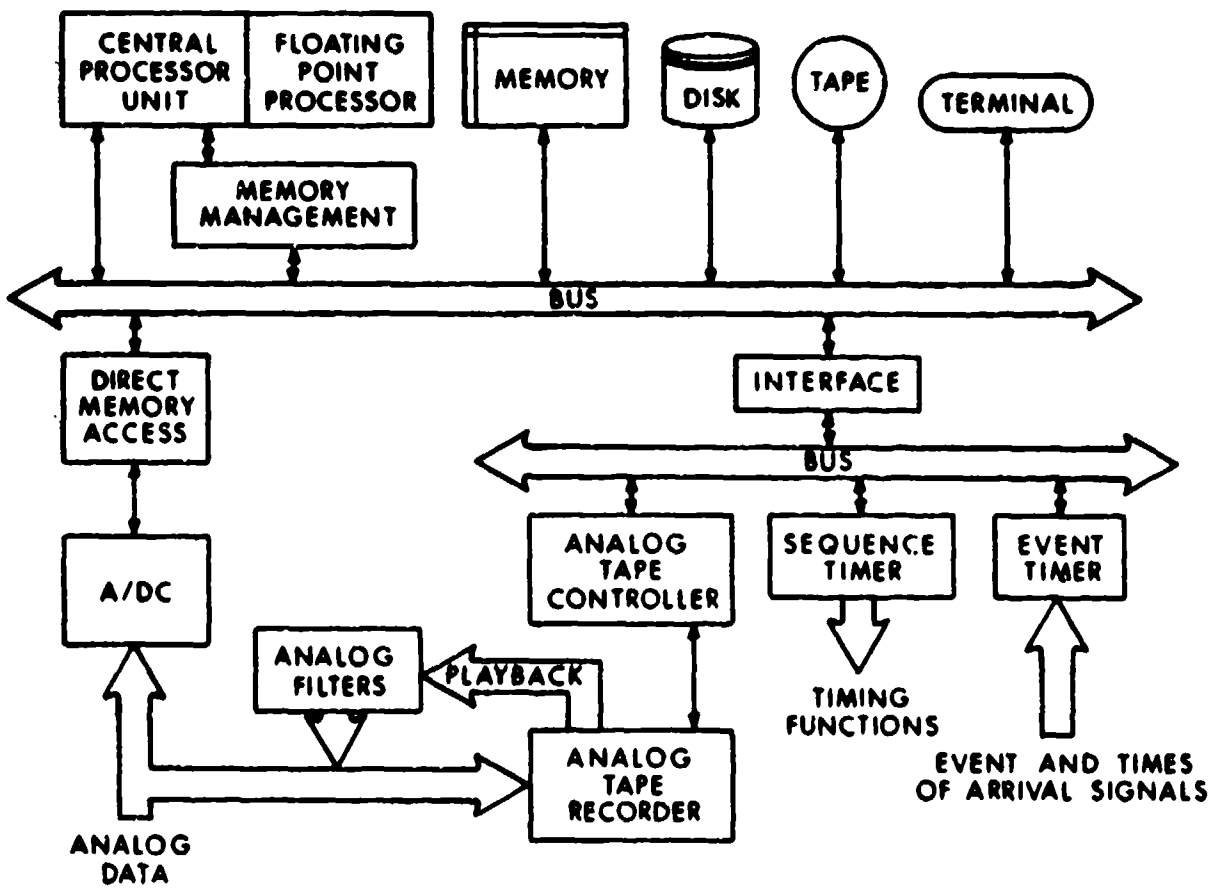

Figure 18. Ballistic Data Acquisition System, Block Diagram

Software for the system is written in an interactive mode. With the appropriate hardware configuration, an operator at the terminal can set up the desired experiment, perform data acquisition, and reduce the data to have hard copy of the experimental results the same day. During system setup, the operator inputs the appropriate parameters to perform the experiment. These include the measurand calibration constants for each channel, the system calibration for each channel, the engineering units for each measurand, the number of channels, digitization rate, analog tape speed, and timing for the various hardware starts. Information describing the experiment is also input for permanent storage on digital magnetic tape along with the data acquired during the event.

After the data acquisition, the operator can output the data in the form of plots or listings on the printer/plotter. This is done from the interactive terminal using the interactive software. The first operation is to scale the raw binary data to engineering units. This is done by a calibration routine. A least square parabolic fit is made to the calibration staircase. This fit is convoluted with the the parabolic fit using the measurand calibration constants to determine what magnitude in engineering units the raw binary data represents. At this point, the operator can display plots of the various data channels on the interactive terminal. A variety of options are available in the data reduction routines. Through these interactive routines, the operator can perform a variety of mathematical operations as well as select the plot window, select the number of plots on an axis, label the axis, and annotate the plot before hard copy is plotted. Permanent storage of the digitized data is on digital magnetic tape. From this tape, the operator can recall the data for additional data reduction or re-evaluation.

VII. TEST PROJECTILES

Standard artillery projectiles are modified to accept the transducers and telemetry transmitting instrumentation package. An effort is made not to significantly modify any feature of the projectile that affects the interior ballistic performance. The rotating band and bourrelet are not altered and the projectiles are ballasted to the standard weight.

A. 155-mm, M101 Free-Flight Projectiles

An instrumented 155-mm, M101 projectile is presented as Figure 19. This free-flight projectile contains a telemetry transmitting system configured to measure base pressure and projectile acceleration. The electronics and battery pack are packaged in a modified fuze housing that is threaded into the nose of the projectile. This is a self-contained unit with the transmitting antenna connected as an integral part. The only required electrical interfacing is with the transducers. The base of the projectile is modified to accept the transducer housing (Figure 20). This housing contains the pressure transducer, that is exposed to the propelling gases, and the accelerometer located forward of the pressure transducer. Both transducers are located on the center line of the projectile. The housing is fastened to the projectile by eight 1/4 - 28 machine screws. An aluminum crush seal, located in a groove in the base structure, is used to

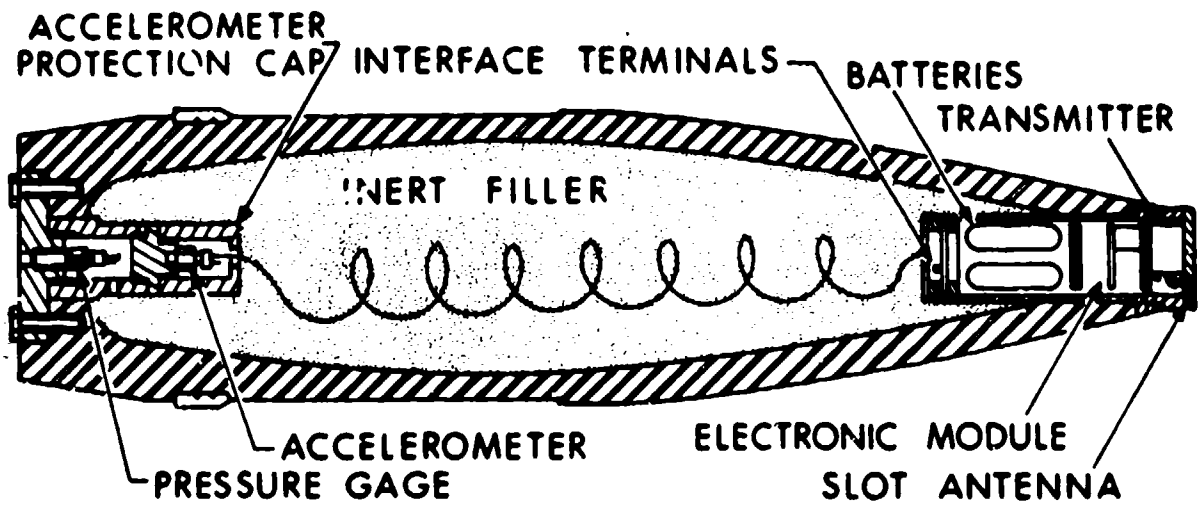

Figure 19. Instrumented Free-Flight 155-mm, M101 Projectile

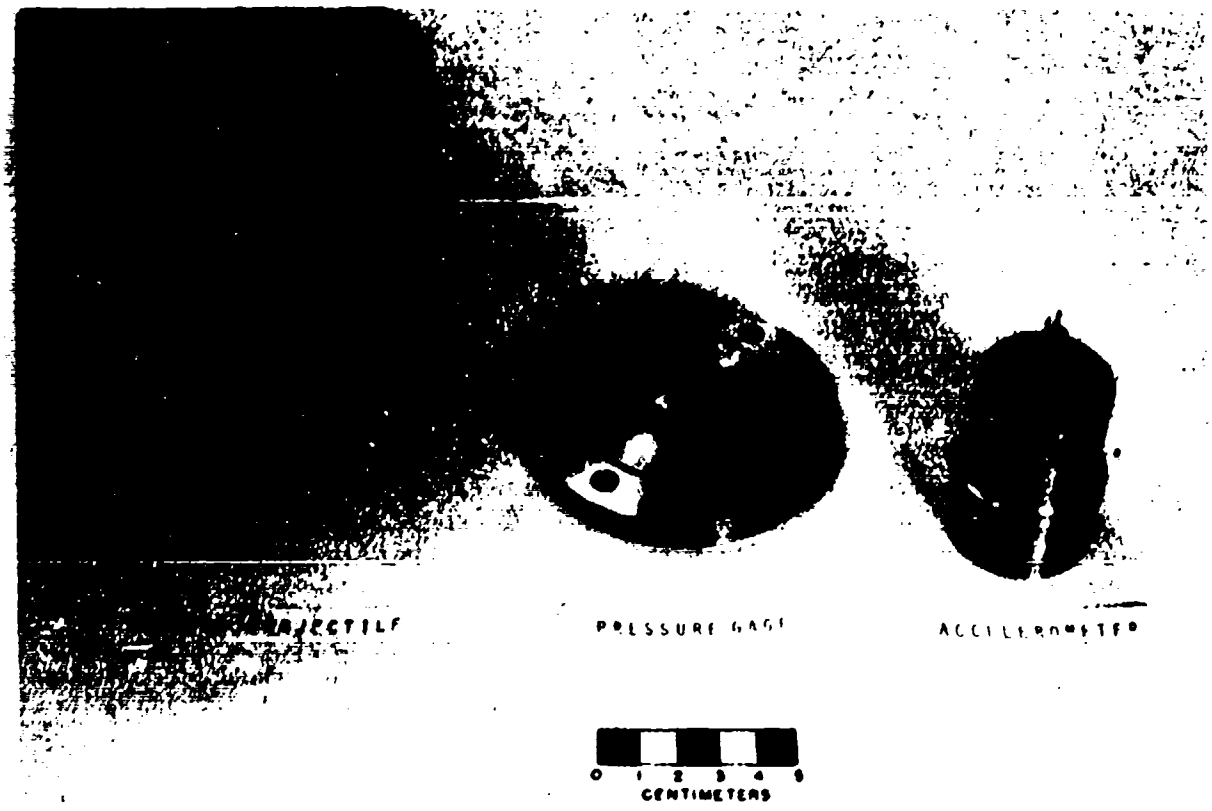

Figure 20. 155-mm, M101 Projectile Base Modification and Transducer Housing

seal against the propelling gases. After connecting the telemetry transmitting system to the transducer using stranded, teflon-coated, hook-up wire, the projectile is filled with an epoxy that has the same density as the high explosive that would normally fill the projectile. This is

accomplished through the projectile base and a small hole, tapped for a pipe plug, in the side wall of the projectile.

When there is a requirement to measure angular accelerations, additional accelerometers are added to this type experiment. An accelerometer to measure tangential acceleration, an accelerometer to measure radial acceleration, and their required constant current sources and VCOs are mounted in an enclosed metal box. The box is then assembled in the projectile (Figure 21) and held in place with machine screws. It is then electrically connected to the telemetry transmitting system and the projectile is filled with epoxy which keeps the box in place during firing.

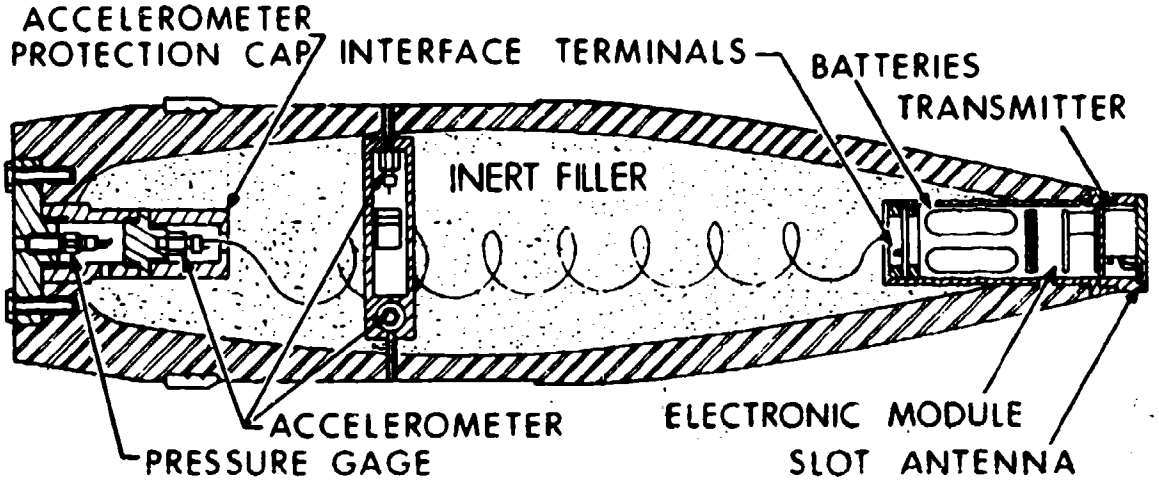

Figure 21. Instrumented Free-Flight 155-mm, M101 Projectile for Measuring Angular Acceleration

B. Instrumented/Recoverable 155-mm, M101 Projectiles

An instrumented, 155mm, M101 projectile modified for recovery in the LCSRS is presented as Figure 22. This projectile contains a telemetry transmitting system configured to measure base pressure, axial acceleration, and tangential acceleration. On some rounds it contained a pressure transducer that is not exposed to the propelling gases to measure the acceleration effect on the transducer. The water scoop is attached to the front with the transmitting antenna located in the center as shown in Figure 22. A drawing showing the modifications to the projectile and the location of the various components is presented as Figure 23. The water scoop, transducer housing, and telemetry transmitting system are designed to be easily assembled and disassembled so a projectile body, that had been launched and recovered, can be easily replaced. The base of the projectile is modified to accept a transducer housing similar to the free-flight rounds. The ogive is cut off 25.4 cm from the original front, and threaded to fasten the scoop. This length is removed to provide ample bearing surface to sustain the load of the scoop assembly during the launch acceleration. During final assembly, the rear section of the projectile is ballasted to the standard weight using lead wool and epoxy. Photographs of the projectile components and the partially assembled projectile are presented as Figure 24.

Figure 22. Instrumented/Recoverable 155-mm, M101 Projectile

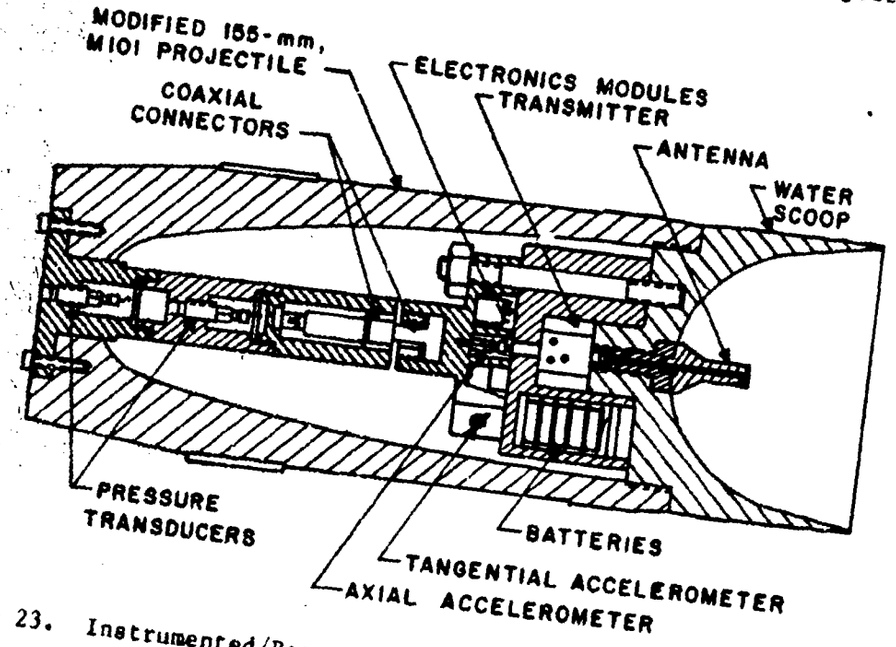

Figure 23. Instrumented/Recoverable 155-mm, M101 Projectile Modification

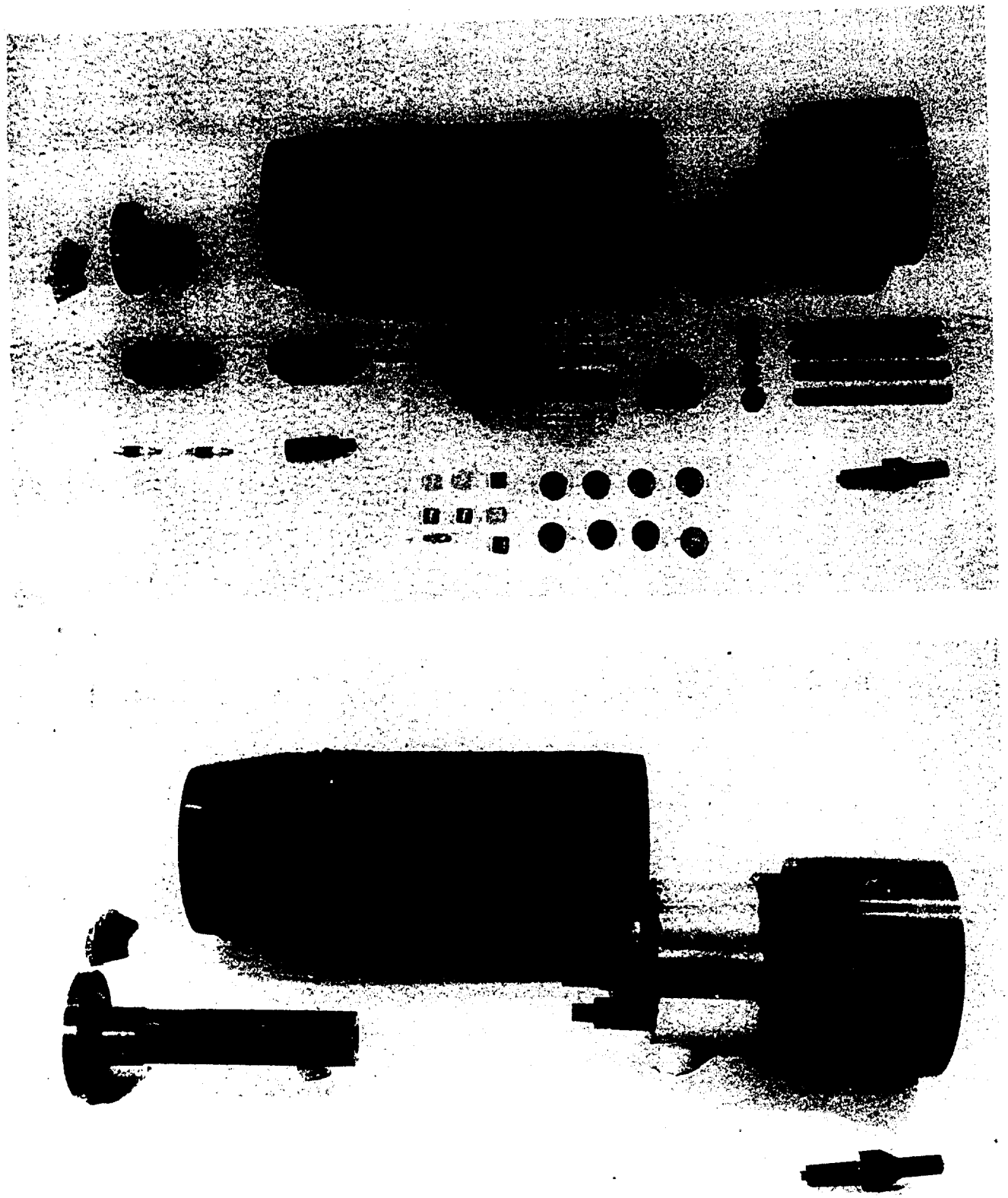

Figure 24. Instrumented/Recoverable 155-mm, M101 Projectile Components

The transducer housing is fabricated in sections so the transducers can be changed for subsequent rounds. The rear most section carries the base pressure transducer, the center section carries a cargo pressure transducer or an accelerometer, and the forward section carries the jacks of a two-conductor, coaxial connector for interfacing with the telemetry electronics. Interconnections within the transducer housing are made using teflon-coated wire through the wiring channels on the sides. After the connections are made, the wiring channels are filled with a rubber encapsulant (Dow Corning, 3120 RTV) and the transducer housing is covered with shrinkable tubing.

The scoop assembly is fastened together using four threaded studs. The battery housing carries the transmitter and eighteen B-250 cells for the power supply. This module also contains the test jacks for battery charging and system turn-on. All other electronic modules are contained in the telemetry carrier along with an axial accelerometer and a tangential accelerometer. The telemetry carrier also carries the plugs of the two-conductor, coaxial connector. The electronic modules are interconnected and cast in an epoxy.

After a structure failure, the projectile system was redesigned to eliminate weight from the scoop assembly. The battery housing was redesigned to carry B-50 cells for the power supply. The telemetry electronics were moved to the transducer housing by adding a section. The tangential accelerometers were attached to the wall of the projectile and were encapsulated by the epoxy used for ballast. A drawing of the redesigned projectile, showing the location of the various components, is presented as Figure 25.

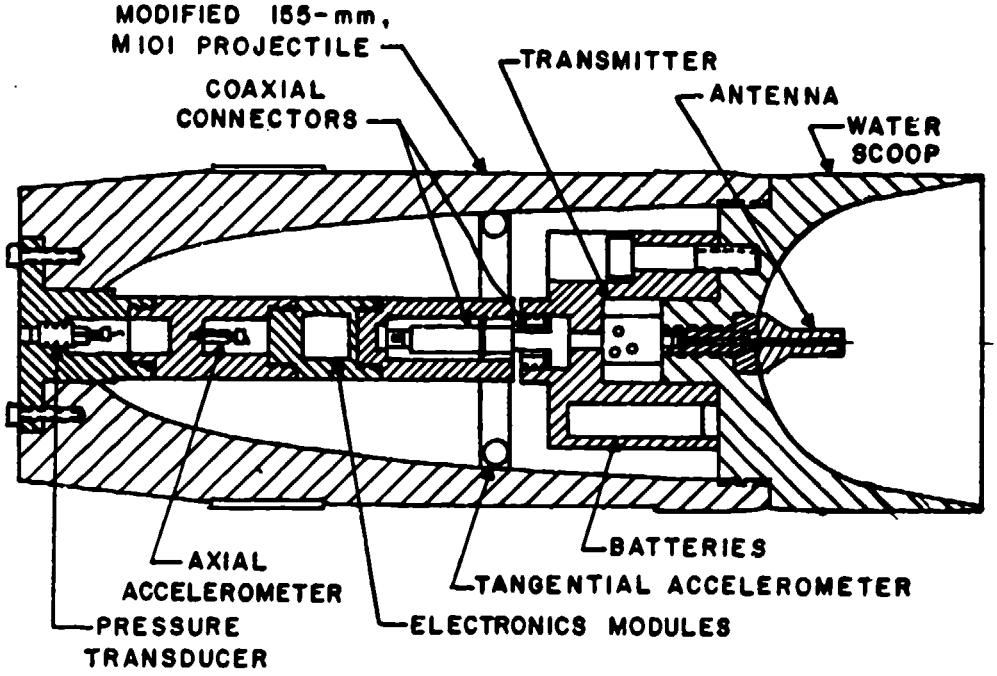

Figure 25. Redesigned 155-mm, M101 Recoverable Projectile

VIII. FIRING PROGRAMS

All firing programs are conducted at the Interior Ballistic Division, BRL Sandy Point Facility (Range 18). The data are received, recorded, and reduced using the on-site BALDAS system.

A photograph of the howitzer and the test setup, used for the free-flight projectiles, is presented as Figure 26. This photograph shows the position of the telemetry receiving antenna, a doppler radar, and the reflector used to reflect the doppler signal into the gun tube. The doppler radar is used as an independent measure of projectile displacement. Before firing, the gun tube is filled with nitrogen. A polyethylene diaphragm is taped across the muzzle as the projectile is readied for ramming. Nitrogen is admitted through a small hole in the polyethylene and allowed to purge the tube. The projectile is then rammed capturing a full tube of nitrogen. This is done to eliminate any oxygen in the tube that could react with the hot propelling gases that may precede the projectile due to incomplete obturation. It has been determined that these reactions can attenuate the RF signals from the telemetry system and

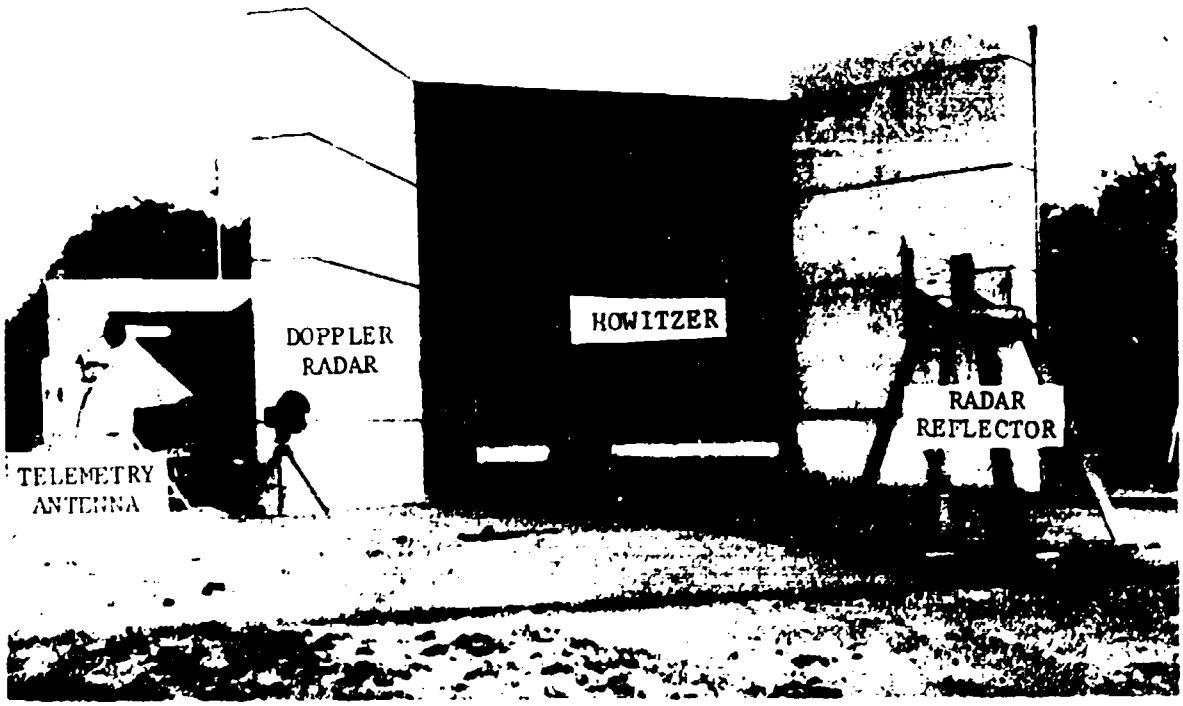

Figure 26. 155-mm Howitzer and Test Setup

the doppler radar. The telemetry link is established with each projectile at turn-on prior to loading. This link is maintained during the loading process, during a warm-up period, and into the event.

A. Free-Flight Projectiles

Five projectiles, of the type shown in Figure 19, were fired from a 155-mm, M185 special howitzer tube using M203E1, Zone 8 propelling charges. The first two projectiles fired did not have the accelerometer protection cap (Figure 19). This caused distortion of the acceleration data due to the mechanical loading of the accelerometer structure by the inert fill. The pressure data were received during the entire in-tube travel. The addition of the cap for subsequent rounds solved the mechanical loading problem. Of the other projectiles fired, two lost signals near peak pressure. It is suspected that this was caused by an open circuit in the battery pack. The other projectile transmitted data during the entire interior ballistic cycle.

Four projectiles, of the type shown in Figure 21, were fired from a 155-mm, M199 howitzer tube using experimental charges that had chamber pressure magnitudes near that of a Zone 8. Two of these rounds transmitted during the entire interior ballistic trajectory, one lost transmission just after peak pressure, and one had a 5 millisecond drop-out during peak pressure.

Unfortunately, the free-flight rounds impacted in the water and were not recoverable. Therefore, the failure modes that existed could not be determined.

B. Soft Recovery of Instrumented Projectiles

The construction of a telemetry transmitting system is expensive. Therefore, it is desirable to recover the projectile so the instrumentation package can be reused. It is also desirable to recover the instrumentation so the transducers and transmitting system can be re-calibrated after being exposed to the launch environment. At the BRL, a LCSRS[10 12] is in operation.

A schematic showing the LCSRS principle of operation is presented as Figure 27. Soft recovery of the projectile is achieved by attaching a water scoop to the test projectile and firing it into a water trough, inclined at a small angle to present an ever-increasing depth of water to the advancing projectile. The momentum of the projectile is transferred to the water ejected forward by the scoop. The water scoop is designed to have the necessary interior contour to eject the impacted water forward. The water enters onto a conical surface of revolution that transitions into a spherical surface of revolution.

The LCSRS apparatus is presented as Figure 28. The projectile is launched through a band cutter, attached to the muzzle, that removes the protruding portion of the rotating band. This allows the tolerance between the projectile body and the LCSRS to be much tighter than if the rotating band were left on. This prevents the rotating band from acting as a fulcrum, thus minimizing balloting during recovery. After passing through

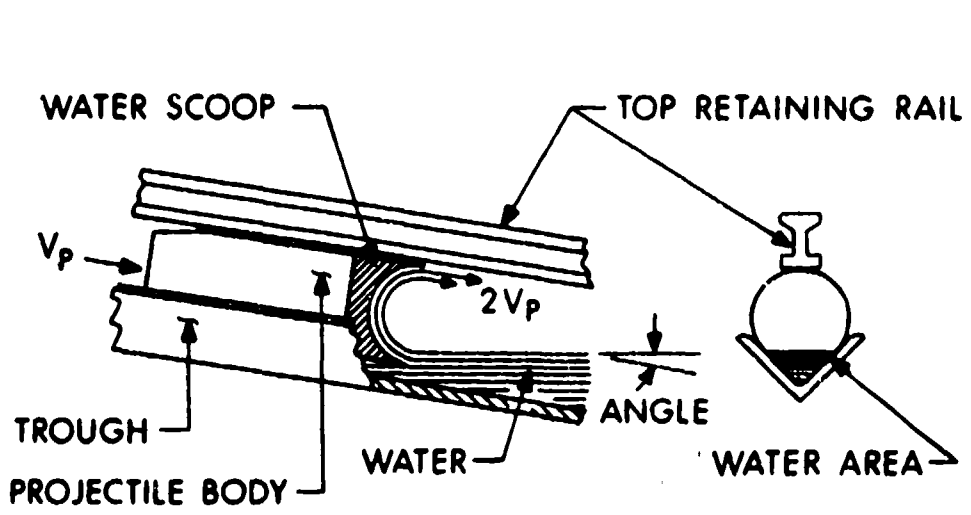

Figure 27. Large Caliber Soft Recovery System, Principle of Operation

Figure 28. Large Caliber Soft Recovery System

the band cutter, the projectile passes through an entrance cone assembly and into the recovery system proper, which consists of the bottom water trough and the overhead, inverted retaining crane rail. The whole assembly is angled slightly by means of five pairs of jacks that cause the projectile to be exposed to the increasing depth of water. The terminal end of the LCSRS is equipped with a specially designed shock absorber to absorb any residual momentum when the projectile has traveled the entire length of the system. The 60-metre length of the system is sufficient to stop the projectile with a maximum deceleration of less than ten percent of the maximum launch acceleration.

C. Recoverable Projectiles

The projectile system, as configured in Figure 23, was fired from an 155-mm, M185 howitzer on five occasions, changing the projectile body after each round. Since different zone propelling charges were used, the transducers were changed as required so a transducer with the range of the predicted measurand magnitudes was used. The propelling charges used were M3A1, Zones 1, 3, and 5 and M4A2, Zone 7. Removing the water scoop assembly required machining of the projectile since the torque experienced during launch tightened the threads. The fifth round was indexed on the projectile body and the scoop to determine their relative angular displacement during launch and recovery. The threads on this round tightened by 24 degrees, corresponding to an 0.21-mm linear distance, causing an interference fit. It was determined on subsequent rounds that eliminating the antiseize lubricant (Hi-Temp, C5-A), used on the threads during assembly, permitted scoop removal without machining.

The telemetry link, with each of the projectiles, was maintained during the entire interior ballistic cycle for all rounds except the fifth. This round lost signal at about one millisecond past maximum pressure. After recovery, each projectile was refitted with a new antenna and the system was turned on and evaluated. All measurable parameters (VCO frequencies, transmitter frequency, battery voltage, and transducer quiescent points) on all five rounds were within the pre-launch specifications except for fifth, that appeared that the constant current source to the transducers in the rear section had an open circuit. The transmitted base pressure and acceleration data for all rounds appeared normal except for a 1.5 millisecond dropout of the pressure near peak on the third round. This was determined to be caused by a bent jack on the coaxial connector that was not properly engaged. The tangential acceleration data had large ringing due to structural vibration and did not represent the tangential acceleration of the projectile, but rather that of the scoop because of the relative angular displacement during launch.

The failure on the fifth round was caused by a structural failure in the projectile system. All four bolts that held the scoop assembly together failed just behind the scoop rear surface. The battery housing and the telemetry carrier moved to the rear, disconnecting the antenna. This accounted for the signal loss. The coaxial connector was sheared because of the motion, causing the electrical connection to the transducers to open. On recovery, the telemetry carrier and battery housing returned to their proper position which accounted for the post-launch evaluation results. After disassembly the telemetry system was reconnected and evaluated. All measurable parameters were then at the pre-launch specifications.

The redesigned projectile system (Figure 25) was fired on six occasions from the M185 howitzer. The propelling charges used were M3A1, Zone 5; M4A2, Zone 7; and M119, Zone 8. The telemetry link for Zones 5 and 7 rounds were maintained until the end of the interior ballistic cycle. The transmitted base pressure and axial acceleration data for these rounds appeared normal. The tangential acceleration data showed ringing and on

some rounds was distorted because the accelerometer mounting block had broken loose from the projectile wall. The Zone 8 round lost signal near peak pressure. The acceleration data started to ring at a frequency of 8 kHz (the response of the data channel) at the start of motion. It was noisy during the acceleration and dropped out at seven milliseconds after start of motion. The RF signal for this round, as indicated by the incidental frequency modulated output, was maintained for ten milliseconds after loss of the subcarriers. The loss of the subcarrier could have been caused by structural failure. On recovery, the water scoop and battery housing had fractured along a centerline of the structure. Although the water scoop was in two pieces, it remained attached to the projectile and the recovery process was normal with only superficial damage to the LCSRS. The cause of the structural failure was not determined, but it was suspected that repeated impulse loading during the eleven launch and recovery cycles was a contributing factor.

IX. RESULTS AND DATA REDUCTION

Representative data of interior ballistic performance are presented for both the free-flight and recoverable projectiles. The data are plotted by the BALDAS after being reduced and manipulated using the interactive software. It is presented in a form useful for evaluating the interior ballistic performance or as an input to an interior ballistic model.

A. Measured Projectile Acceleration

The acceleration data are affected by the structural vibration of the transducer mounting. This is evident by comparing the acceleration from two accelerometers on a recoverable round (Figure 23) that were located in the scoop assembly and the transducer housing. As shown in Figure 29, both transducers produce essentially the same gross acceleration but the vibrations or ringing are at different frequencies. Loss of data was due to the structure failure.

Since the data are required to be manipulated with that of the pressure channel, it was desirable to remove the vibration and/or noise component. Two techniques are used to accomplish this. Figure 30 shows the results obtained from a free-flight round using a smoothing routine on the BALDAS. This is a moving arc polynomial routine that worked well on the free-flight rounds where the unwanted signal components are at a relative high frequency. On the recoverable rounds, the vibrating frequencies are lower and the smoothing routine did not remove the vibrating component. Therefore, a filtering technique is used. The data are played back from the analog tape recorder through a low pass analog filter into the BALDAS A/DC. A cutoff frequency is selected that eliminates the undesired signal component. Figure 31 is a comparison of the unfiltered and filtered acceleration. The data were recorded at 120 inches per second (ips) and played back at 7 1/2 ips. The cut-off frequency was set for 93.8 Hz that is an effective 1500 Hz real time frequency.

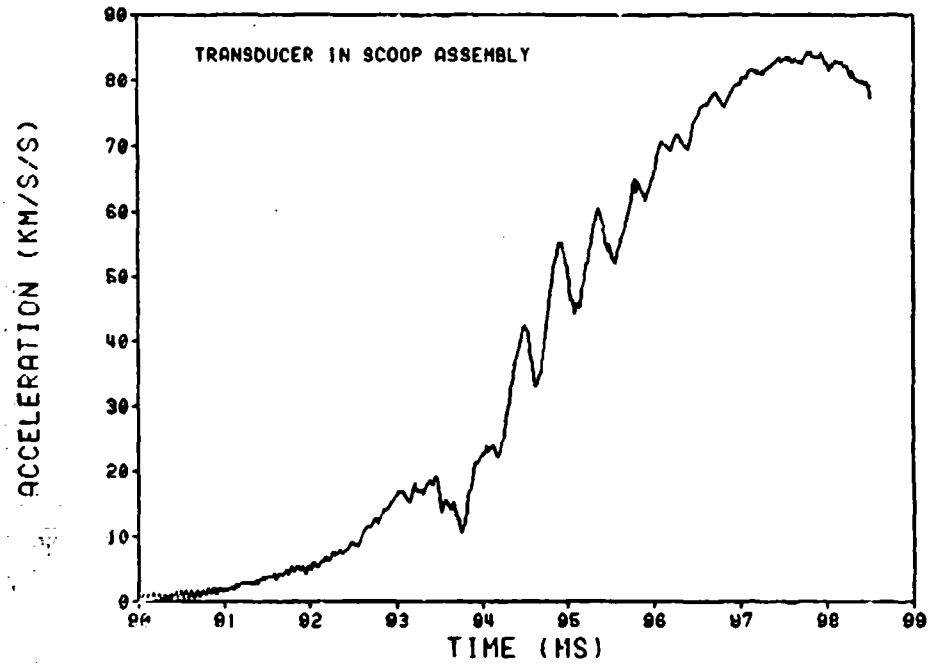

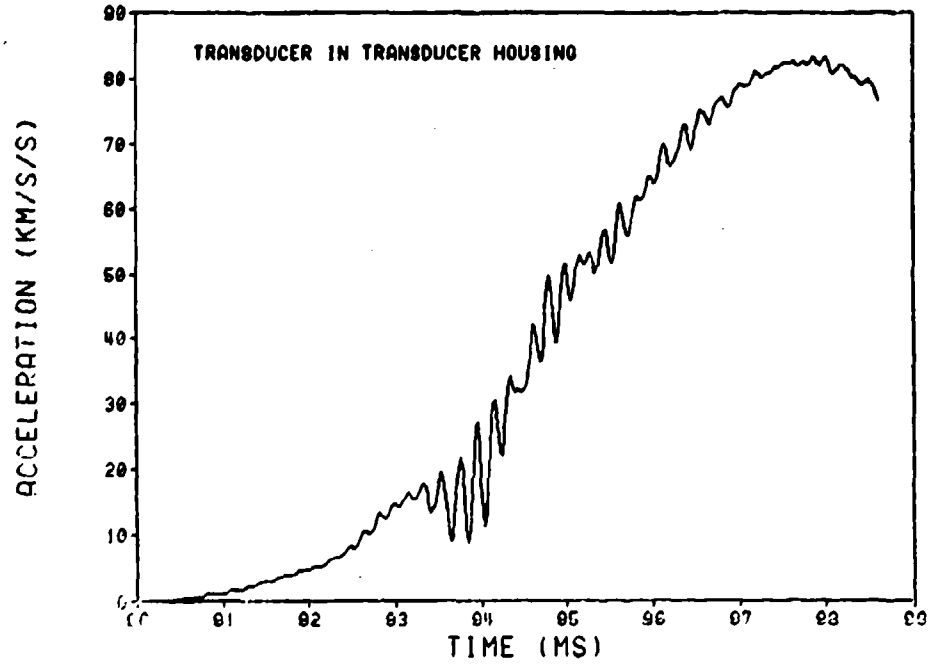

Figure 29. Acceleration versus Time, M4A2, Zone 7 Propelling Charge, LCSRS Projectile

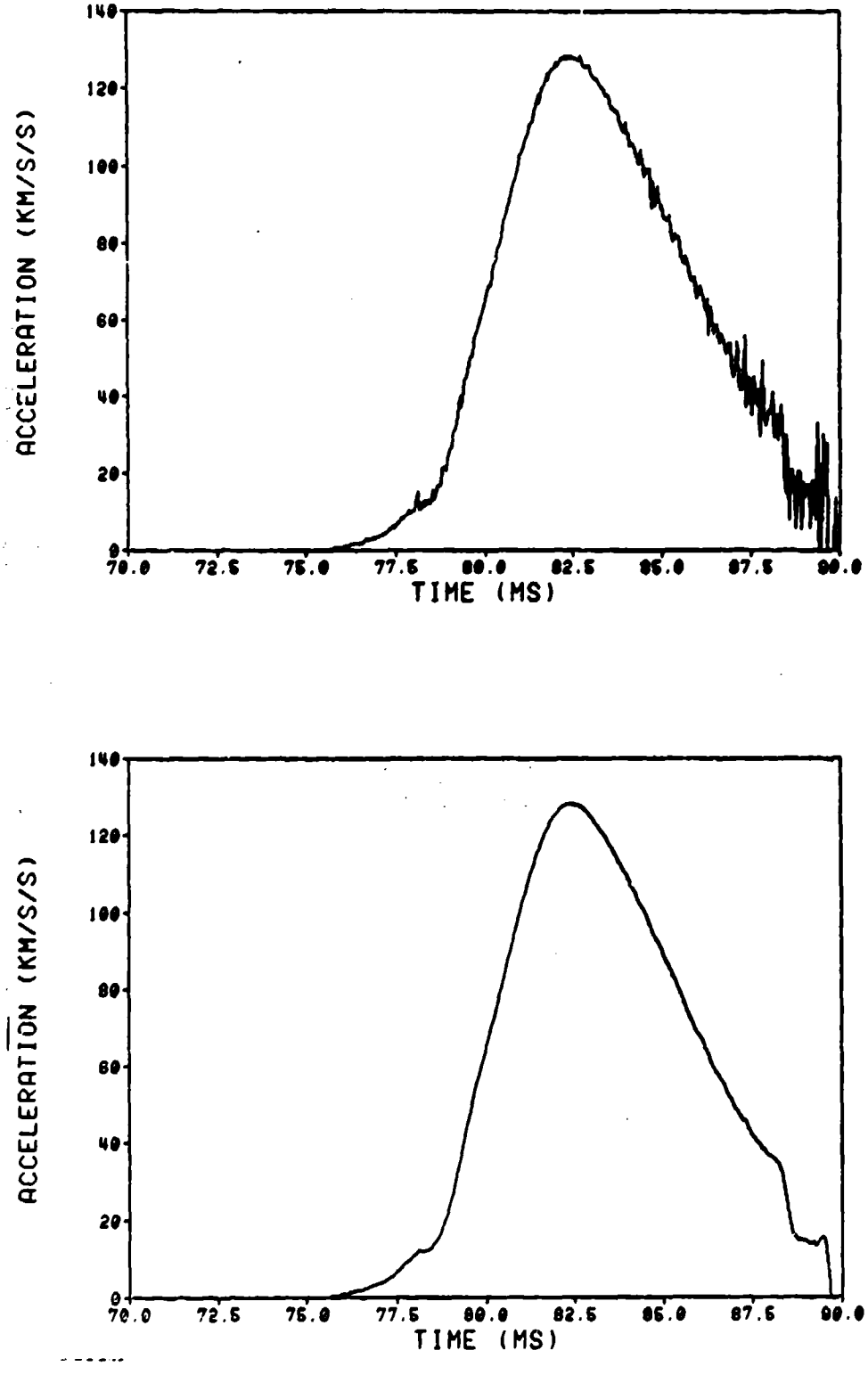

Figure 30. Acceleration versus Time, M203E1, Zone 8 Propelling Charge, Free-Flight Projectile

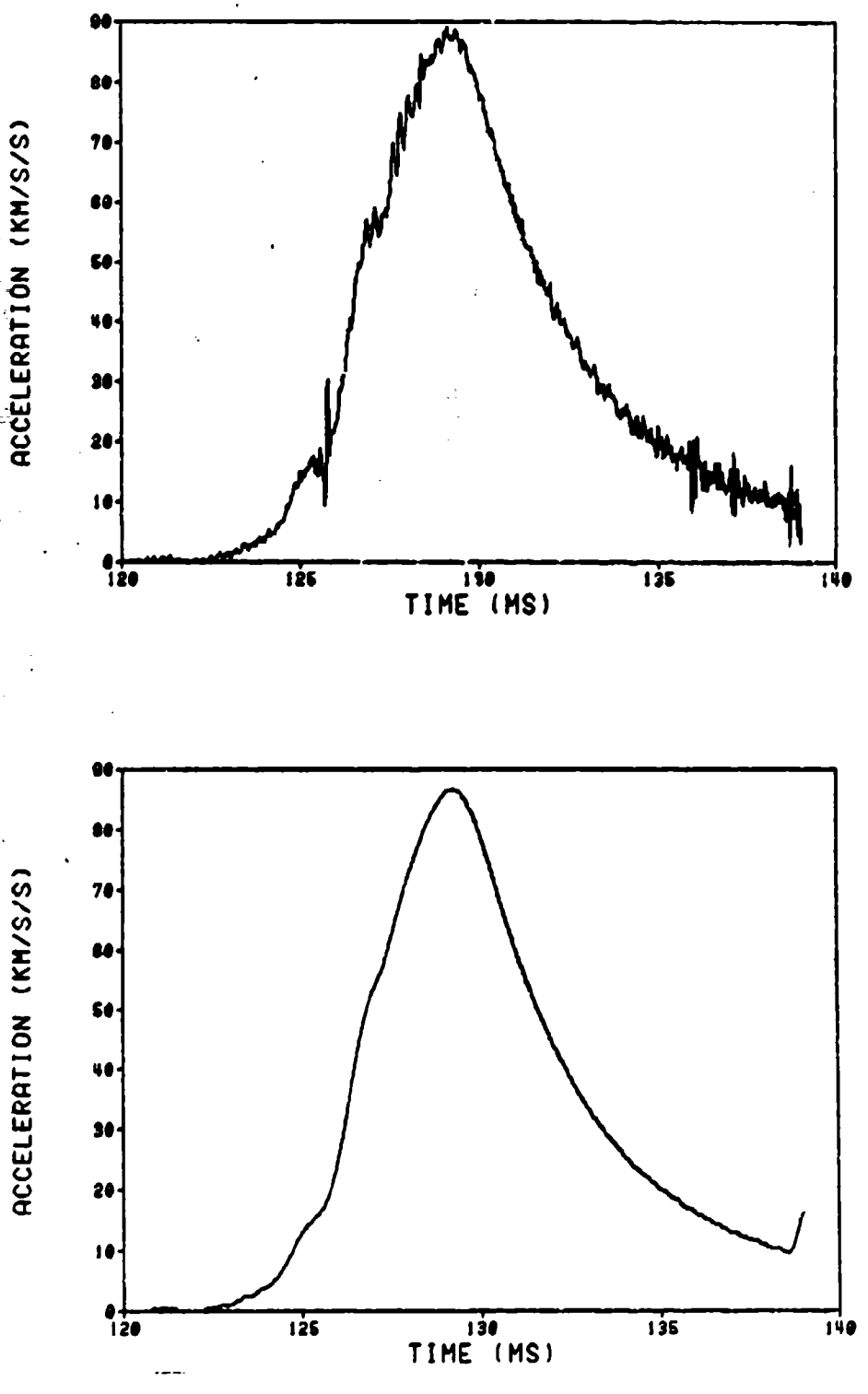

Figure 31. Acceleration versus Time, M4A2, Zone 7 Propelling Charge, LCSRS Projectile

The acceleration data are used to determine the interior ballistic trajectories. The velocity is determined by integrating the acceleration and the displacement is determined by integration of the velocity. Since there is not an available in-house calibration facility for accelerometers, the manufacturer's calibration constant can not be verified. When the interior ballistic trajectories are plotted, the displacements are compared with known displacement points acquired from the projectile rotating band passage across pressure transducer ports located in the gun tube side wall. In all cases, the accelerometer acquired displacement data were found to be lower. It is believed that the pressure port displacements are more accurate since the pressure port locations are well defined as are the times of pressure rise due to band passage. Therefore, the acceleration data are corrected by multiplying by a constant that gives the best fit of the displacement curve through the points acquired by the pressure port passage. The required correction factor varied from transducer to transducer with a range of 1.012 to 1.12. Figures 32 through 36 are interior ballistic trajectories for rounds fired at various zones, obtained using this correction/calibration technique.

B. Measured Base Pressure

Pressures measurements from various zone propelling charges are presented as Figures 37 through 41. The spindle and forward chamber pressures are hard wire data recorded from Kistler, Model 607 pressure transducers. Since the base pressure data are manipulated with the measured acceleration, they are both smoothed or filtered in a similar manner. Cargo pressure transducers, not exposed to the propelling gases, on several rounds did not have a significant output caused by the launch acceleration and vibration environment.

C. Resistive Pressure Profile

Applying Newton's Second Law, the axial forces acting on the projectile are defined by the equation:

$$P_b A - f = ma \qquad (3)$$

where: P_b = Base Pressure

A = Cross-Sectional Area of the Tube

f = Frictional Forces

m = Mass of the Projectile

a = Projectile Acceleration

The frictional forces include the engraving forces of the rotating band, the sliding friction for the projectile/tube, and the pressure buildup ahead of the projectile due to the velocity. This force balance equation is rearranged to make each term have units of pressure as follows:

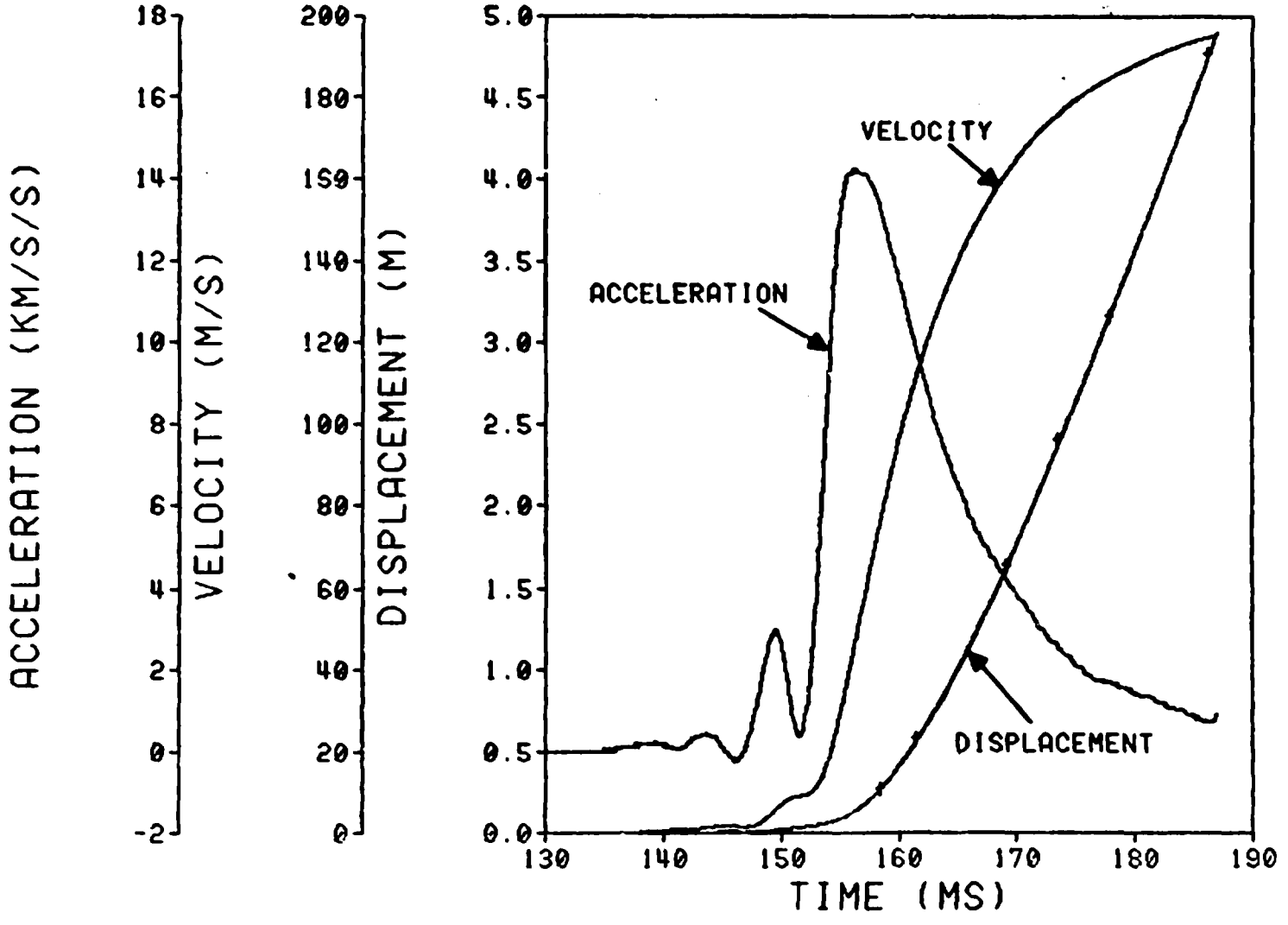

Figure 32. Interior Ballistic Trajectory, M3A1, Zone 1 Propelling Charge, LCSRS Projectile

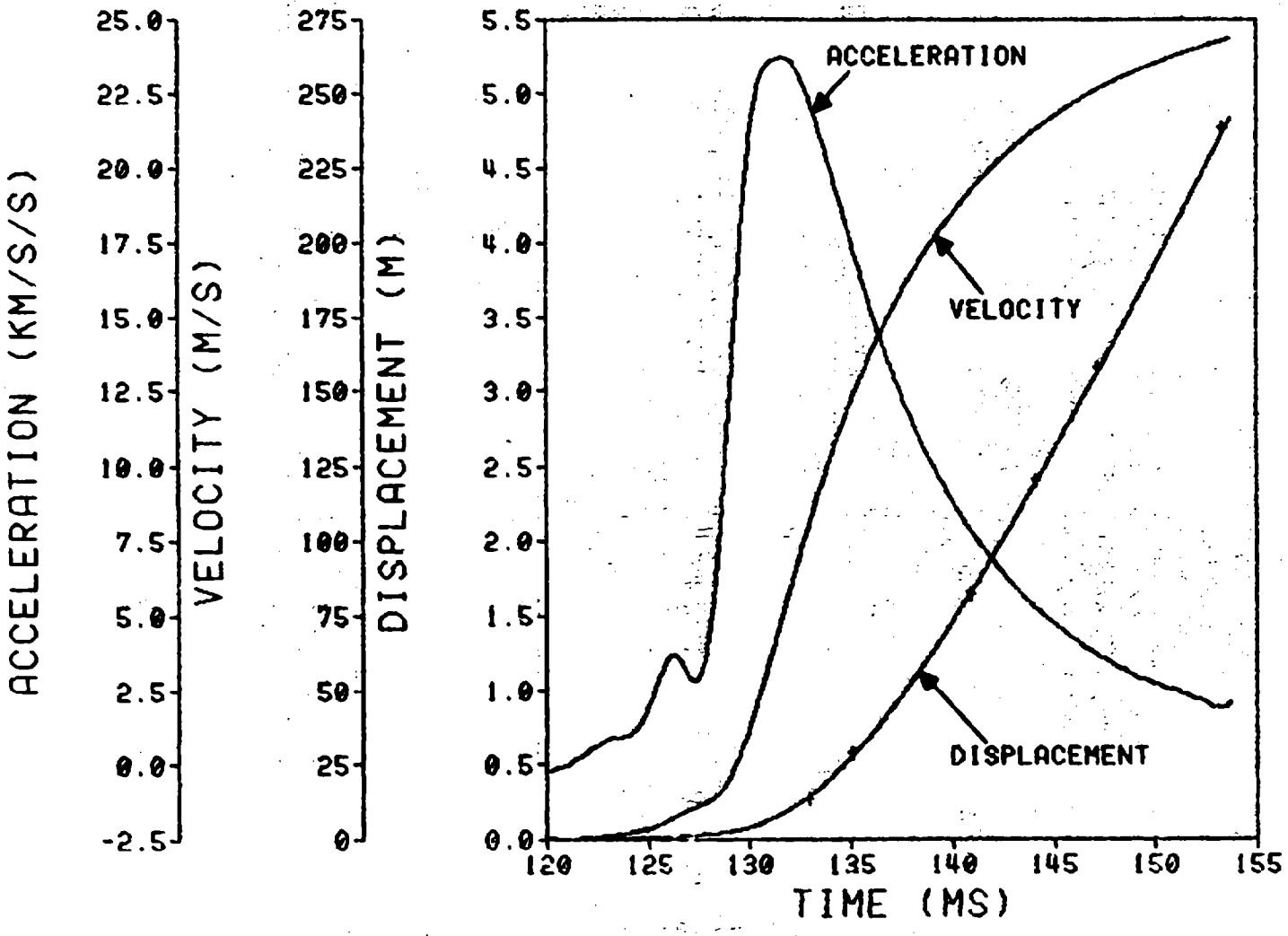

Figure 33. Interior Ballistic Trajectory, M3A1, Zone 3 Propelling Charge, LCSRS Projectile

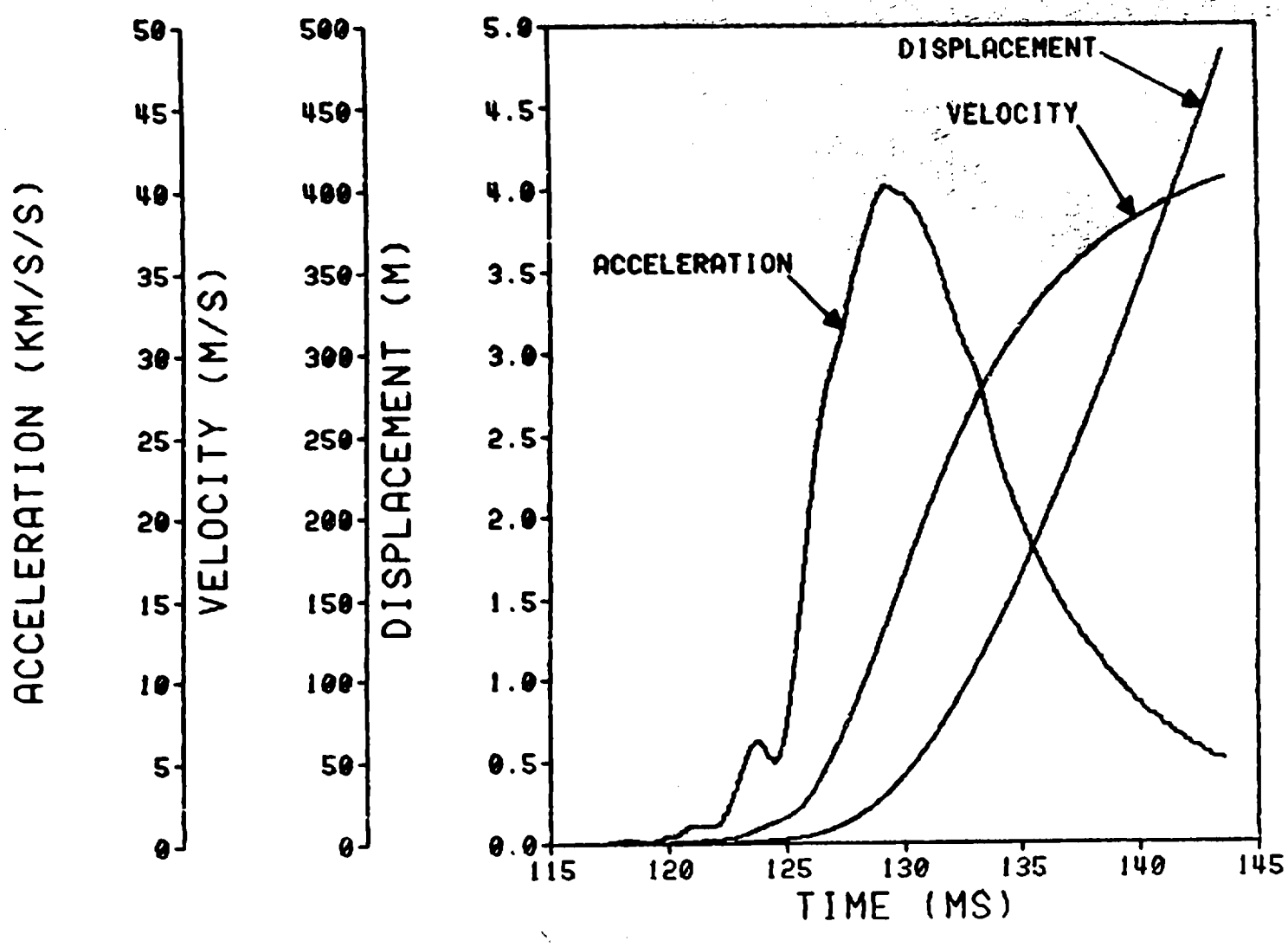

Figure 34. Interior Ballistic Trajectory, M3A1, Zone 5 Propelling Charge, LCSRS Projectile

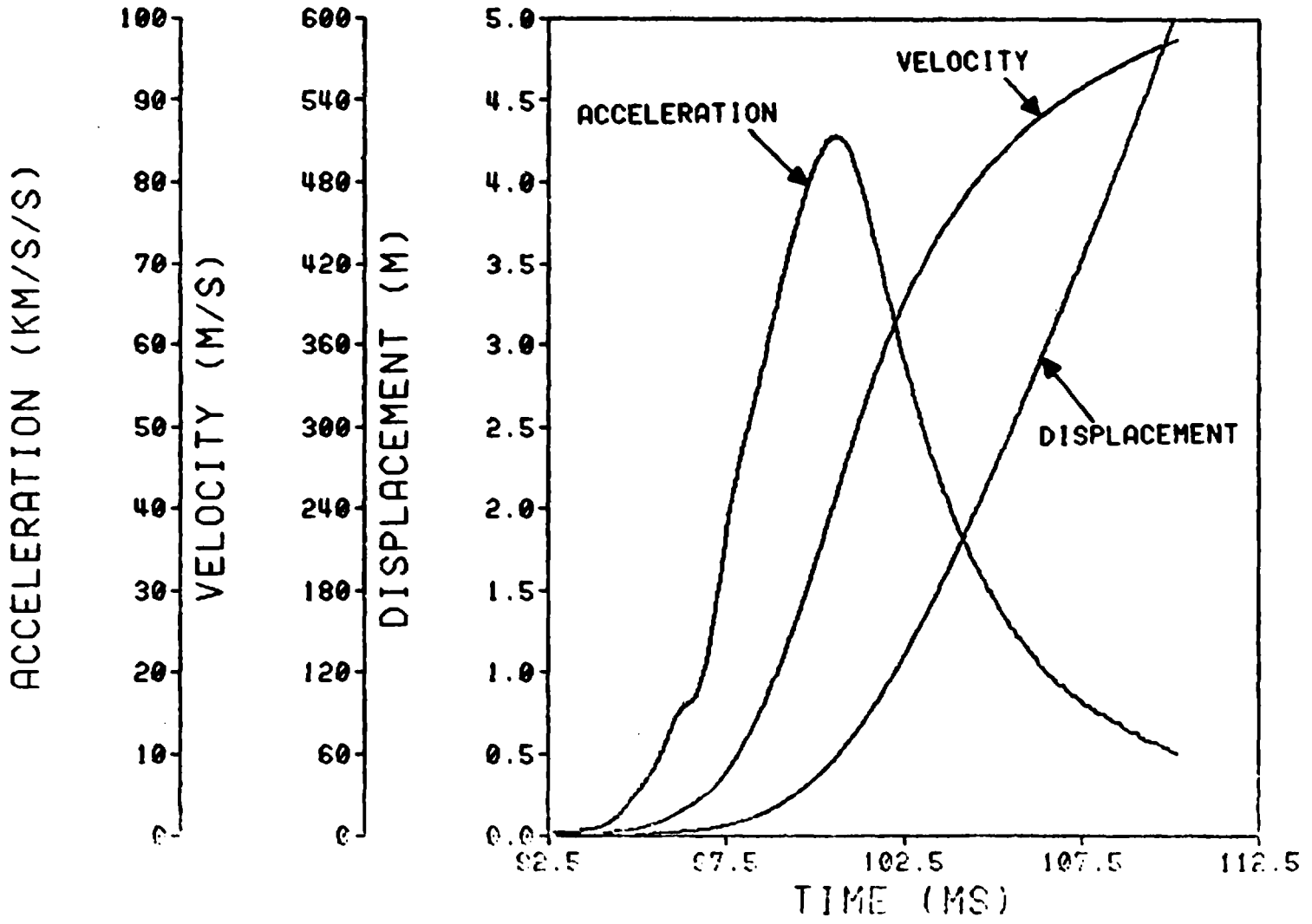

Figure 35. Interior Ballistic Trajectory, M4A2, Zone 7 Propelling Charge, LCSRS Projectile

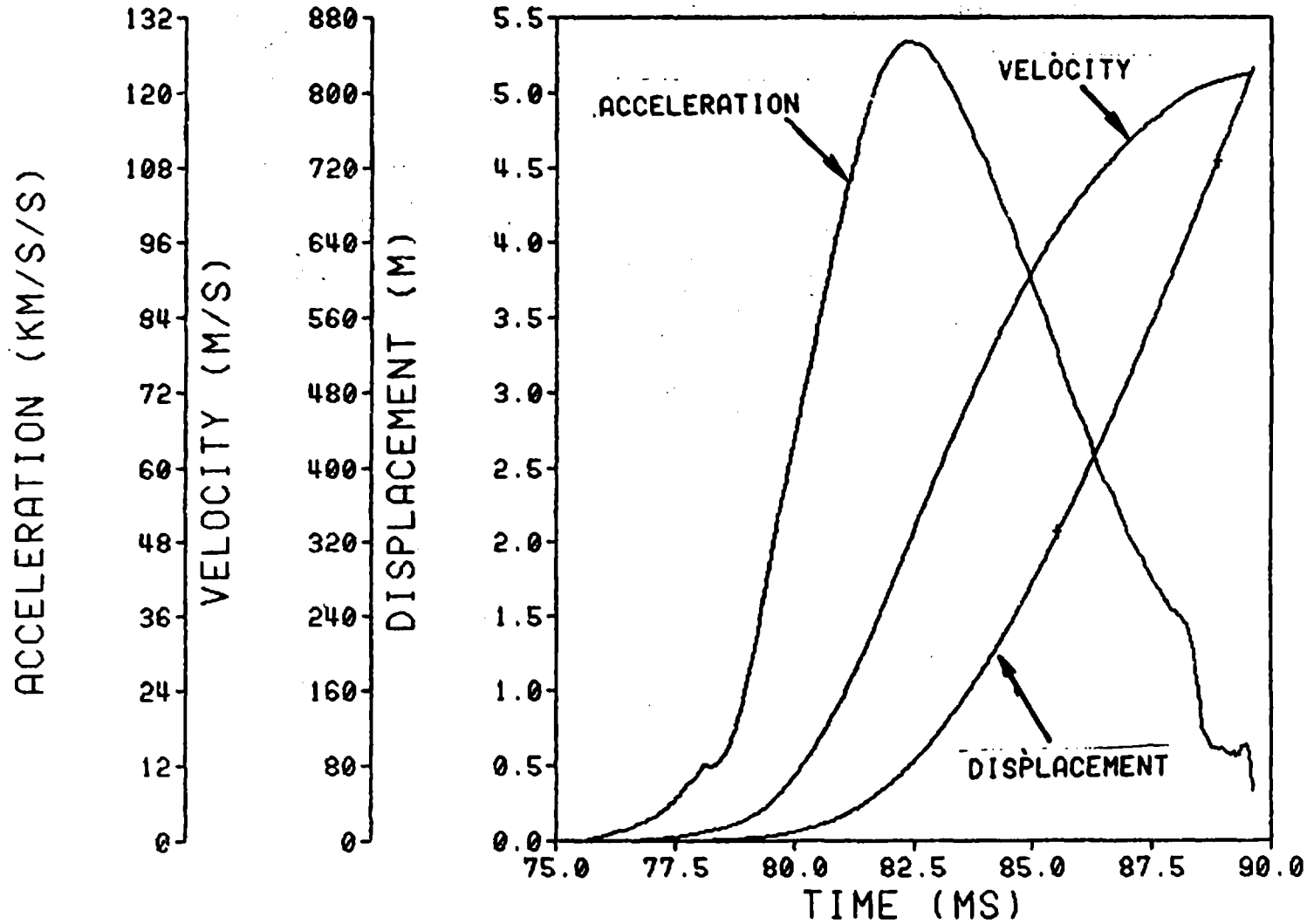

Figure 36. Interior Ballistic Trajectory, M203E1, Zone 8 Propelling Charge, Free-Flight Projectile

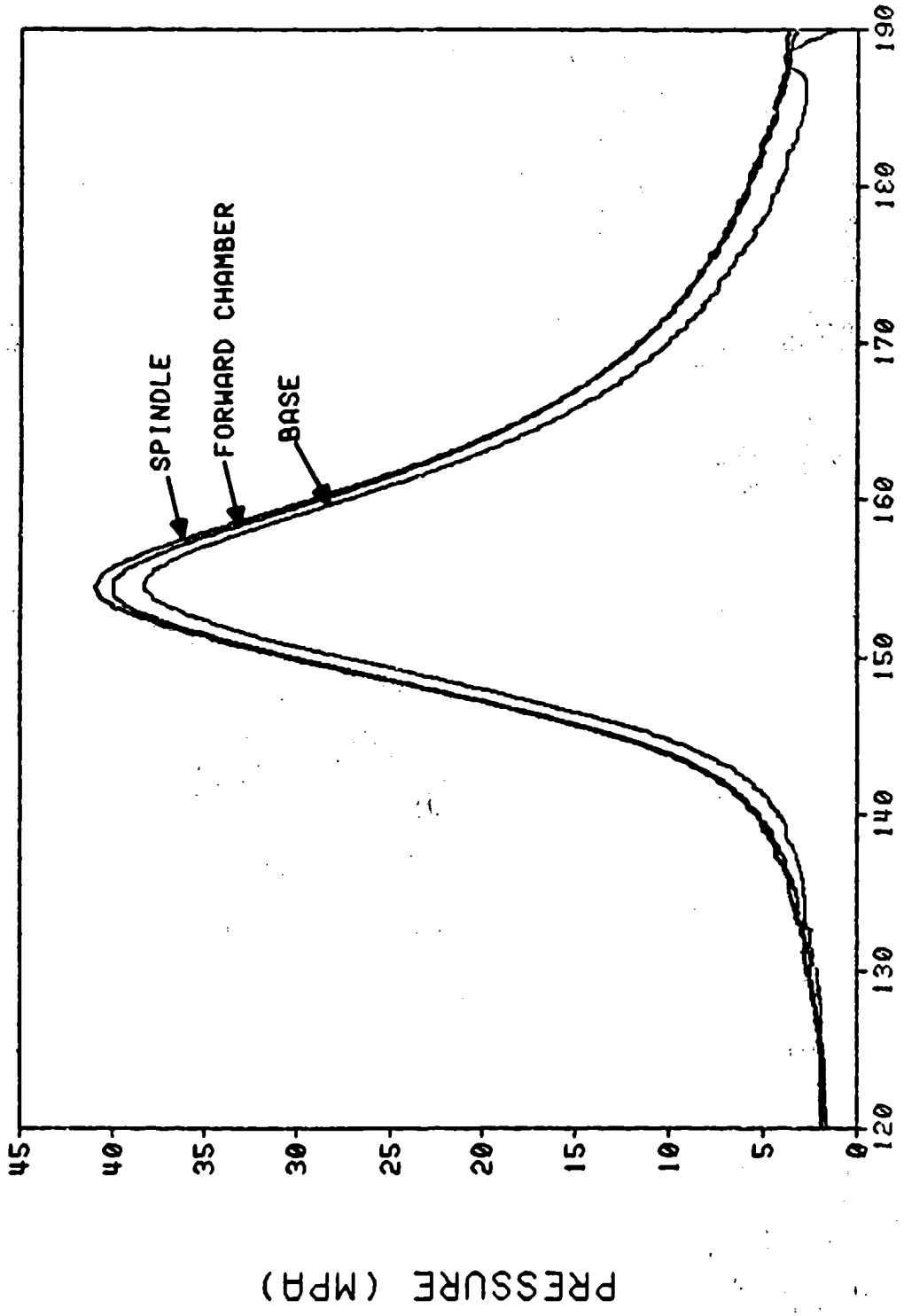

Figure 37. Pressure versus Time, M3A1, Zone 1 Propelling Charge, LCSKS Projectile

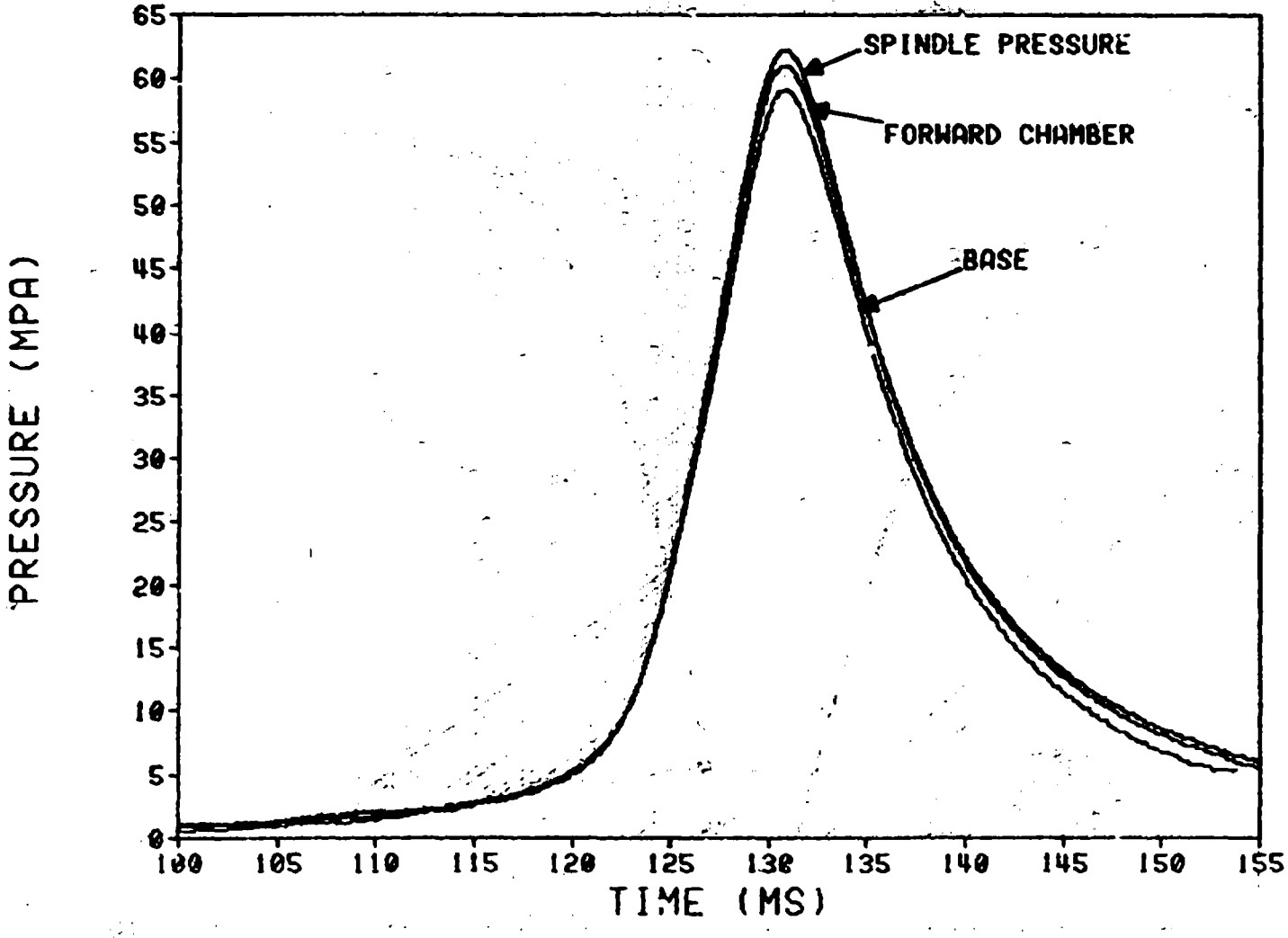

Figure 38. Pressure versus Time, M3A1, Zone 3 Propelling Charge, LCSRS Projectile

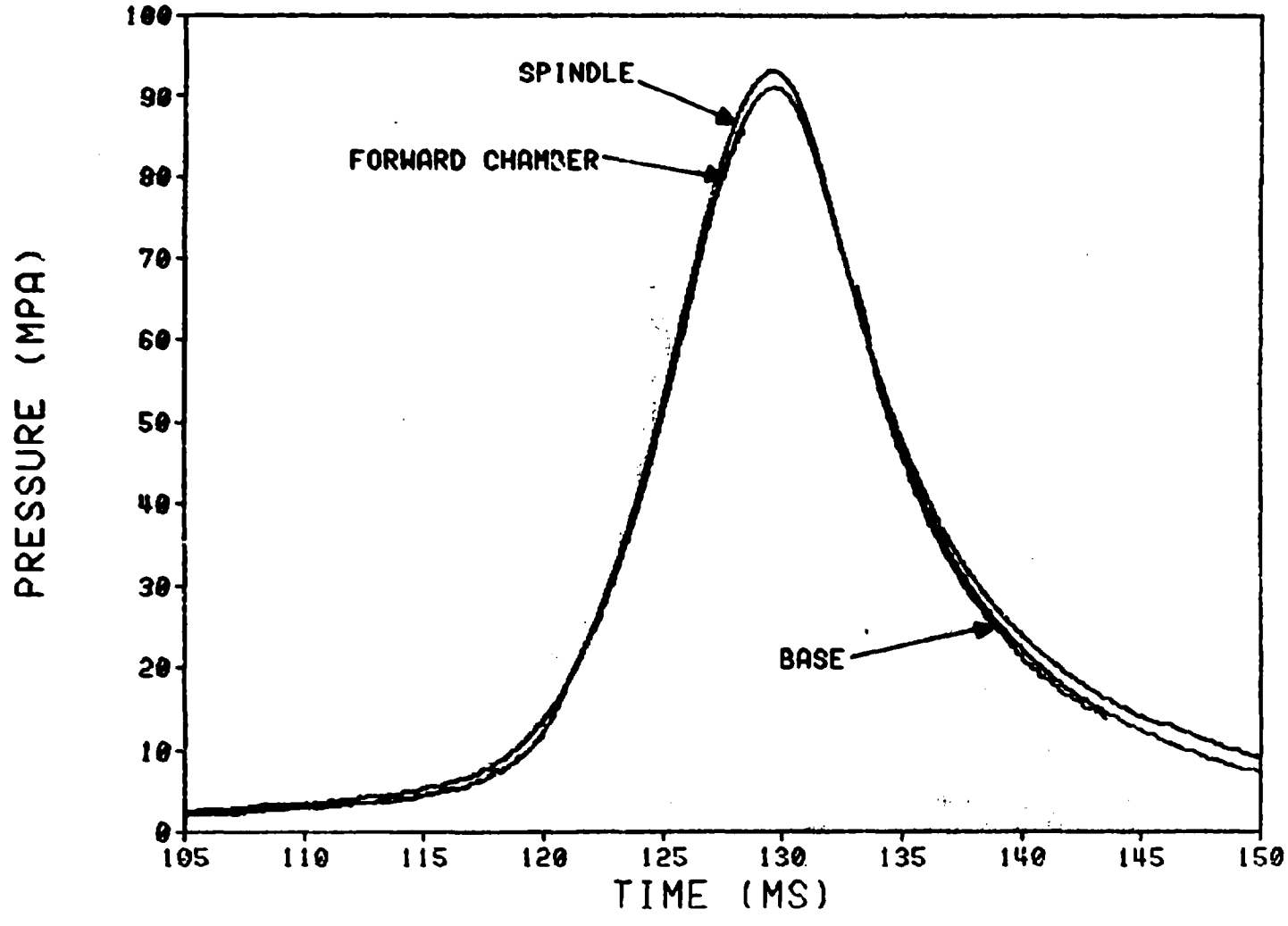

Figure 39. Pressure versus Time, M3A1, Zone 5 Propelling Charge, LCSRS Projectile

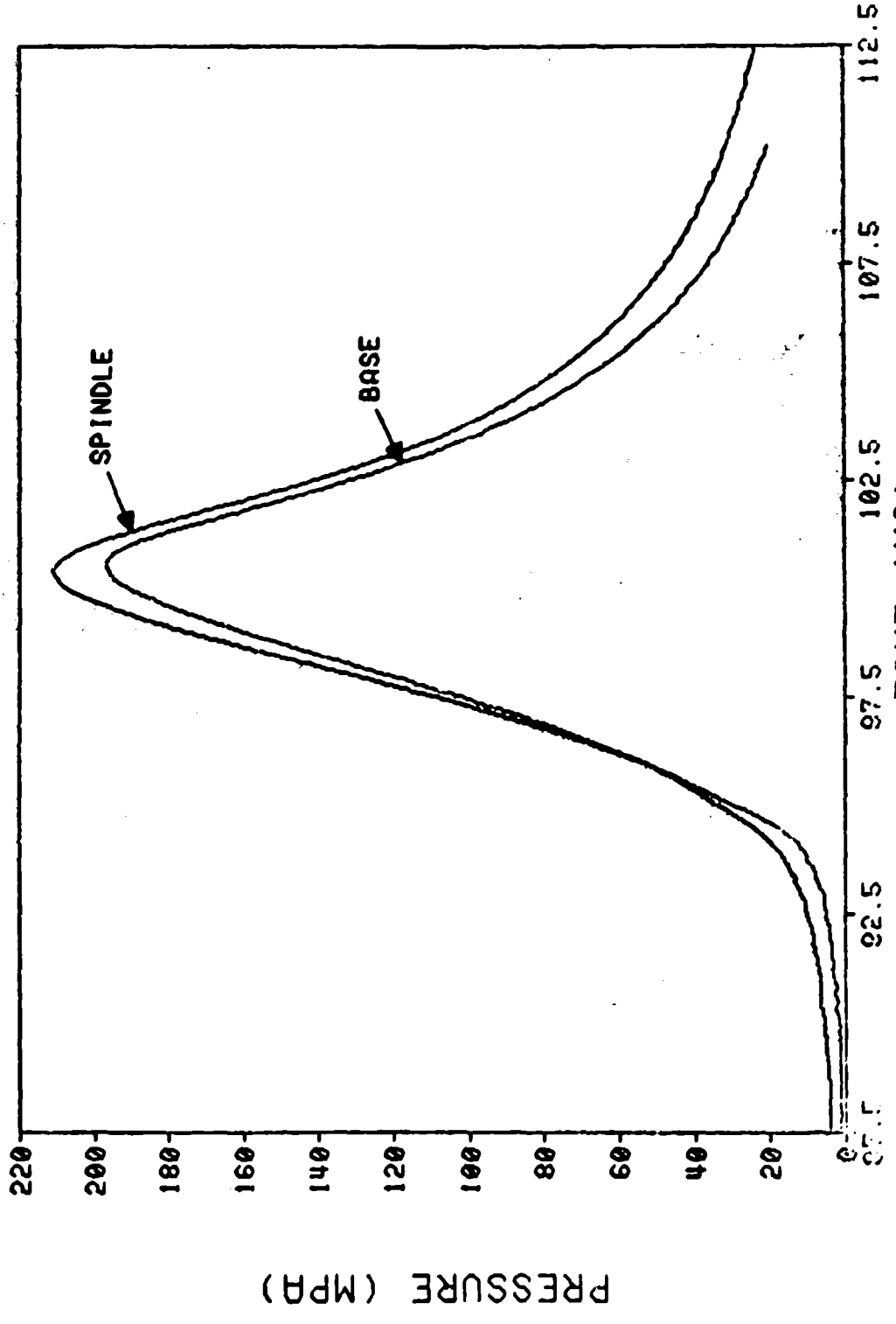

Figure 40. Pressure versus Time, M42, Zone 7 Propelling Charge, LCSRS Projectile

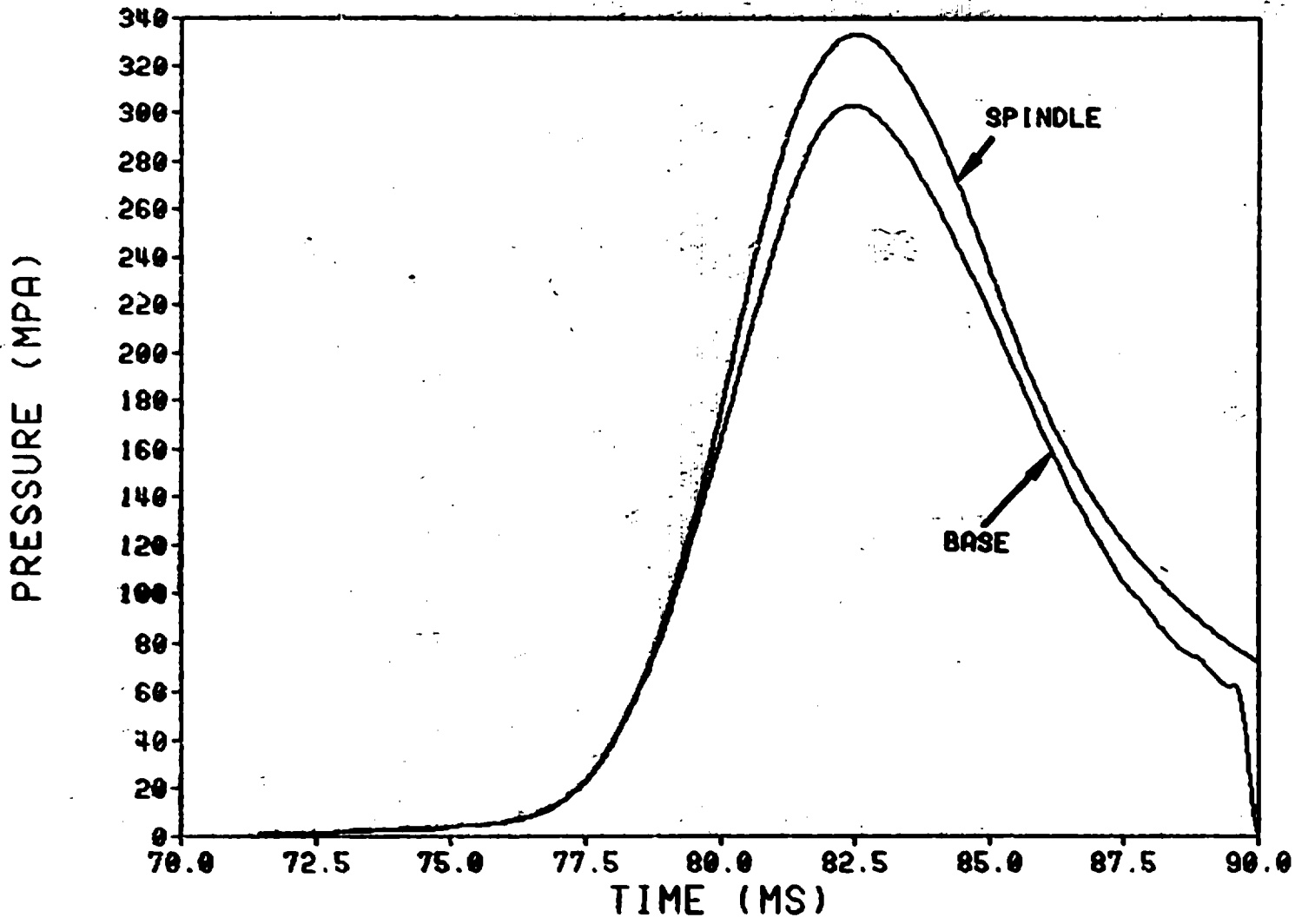

Figure 41. Pressure versus Time, M203E1, Zone 8 Propelling Charge, Free-Flight Projectile

$$P_r = P_b - ma/A \quad (4)$$

where: $P_r = f/A$ = Resistive Pressure

For the 155-mm, M101 projectile weight (422.6 newtons) and the tube cross-sectional area (0.01914 square metres), the relationship for determining the resistive pressure is:

$$P_r = P_b - (2.2516)\, a$$

where pressure is in megapascals and acceleration is in kilometre/second/second. The resistive pressure is then determined by multiplying the measured acceleration by the constant and subtracting it from the base pressure. This manipulation is easily accomplished using the BALDAS data reduction routines. A plot of the three terms of the force balance equation for various zone propelling charges are presented as Figures 42 through 46. The resistive pressure as a function of displacement for the engraving region for several zone propelling charges are presented as Figures 47 through 51. The displacements are acquired from the previously determined interior ballistic trajectory.

D. Angular Acceleration Measurements

Tangential acceleration measurements are made using accelerometers similar to the ones used for the axial measurements. They are orientated so their sensitive axis is on a tangent and the center of gravity of the seismic mass is located on a radius of the projectile. The purpose of this measurement is to determine the torsional impulse during the rotating band engraving.[23] [24] [25] This measurement was first added to recoverable rounds, but unfortunately adequate consideration was not given to the mounting structure for the accelerometer. The accelerometers were located on the

---

[23] A.E. Schmidlin, "Torsional Impulse In Gun Launched Projectiles, "ARLCD-TR-80037, Large Caliber Weapons System Laboratory, USA ARRADCOM, Dover, NJ, March 1981.

[24] Minutes of Meeting, "Measurements of Torsional Impulse Using In-Bore Telemeter," Program Manager/Cannon Launched Weapon Systems, ARRADCOM, Dover, NJ, 5 March 1980

[25] Minutes of Meeting, "Internal Ballistics Characterization Briefing," Project Manager for Nuclear Munitions, ARRADCOM, Dover, NJ, 28 April 1981.

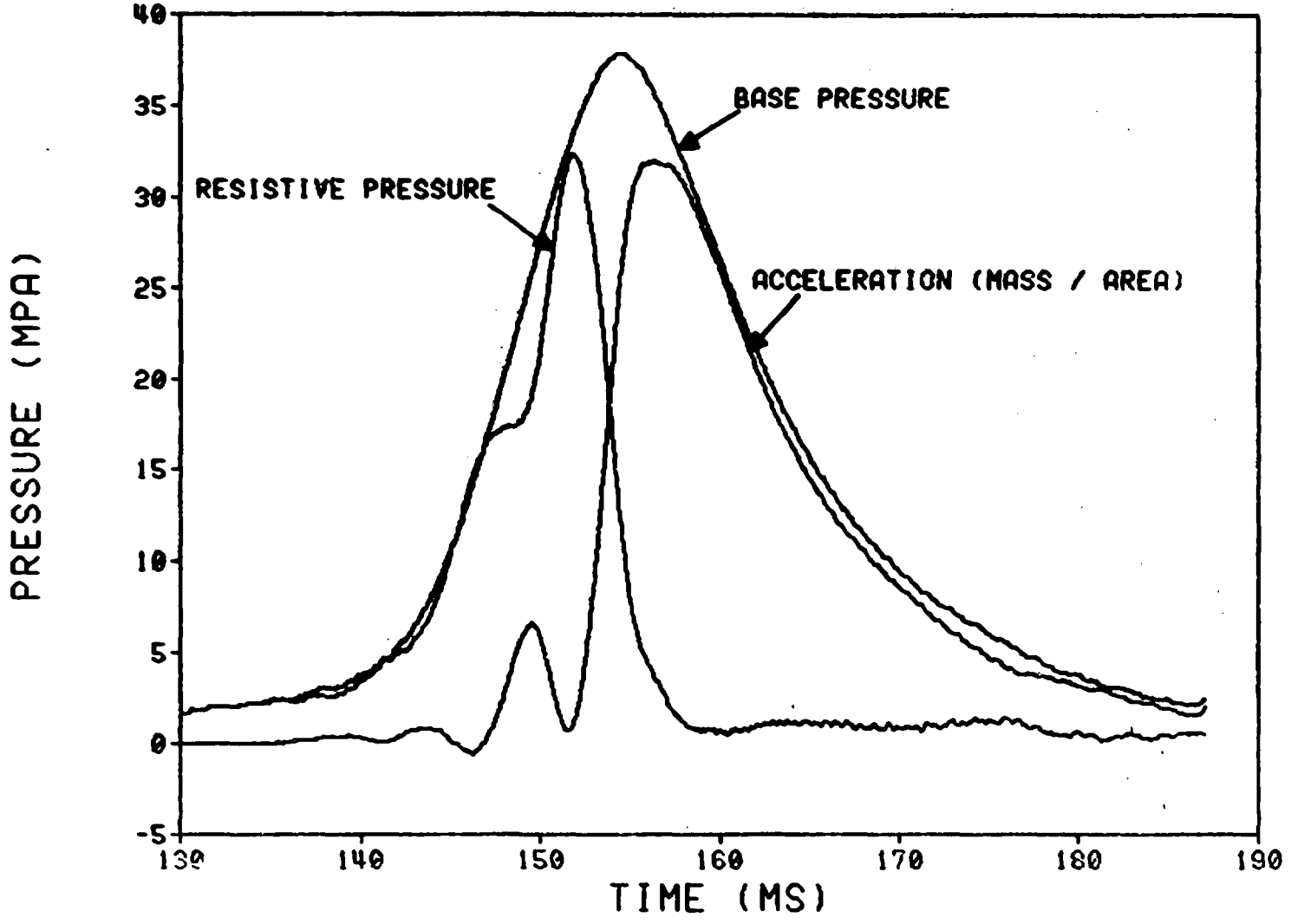

Figure 42. Base Pressure, Acceleration, Resistive Pressure versus Time, M3A1, Zone 1 Propelling Charge, LCSRS Projectile

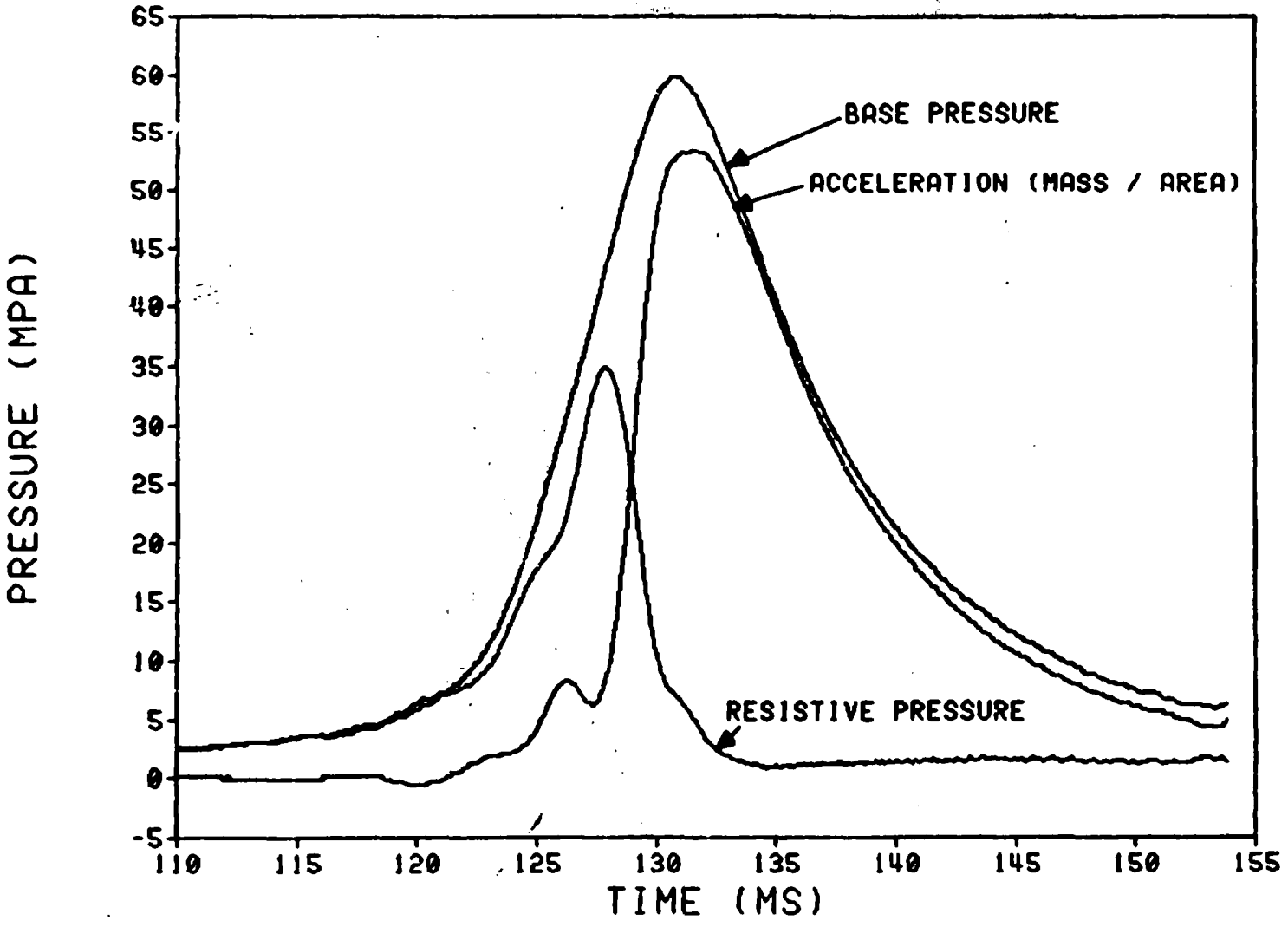

Figure 43. Base Pressure, Acceleration, Resistive Pressure versus Time, M3A1, Zone 3 Propelling Charge, LCSRS Projectile

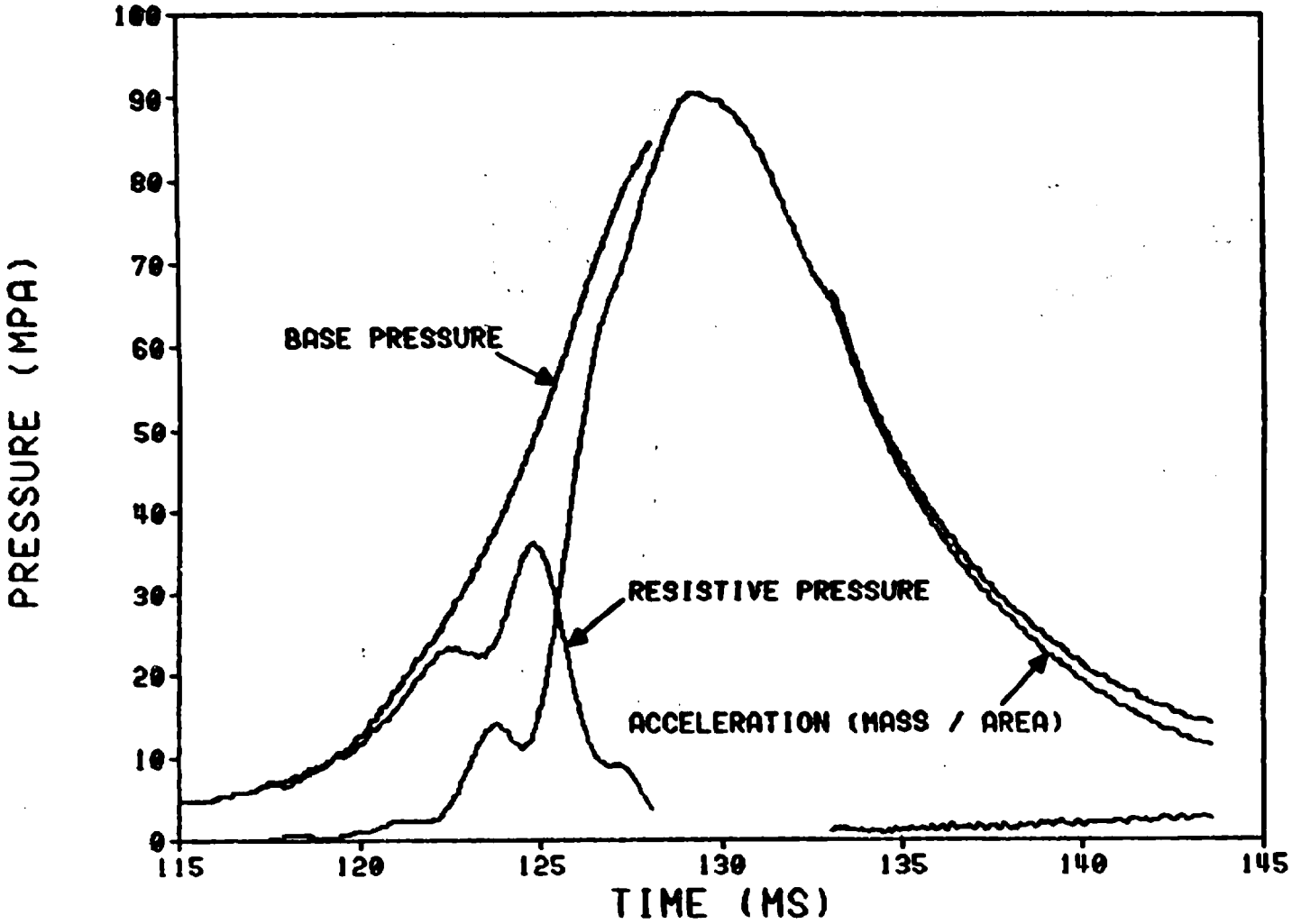

Figure 44. Base Pressure, Acceleration, Resistive Pressure versus Time, M3A1, Zone 5 Propelling Charge, LCSRS Projectile

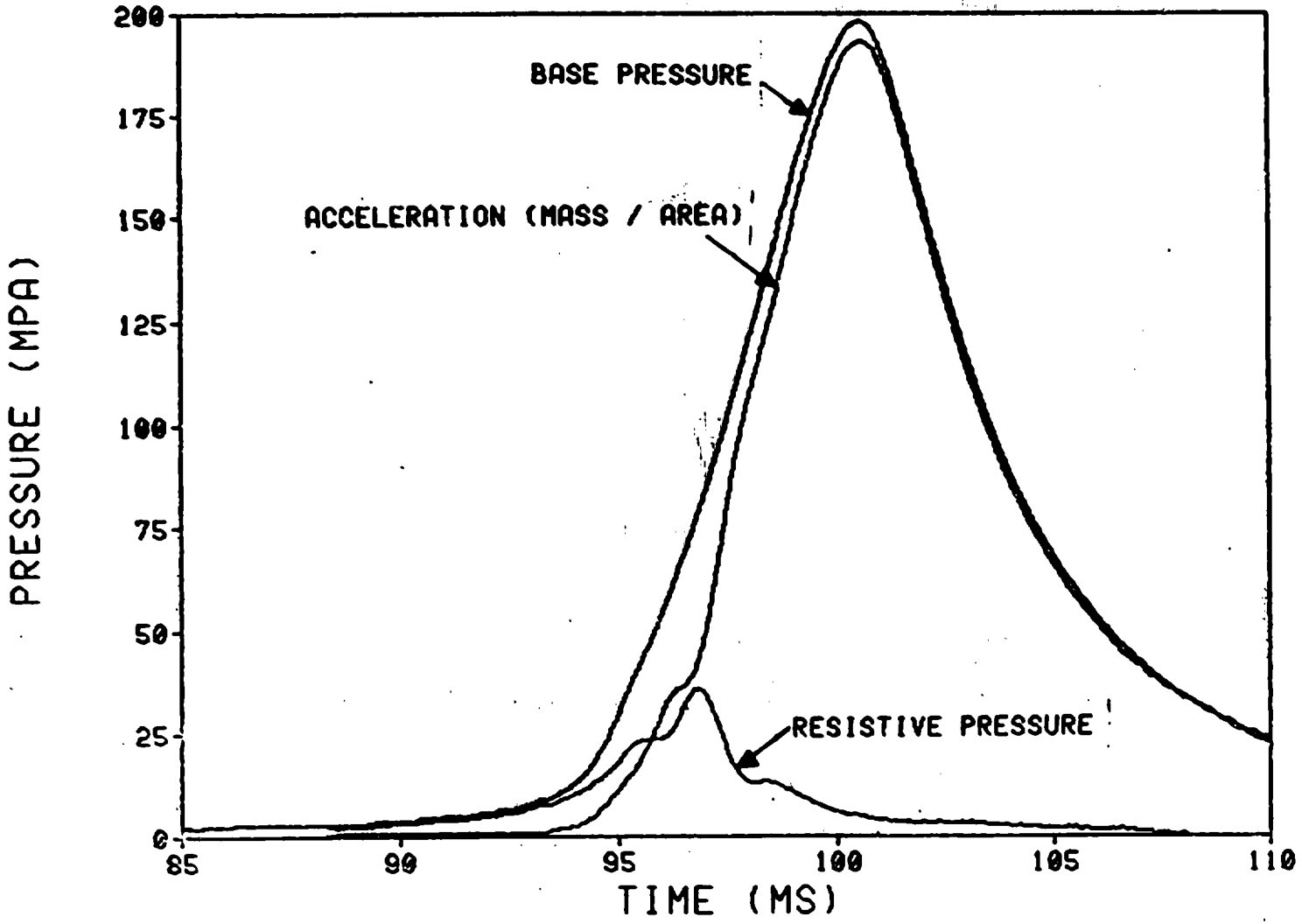

Figure 45. Base Pressure, Acceleration, Resistive Pressure versus Time, M4A2, Zone 7 Propelling Charge, LCSRS Projectile

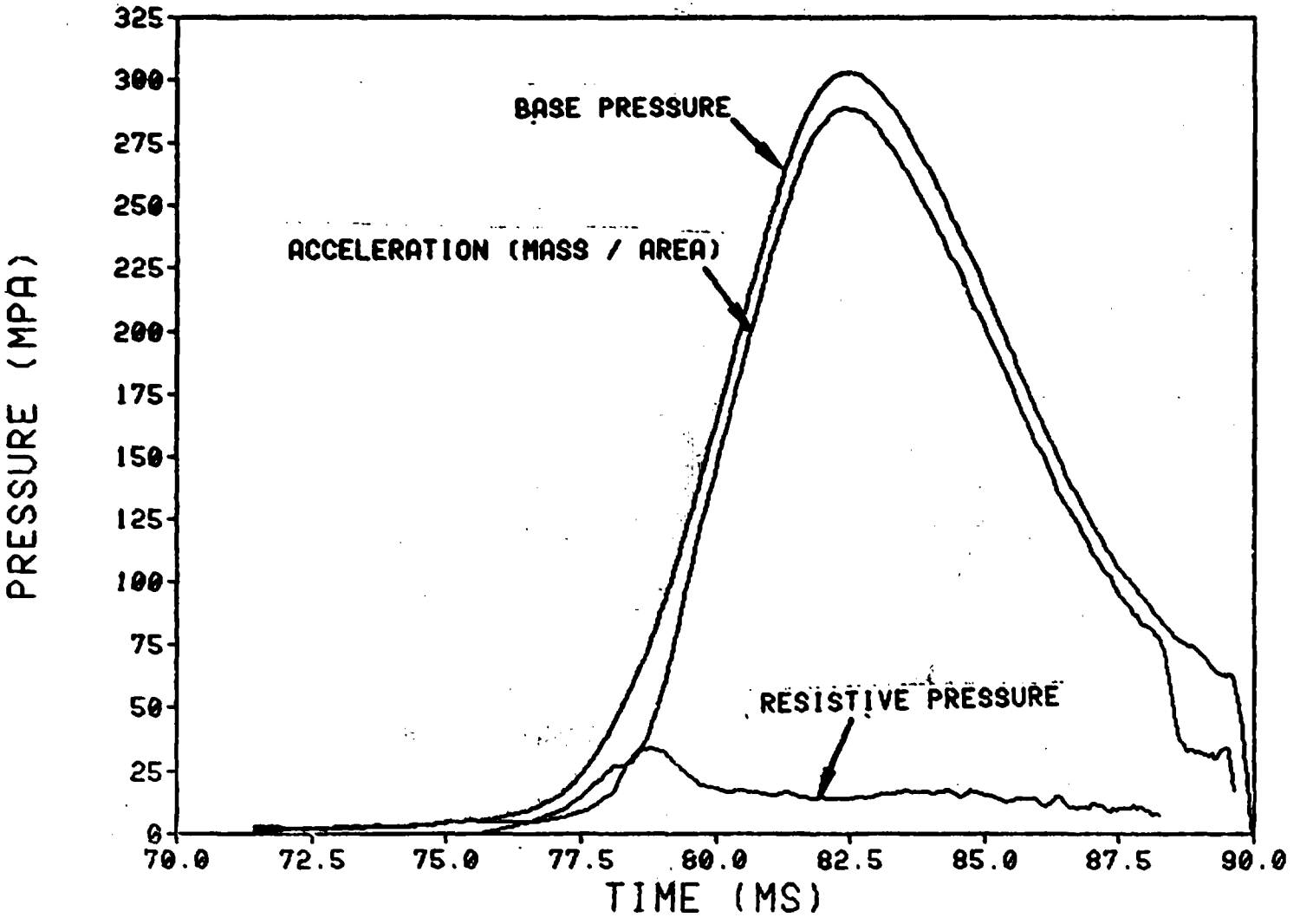

Figure 46. Base Pressure, Acceleration, Resistive Pressure versus Time, M203E1, Zone 8 Propelling Charge, Free-Flight Projectile

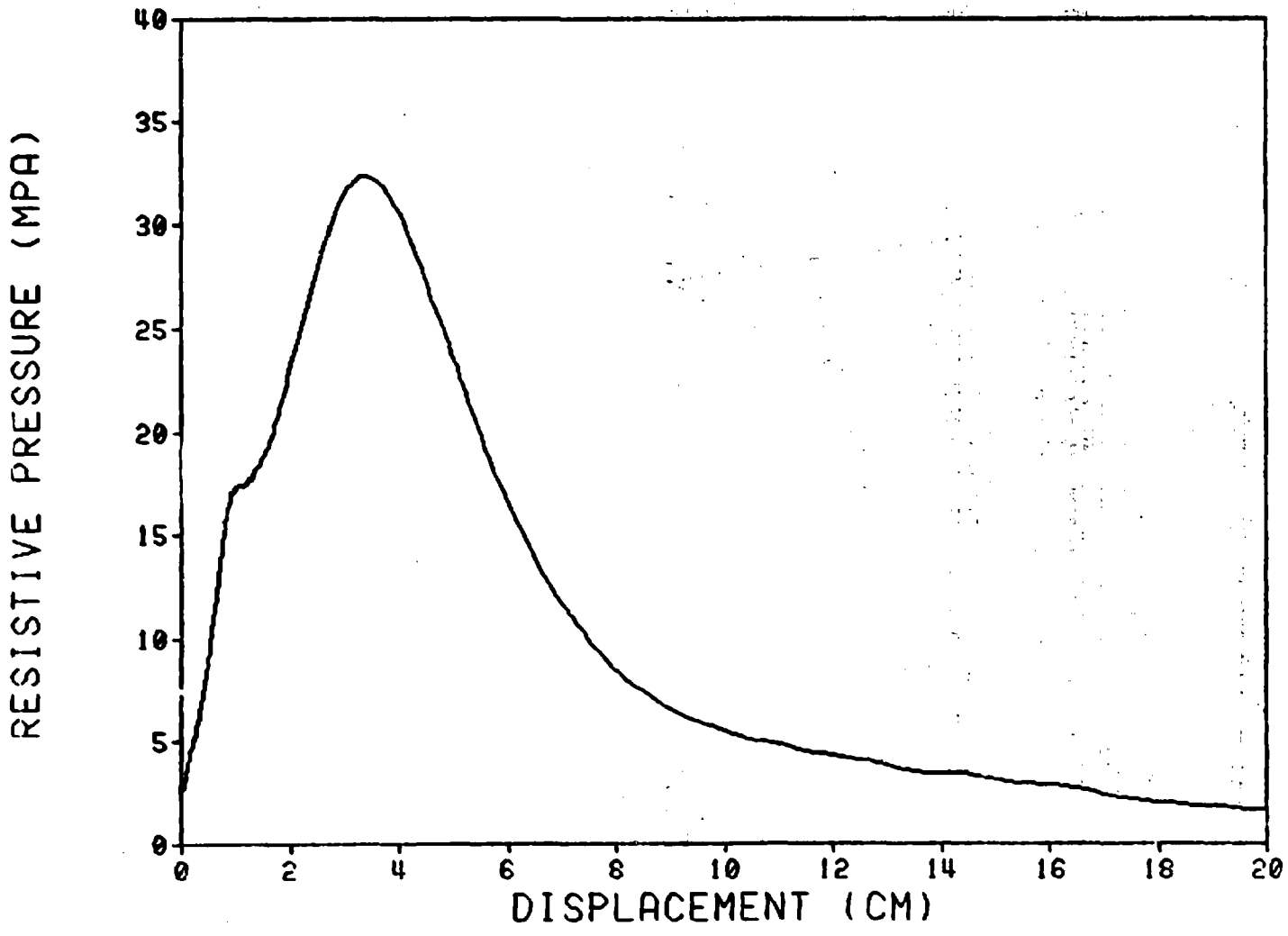

Figure 47. Resistive Pressure versus Displacement, M3A1, Zone 1 Propelling Charge, LCSRS Projectile

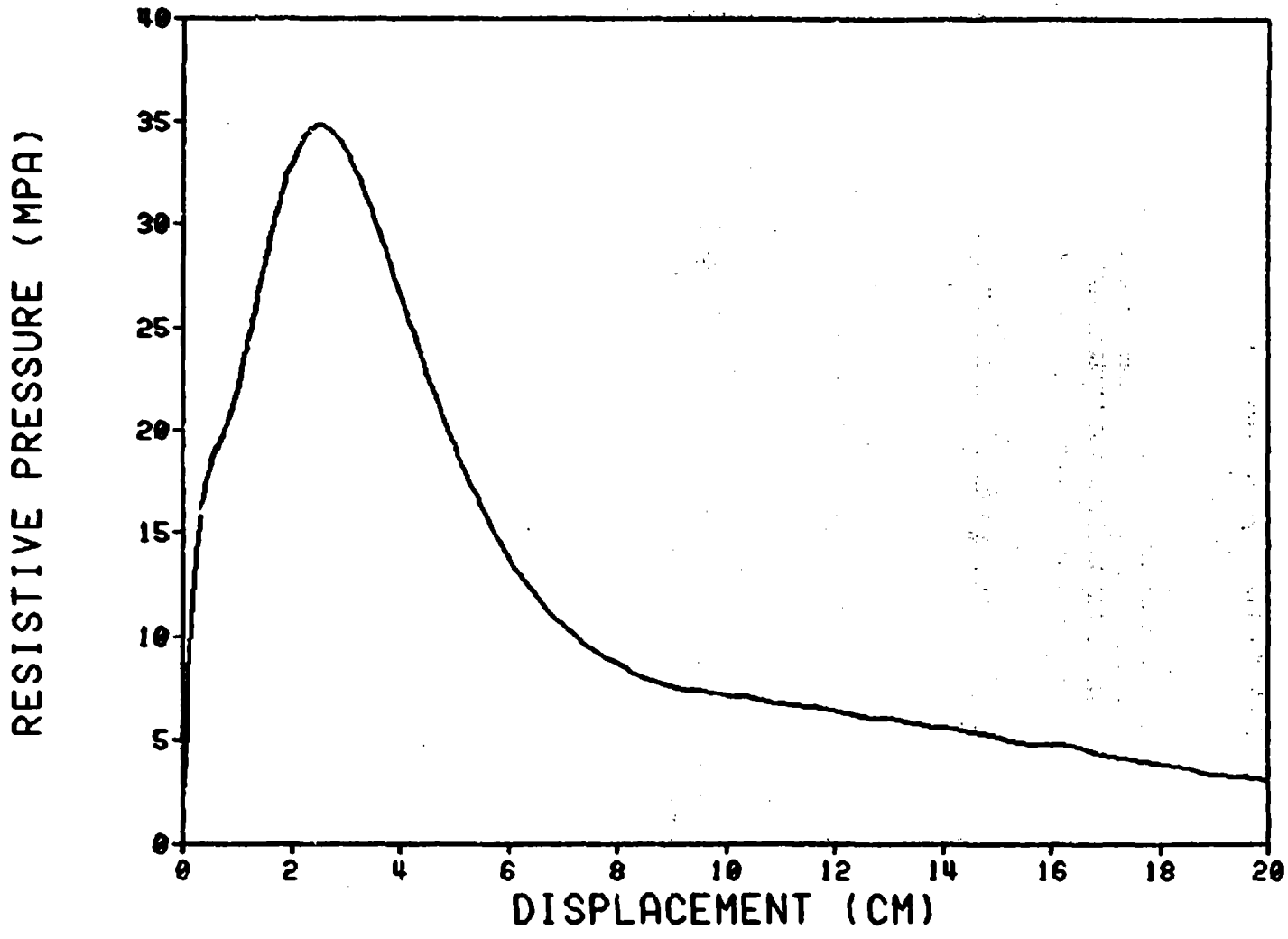

Figure 48. Resistive Pressure versus Displacement, M3A1, Zone 3 Propelling Charge, LCSRS Projectile

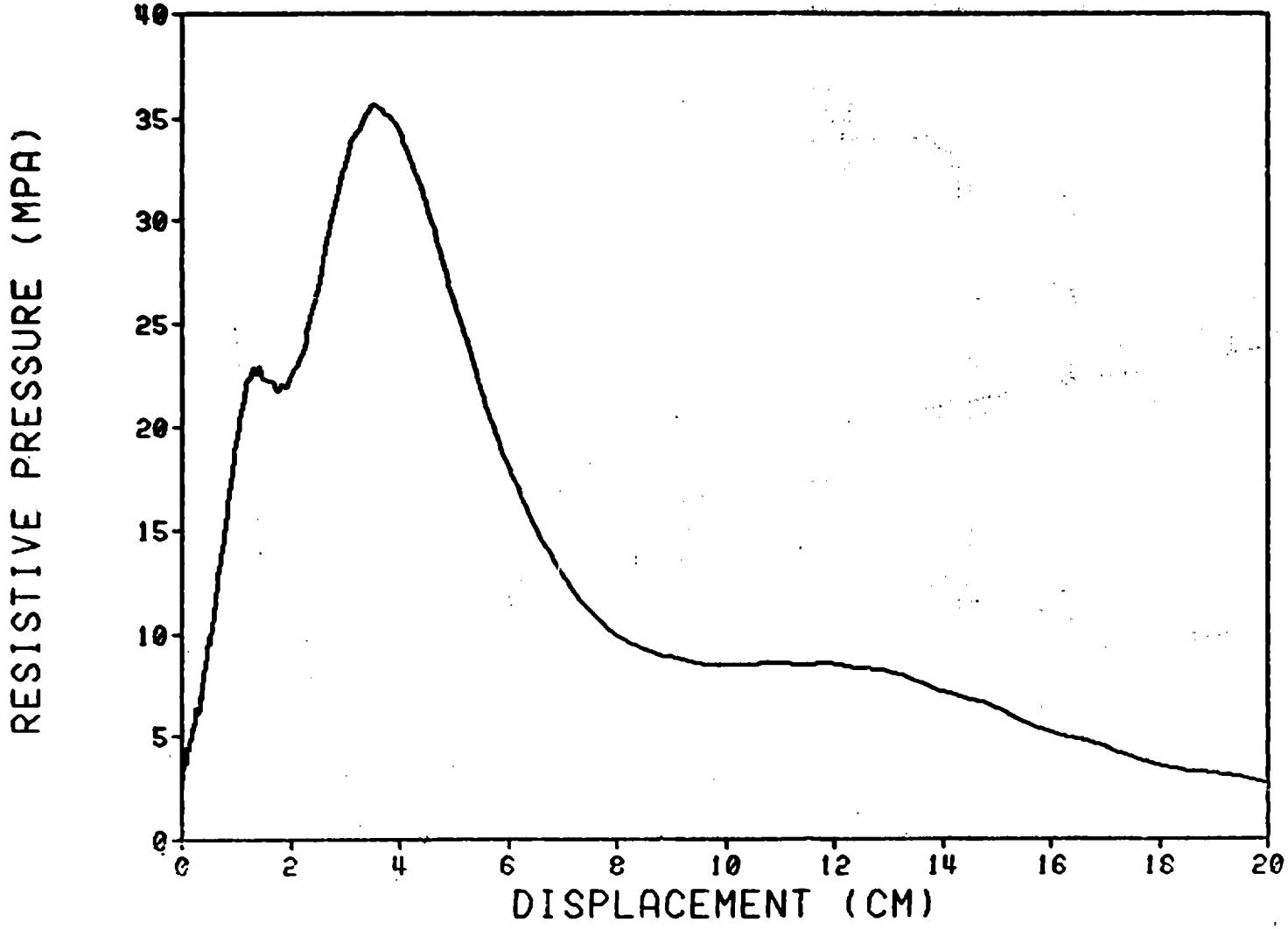

Figure 49. Resistive Pressure versus Displacement, M3A1, Zone 5 Propelling Charge, LCSRS Projectile

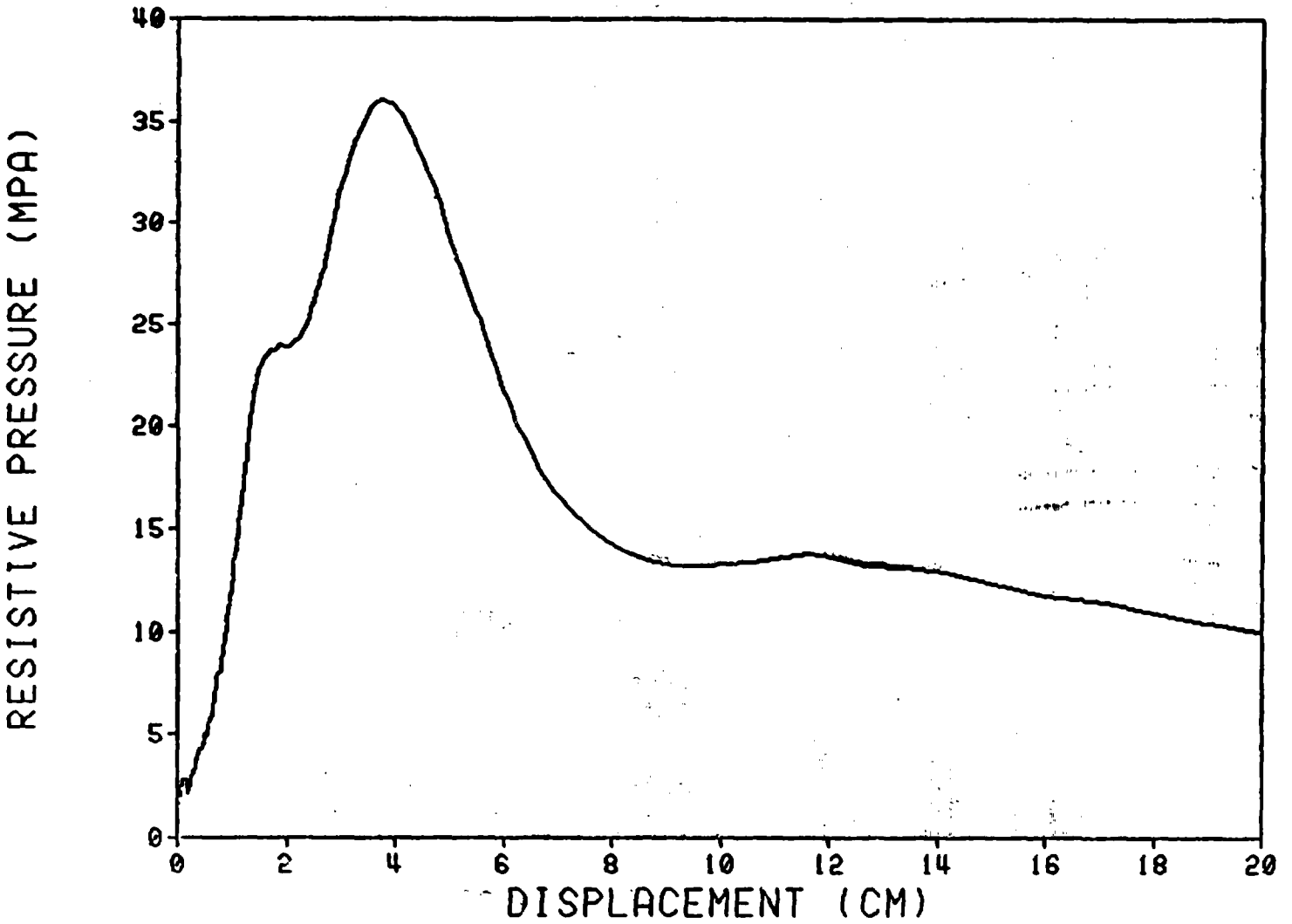

Figure 50. Resistive Pressure versus Displacement, M4A2, Zone 7 Propelling Charge, LCSRS Projectile

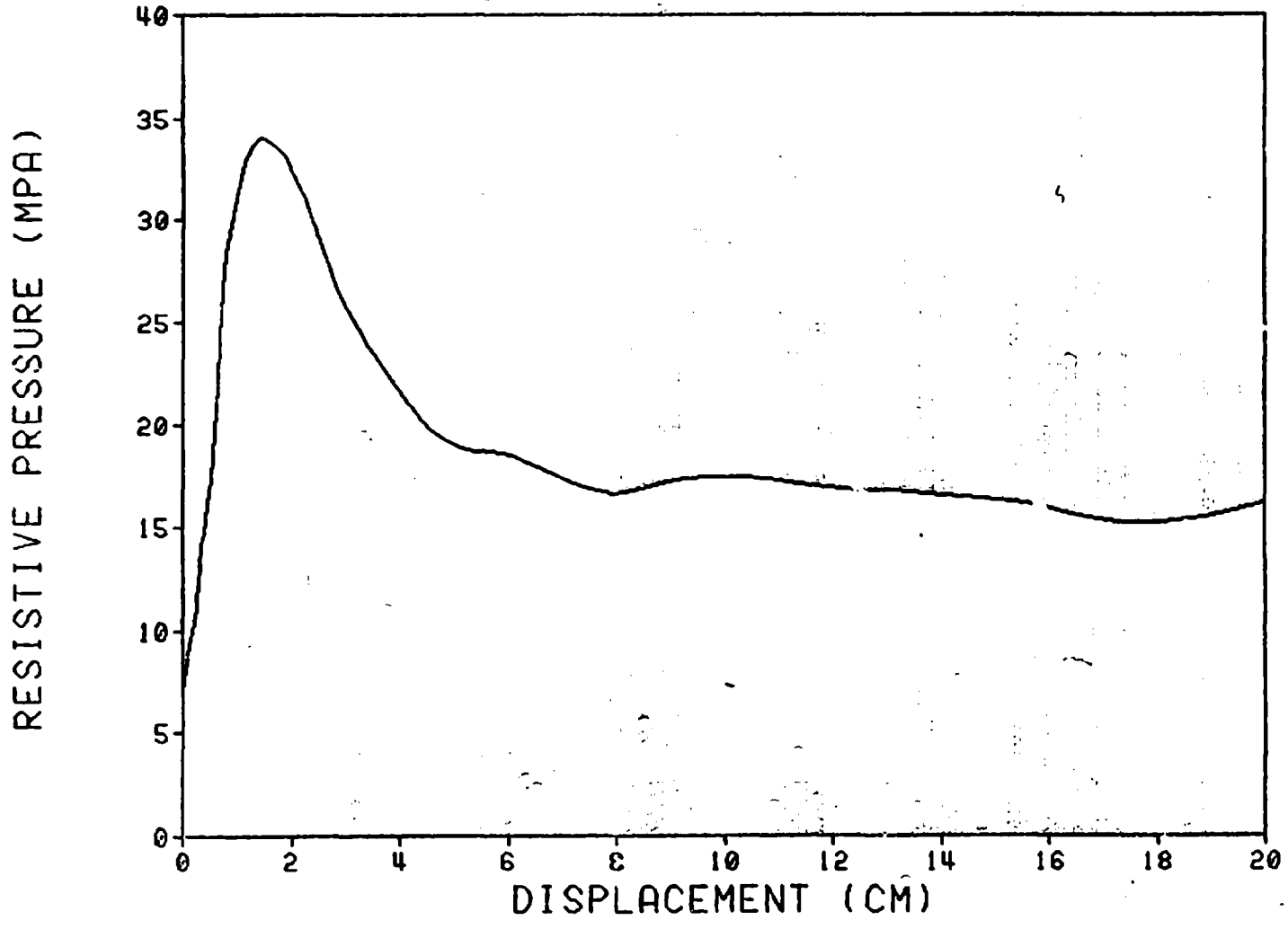

Figure 51. Resistive Pressure versus Displacement, M203E1, Zone 8 Propelling Charge, Free-Flight Projectile

scoop assembly. Because of the relative motion between the scoop and projectile body during launch, the measured tangential acceleration was of the scoop assembly and not the projectile. On subsequent rounds, the accelerometers were mounted in an adapter that fastened to the wall of the projectile and were encapsulated in the epoxy that was used for the ballast (Figure 25). This structure on several of the rounds broke loose during launch and distorted the data. In response to the projectile community's interest in angular acceleration/torsional impulse measurements, four free-flight rounds, originally configured for evaluation of an experimental propelling charge, were also configured with accelerometers located in a small metal box suspended 'n the epoxy fill as shown in Figure 21.

The relationship between the angular acceleration, axial acceleration, and the tangential acceleration is as follows:

$$\ddot{\theta} = a_x \; T = a_t / r \qquad (5)$$

where: $\ddot{\theta}$ = angular acceleration

a_x = axial acceleration

T = twist of the tube
= 1 revolution / 20 calibers
= 2.0268 radians / metre
(for 155-mm tube)

a_t = tangential acceleration

r = radius of the tangent

If the rotating band immediately engraves the rifling and there is no free run, the axial acceleration and tangential acceleration-time histories will have identical shapes differing only by magnitude. The difference in the shapes of these two curves is a measure of the torsional impulse during the engraving process.

Unfortunately, accelerometers also measure any vibration of the structure on which they are mounted. This effect can mask the desired quantity being measured. The cross-axis sensitivity of the accelerometer also distorts this measurement. It can be as much as five percent according to the manufacturer's specifications. Several of the accelerometers used for these measurements were subjected to an acceleration, on a drop table, at right angles to the sensing axis to try to determine the cross-axis characteristics. However, the transverse motion of the drop table caused substantial output and no conclusions could be made.

The tangential accelerometer is subjected to two cross-axis accelerations. They are the axial acceleration of the projectile and the centrifugal force of the spinning projectile. The acceleration due to the centrifugal force is directed along a radius and is related to the axial acceleration by the relationships:

$$a_r = v_r^2/R \qquad (6)$$

where: a_r = radial acceleration

R = radius at (a_r)

v_r = velocity at R

$$a_r = T^2 R v_x^2$$

where: v_x = axial velocity

The radial acceleration-time history should have a shape of the squared axial velocity curve and only differ in the magnitude.

Using a measured axial acceleration for a 155-mm, M101 projectile and the above relationships, the resultant cross-axis acceleration on a tangential accelerometer located on a 4.29 cm radius is presented as Figure 52. The acceleration vector is aligned with the projectile axis at the start of motion, rotates 90 degrees during the in-tube travel, and is aligned with the radius at projectile/tube separation. The tangential acceleration for this location is 8.7% of the axial acceleration. Therefore, several percent of cross-axis sensitivity for the tangential accelerometer would result in a significant distortion of the measurement. During the engraving region, the cross-axis influence is at the minimum. Therefore, indications of torsional impulse may be determined provided the vibrational component can be identified and separated from the torsional impulse.

The free-flight rounds, modified for angular acceleration measurements (Figure 21), were configured with a radial accelerometer located in the small metal box along with the tangential accelerometer. Figures 53, 54, and 55 present the unfiltered acceleration time histories for the axial, radial, and tangential acceleration respectively. This round was propelled with an experimental charge made with slotted stick propellant (74 cm long)[26] and had a chamber pressure magnitude near that of a Zone 8. The magnitude of the axial acceleration was corrected using the pressure-port-passage procedure as previously described. Unfortunately, there are not similar techniques for correcting the tangential and radial acceleration

---

[26] F.W. Robbins and A.W. Horst, "Detailed Characterization of The Interior Ballistics of Slotted Stick Propellant," BRL-TR-2591, Ballistic Research Laboratory, Aberdeen Proving Ground, MD, September 1984.

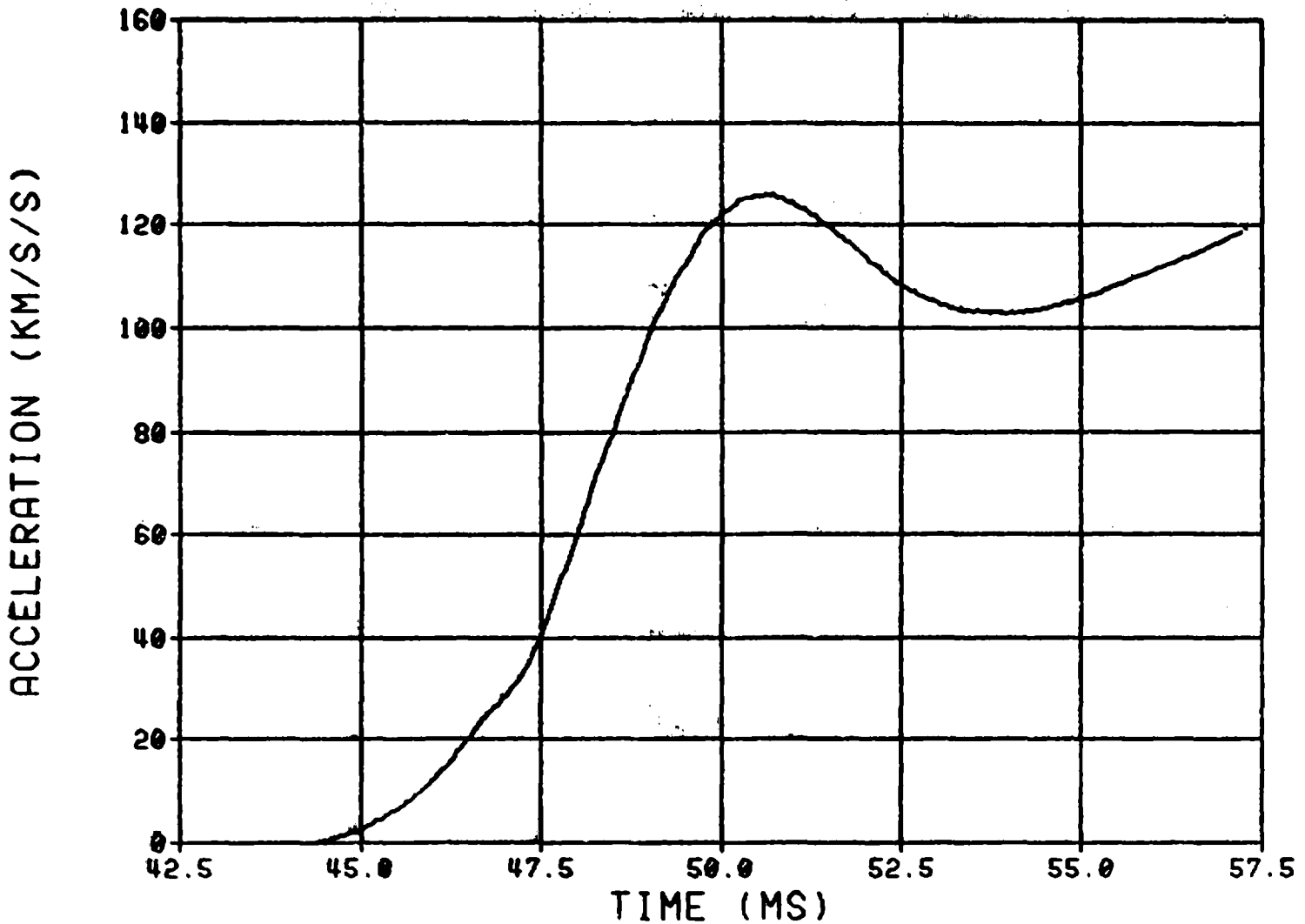

Figure 52. Resultant Cross-Axis Acceleration versus Time, Slotted Stick Propelling Charge, Free-Flight Projectile

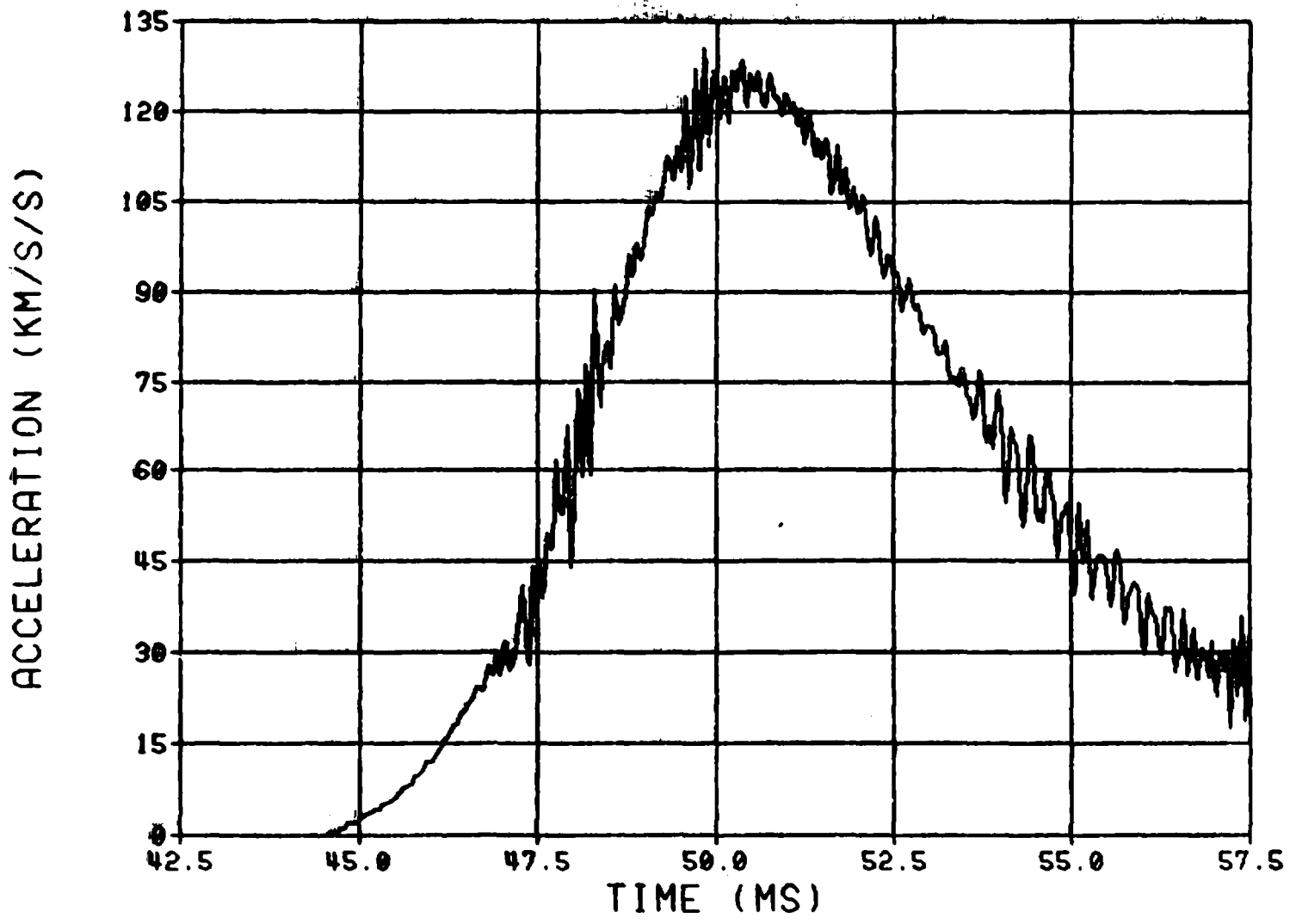

Figure 53. Axial Acceleration versus Time, Slotted Stick Propelling Charge, Free-Flight Projectile

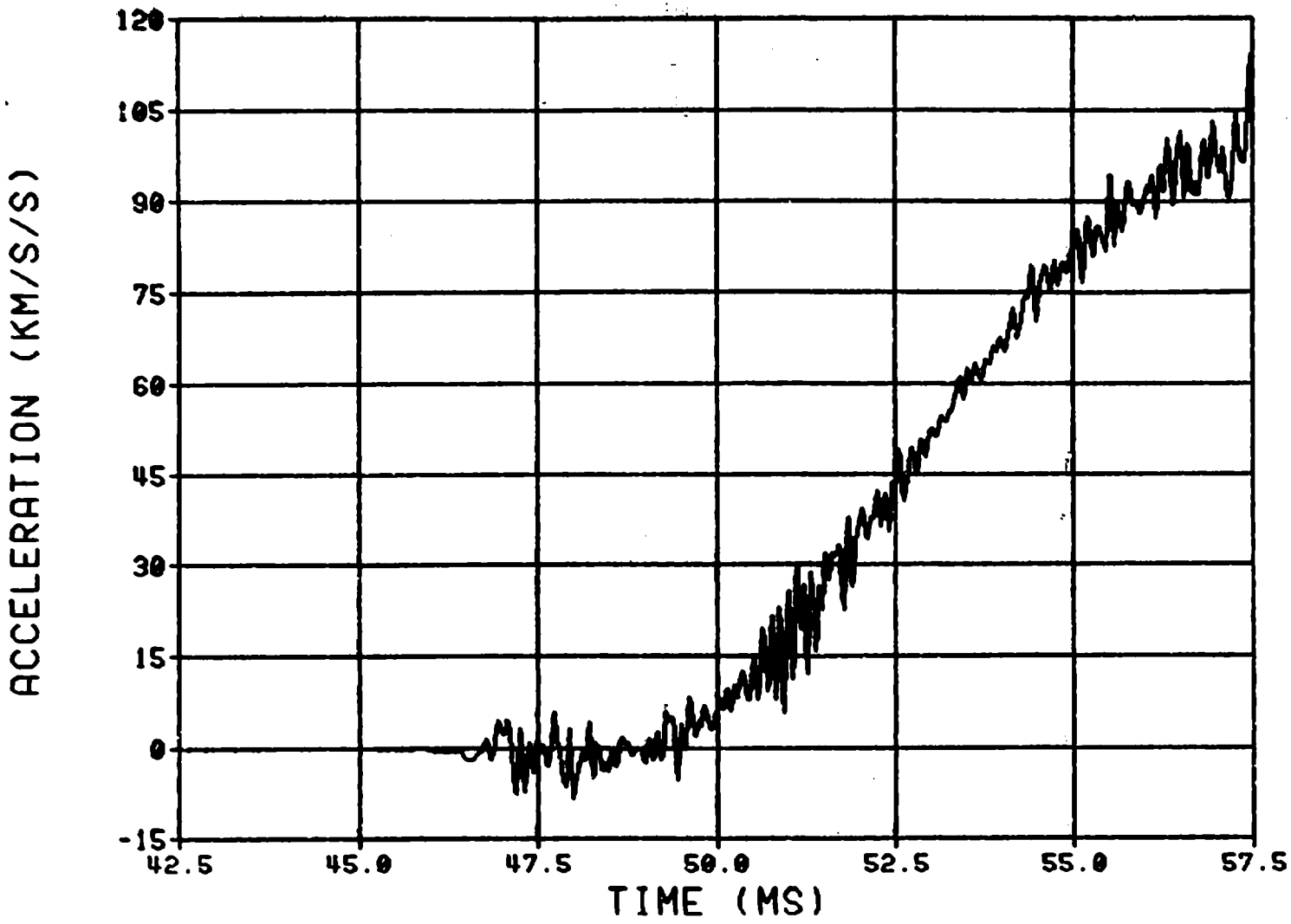

Figure 54. Radial Acceleration versus Time, Slotted Stick Propelling Charge, Free-Flight Projectile

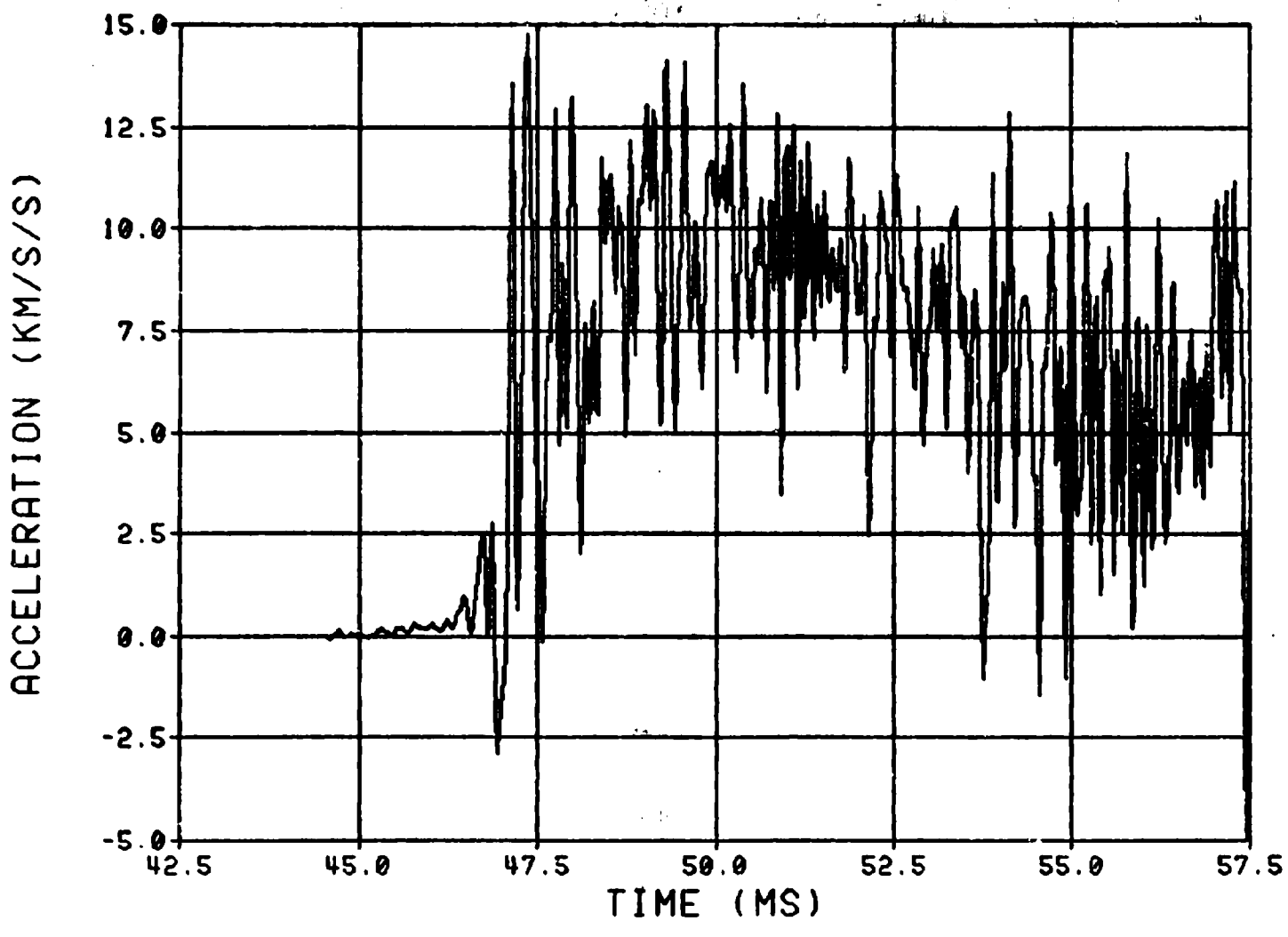

Figure 55. Tangential Acceleration versus Time, Slotted Stick Propelling Charge, Free-Flight Projectile

measurements. Past experience indicates that the magnitude of on-board acceleration measurements are low. The radial and tangential accelerometers were located on 4.32 and 4.29 cm radii respectively. The frequency bandwidth of the telemetry system was 8 kHz and permitted passage of the vibration influence. The vibration component of the tangential acceleration was large and the trace did not return to near baseline at the same rate as the axial acceleration. This indicates the influence of the cross-axis component. Figure 56 presents the three acceleration-time histories for this round after filtering at 2 kHz. The negative excursion of the radial acceleration is not explained. It is possible that it was caused by a lateral motion of the projectile while being centered by the forcing cone.

The angular accelerations derived from the axial and tangential accelerations for this round are presented as Figures 57 through 60. These plots are filtered at 2,3,4, and 5 kHz respectively to try to eliminate the vibration component. A similar free-flight round was propelled by a charge made of slotted granular (2.54 cm long) propellant.[26] A plot of the angular accelerations, filtered at 5 kHz, for this round is presented as Figure 61. It is obvious that the measurement of the torsional impulse, if it exists, is somewhat masked by the structural vibration. Also, the effect of the vibration and cross-axis sensitivity are apparent during the down-tube travel. During the early motion, Figure 60 and 61 show the rotating bands did not immediately engage tube rifling since the angular acceleration derived from the tangential acceleration lagged that derived from the axial acceleration.

X. CONCLUSIONS

The telemetry system has been proven to be reliable for use as the data link from the projectiles during the interior ballistic cycle. The commercial availability of the transmitting subsystems make this type of measurement feasible for routine experiments. Since the LCSRS is operational, the instrumentation can be reused, decreasing the costs per shot. Retrieving the telemetry transmitting system also permits determination of failure modes when they occur. The failure modes of the telemetry system for the expendable free-flight rounds were only surmised.

The interfacing of the transducers to the projectile and structures that house the transducers are problem areas that must be addressed. For better measurements, an effort must be made to improve the design of the modifications to the projectiles and a more detailed analysis must be made of the effect of the added structures. It was shown that vibrations were introduced by the added structure on the recoverable rounds.

Additional efforts are required to gain more confidence in the

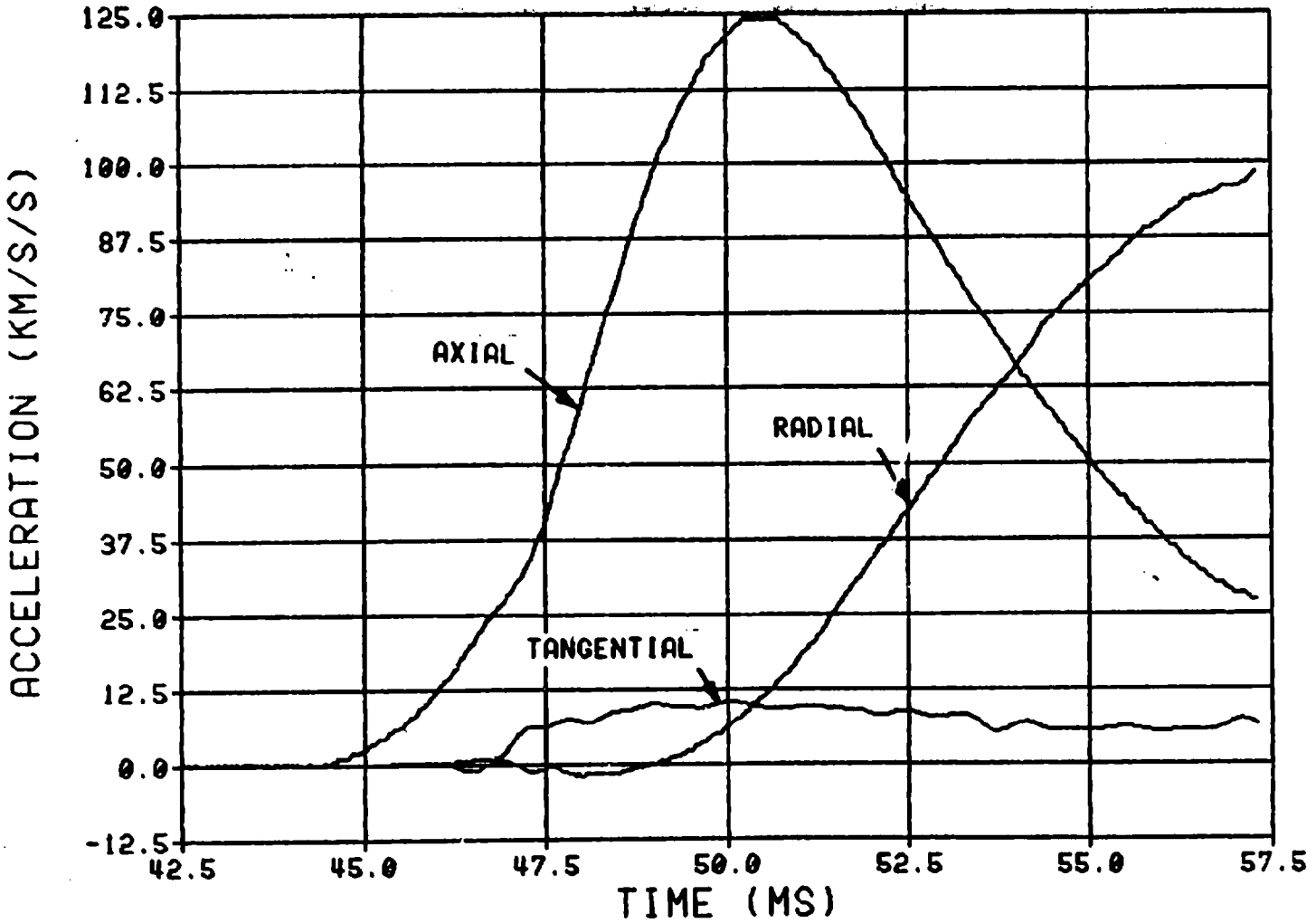

Figure 56. Axial, Radial, and Tangential Acceleration versus Time, Slotted Stick Propelling Charge, Free-Flight Projectile, Filtered at 2 kHz

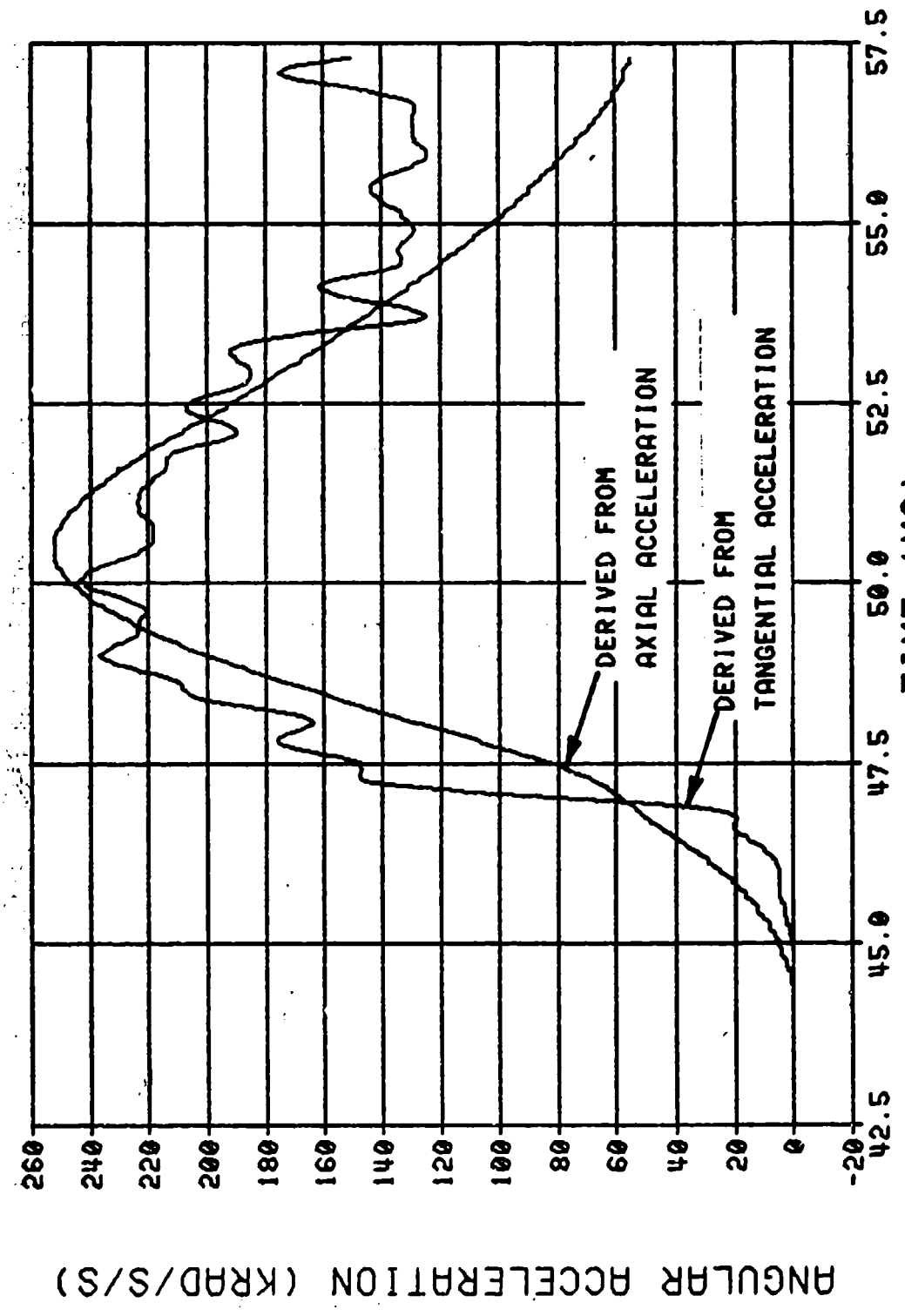

Figure 57. Angular Acceleration versus Time, Slotted Stick Propelling Charge, Free-Flight Projectile, Filtered at 2 kHz

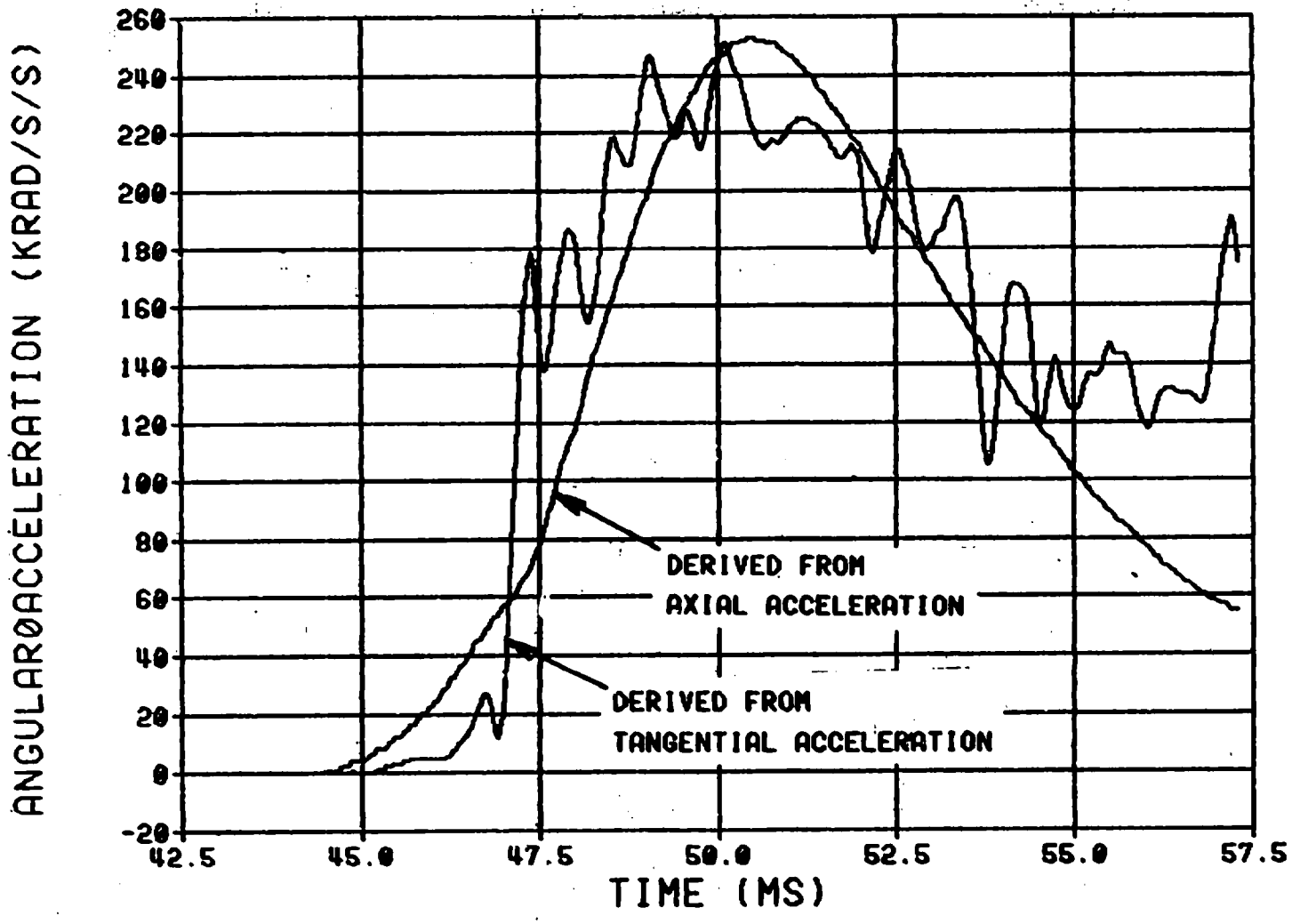

Figure 58. Angular Acceleration versus Time, Slotted Stick Propelling Charge, Free-Flight Projectile, Filtered at 3 kHz

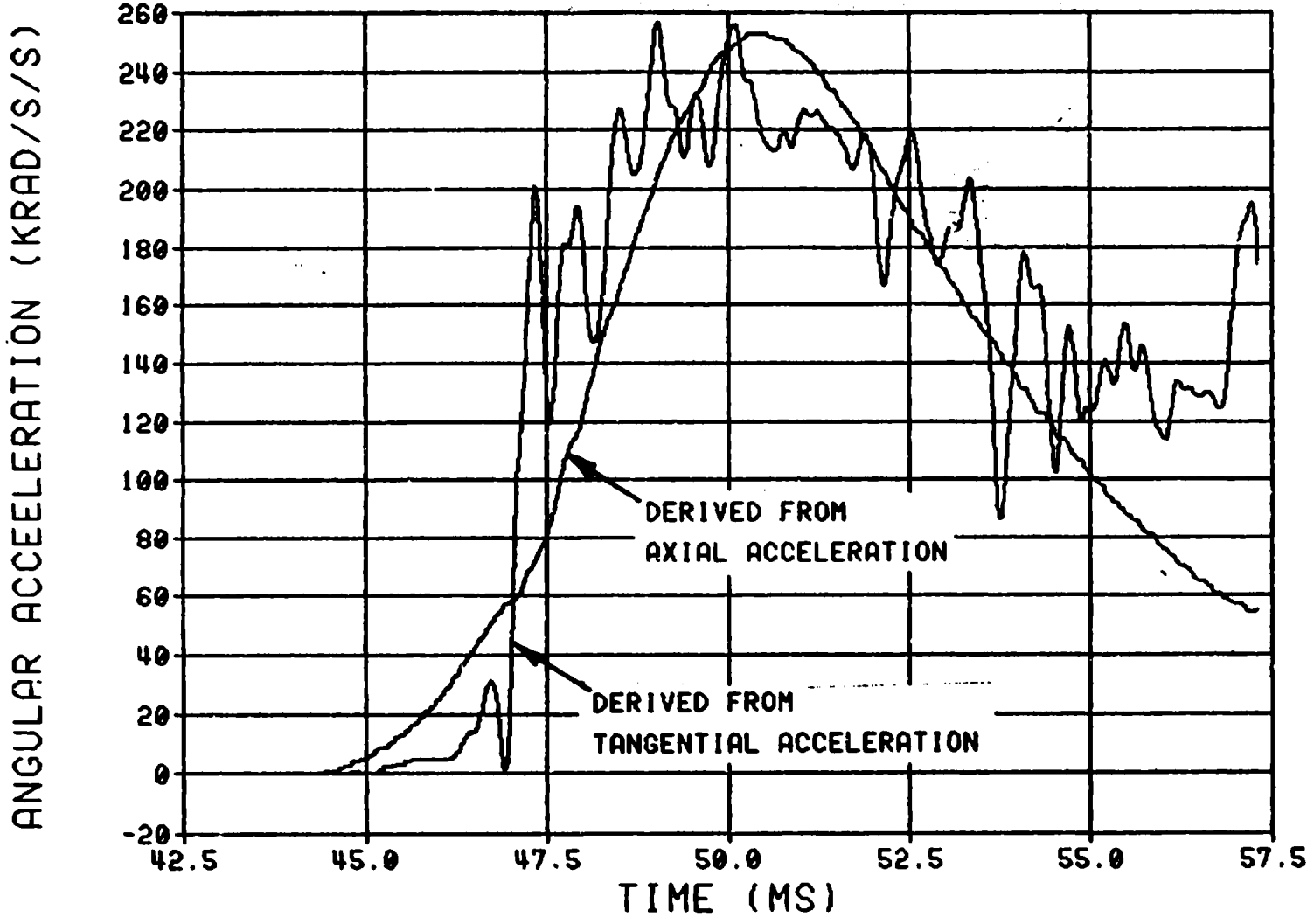

Figure 59. Angular Acceleration versus Time, Slotted Stick Propelling Charge, Free-Flight Projectile, Filtered at 4 kHz

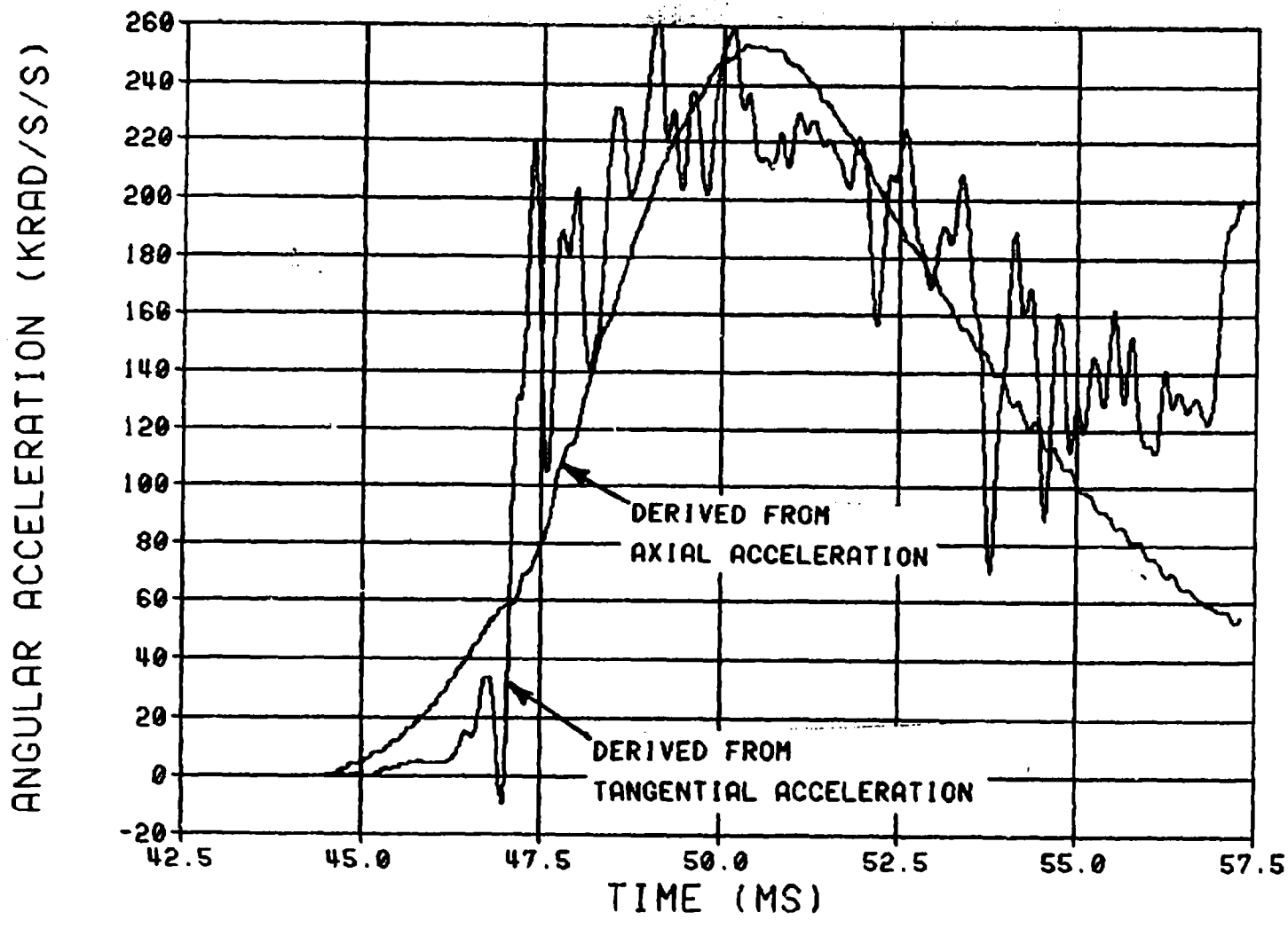

Figure 60. Angular Acceleration versus Time, Slotted Stick Propelling Charge, Free-Flight Projectile, Filtered at 5 kHz

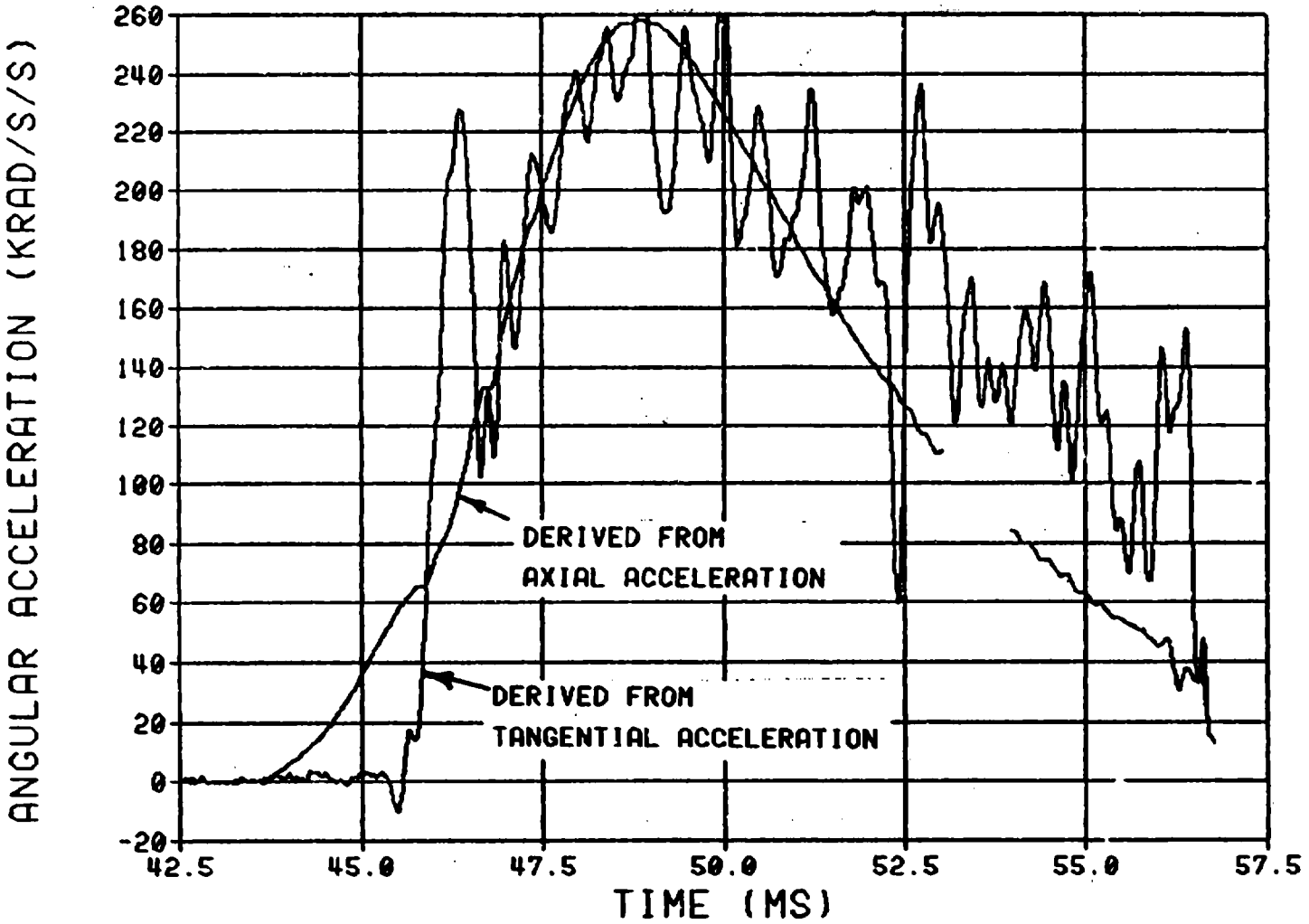

Figure 61. Angular Acceleration versus Time, Slotted Granular Propelling Charge, Free-Flight Projectile, Filtered at 5 kHz

transducer calibrations. Techniques are required for the dynamic calibration of the transducers over the range they will be used. It is necessary to accurately determine their linearity, hysteresis, and repeatability. It is also necessary to determine the cross-axis sensitivity of the accelerometers used for measuring tangential acceleration and establish if super position exists so the axial component of this measurement can be subtracted. Although the telemetry transmission link functions throughout most of the in-tube travel, the characteristics of the transducers distort the data for tangential acceleration measurements. It is obvious that additional research and development is required in this area before routine measurements are made of the torsional impulse. Possible solutions of the problems are: mechanical filtering to eliminate the vibration component, developing transducers with minimum cross-axis sensitivity, and/or developing a new class of transducers that measure the angular acceleration directly.

The data presented in this report are a small sample. Additional measurements are required to establish a data base large enough to be useful as input parameters to new weapon systems designs and newly formulated interior ballistic models.

XI. ACKNOWLEDGMENTS

The author is grateful to Messrs. C.R. Ruth, J.E. Bowen, and J.R. Hewitt for their invaluable service of conducting the firing programs and managing the LCSRS. Mr. J.L. Stabile was invaluable for his assistance with the instrumentation, telemetry receiving system, and data reduction. Mr. Ruth was particularly helpful with the BALDAS and instrumentation set-up. Messrs W.J. Cruickshank and J.O. Pilcher contributed many suggestions during the projectile modification and telemetry transmitting systems design. Mr. F.W. Robbins provided guidance during data evaluation.

REFERENCES

1. E.B. Fisher, "Continued Development and Documentation of the Calspan Interior Ballistics Code," ARBRL-CR-00465, Calspan Corporation, Ballistic Research Laboratory, USA ARRADCOM, Aberdeen Proving Ground, MD, September 1981.

2. J.W. Evans, "In-Bore Measurements of Projectile Acceleration and Base Pressure Using an S-Band Telemetry System," Proceedings of The International Telemetry Conference, Volume XI, October 1975.

3. J.W. Evans, "In-Bore Measurements of Projectile Acceleration and Base Pressure Using an S-Band Telemetry System," Proceedings of The Fuze/ Munitions Environment Characterization Symposium II, October 1975.

4. J.W. Evans, "In-Bore Measurements of Projectile Acceleration and Base Pressure Using an S-Band Telemetry System," Memorandum Report No. 2562, Ballistic Research Laboratories, Aberdeen Proving Ground, MD, December 1975.

5. J.W. Evans, "Pressure and Acceleration Measurements In Large Caliber Cannons," Proceedings of The Tenth Transducer Workshop, June 1979.

6. J.W. Evans, "Measurements On-Board A Projectile During The In-Tube Travel Using An FM/FM Telemeter," Proceedings of DEA-G-1060 Germany-United States Ballistic Research and Development, October 1980.

7. J.W. Evans, "A Technique for Measuring Engraving and Bore Frictional Forces in Large Caliber Guns," Proceedings of the 1983 JANNAF Propulsion Meeting, CPIA Publication Number 370, February 1983.

8. J.W. Evans, C.R. Ruth, and E.V. Clarke, Jr., "Soft Recovery Tests of A 155-mm Cannon Launched Guided Projectile, Type T," ARBRL-MR-03107, Ballistic Research Laboratory, USA ARRADCOM, Aberdeen Proving Ground, MD, May 1981.

9. M.H. Nichols and L.L. Rauch, Radio Telemetry, 2nd Edition, John Wiley and Sons, Inc., New York, NY, 1956.

10. E.J. Halcin and J.A. Pratt, "Design of A Large Caliber Soft Recovery System For The Ballistic Research Laboratories," Contract Report No. 308, Honeywell Inc., Ballistic Research Laboratories, Aberdeen Proving Ground, MD, August 1976. (AD #B013626L)

11. J.W. Evans, E.V. Clarke, Jr., and C.R. Ruth, "Large Caliber Projectile Soft Recovery," Proceedings of The 1979 JANNAF Propulsion Meeting, CPIA Publication Number 300, Volume I, March 1979.

12. E.V. Clarke, Jr., C.R. Ruth, J.W. Evans, J.E. Bowen, J.K. Hewitt, and J.L. Stabile, "Large Caliber Projectile Soft Recovery," ARBRL-MR-03083, Ballistic Research Laboratory, USA ARRADCOM, Aberdeen Proving Ground, MD, February 1981.

13. "Model 109A Pressure Transducer Instrumentation Manual," PCB Piezotronics, Inc., Buffalo, NY, 14225

14. "Model 305M Accelerometer Instrumentation Manual," PCB Piezotronics, Inc., Buffalo, NY, 14225.

15. PCB Piezotronics, Inc., General Guide To ICP Instrumentation, Pamphlet G-0001, Buffalo, NY.

16. L.A. Ware and H.R. Reed, Communication Circuits, 3rd Ed., John Wiley and Sons, Inc., New York, NY, 1958.

17. A. Adamian, "Voltage Regulator Handbook," Fairchild Camera and Instrument Corporation, Mountain View, CA, 1978

18. C.L. Henry, R.L. Martz, and E.M. Wineholt, "An Improved Procedure For The Reduction of Interior Ballistic Data Recorded On Analog Tape," Memorandum Report No. 2374, Ballistic Research Laboratories, Aberdeen Proving Ground, MD, April 1974. (AD #919924L)

19. Telemetry Working Group, Inter-Range Instrumentation Group, Range Commanders Council, Telemetry Standards, Document 106-71, White Sands Missile Range, NM, 88002.

20. W.J. Cruickshank, "A Feasibility Test of An "S" Band Telemetry System For Making In-bore Projectile Measurements," Memorandum Report No. 2335, Ballistic Research Laboratories, Aberdeen Proving Ground, MD, October 1973.

21. W.J. Cruickshank, "Radio Telemetry Formula Applications, A Practical Users Guide," ARBRL-MR-03364, Ballistic Research Laboratory, Aberdeen Proving Ground, MD, August 1984.

22. M. Schwartz, "Information Transmission, Modulation, and Noise," McGraw-Hill Book Company, INc., New York, NY, 1959.

23. A.E. Schmidlin, "Torsional Impulse In Gun Launched Projectiles," ARLCD-TR-80037, Large Caliber Weapons Systems Laboratory, USA ARRADCOM, Dover, NJ, March 1981.

24. Minutes of Meeting, "Measurements of Torsional Impulse Using In-Bore Telemetry," Program Manager/Cannon Launched Weapon Systems, ARRADCOM, Dover, NJ, 5 March 1980.

25. Minutes of Meeting, "Internal Ballistics Characterization Briefing," Project Manager for Nuclear Munitions, ARRADCOM, Dover, NJ, 28 April 1981.

26. F.W. Robbins and A.W. Horst, "Detailed Characterization of The Interior Ballistics of Slotted Stick Propellant," BRL-TR-2591, Ballistic Research Laboratory, Aberdeen Proving Ground, MD, September 1984.

DISTRIBUTION LIST

No. Of Copies	Organization
12	Administrator Defense Technical Info Center ATTN: DTIC-DDA Cameron Station Alexandria, VA 22304-6145
1	Commander USA Concepts Analysis Agency ATTN; D. Hardison 8120 Woodmont Avenue Bethesda, MD 20014-2797
1	HQDA/DAMA-ZA Washington, DC 20310-2500
1	HQDA, DAMA-CSM, E. Lippi Washington, DC 20310-2500
1	HQDA/SARDA Washington, DC 20310-2500
1	Commander US Army War College ATTN: Library-FF229 Carlisle Barracks, PA 17013
1	US Army Ballistic Missile Defense Systems Command Advanced Technology Center P. O. Box 1500 Huntsville, AL 35807-3801
1	Chairman DOD Explosives Safety Board Room 856-C Hoffman Bldg. 1 2461 Eisenhower Avenue Alexandria, VA 22331-9999
1	Commander US Army Materiel Command ATTN: AMCPM-GCM-WF 5001 Eisenhower Avenue Alexandria, VA 22333-5001
1	Commander US Army Materiel Command ATTN: AMCDRA-ST 5001 Eisenhower Avenue Alexandria, VA 22333-5001
1	Commander US Army Materiel Command ATTN: AMCDE-DW 5001 Eisenhower Avenue Alexandria, VA 22333-5001
5	Project Manager Cannon Artillery Weapons System, ARDC, AMCCOM ATTN: AMCPM-CW, F. Menke AMCPM-CWW AMCPM-CWS M. Fisette AMCPM-CWA R. DeKleine H. Hassmann Dover, NJ 07801-5001
1	Project Manager Nuclear Munitions ARDC, AMCCOM ATTN: AMCPM-NUC, H. Painter Dover, NJ 07801-5001
2	Project Manager Munitions Production Base Modernization and Expansion ATTN: AMCPM-PBM, A. Siklosi AMCPM-PBM-E, L. Laibson Dover, NJ 07801-5001
3	Project Manager Tank Main Armament System ATTN: AMCPM-TMA, K. Russell AMCPM-TMA-105 AMCPM-TMA-120 Dover, NJ 07801-5001
1	Commander US Army Watervliet Arsenal ATTN: SARWV-RD, R. Thierry Watervliet, NY 12189-5001

DISTRIBUTION LIST

No. Of Copies	Organization
22	Commander US Army ARDC, AMCCOM ATTN: SMCAR-TSS SMCAR-TDC SMCAR-LC LTC N. Barron SMCAR-LCA A. Beardell D. Downs S. Einstein S. Westley S. Bernstein C. Roller J. Rutkowski SMCAR-LCB-I D. Spring SMCAR-LCE SMCAR-LCM-E S. Kaplowitz SMCAR-LCS SMCAR-LCU-CT E. Barrieres R. Davitt SMCAR-LCU-CV C. Mandala SMCAR-LCW-A M. Salsbury SMCAR-SCA L. Stiefel B. Brodman SMCAR-TSE-IT L. Glass D. Everswick Dover, NJ 07801-5001
4	Commander US Army Armament Munitions and Chemical Command ATTN: SMCAR-ESP-L Rock Island, IL 61299-7300
1	HQDA DAMA-ART-M Washington, DC 20310-2500
1	Director Benet Weapons Laboratory Armament R&D Center US Army AMCCOM ATTN: SMCAR-LCB-TL Watervliet, NY 12189-5001
1	Commander US Army Aviation Research and Development Command ATTN: AMSAV-E 4300 Goodfellow Blvd. St. Louis, MO 63120-1702
1	Commander US Army TSARCOM 4300 Goodfellow Blvd. St. Louis, MO 63120-1702
1	Director US Army, Air Mobility Research And Development Laboratory Ames Research Center Moffett Field, CA 94035-1099
1	Commander US Army Communications - Electronics Command ATTN: AMSEL-ED Fort Monmouth, NJ 07703-5301
1	Commander ERADCOM Technical Library ATTN: DELSD-L (Report Section) Fort Monmouth, NJ 07703-5301
1	Commander US Army Harry Diamond Lab. ATTN: DELHD-TA-L 2800 Powder Mill Road Adelphi, MD 20783-1145
1	Commander US Army Missile Command ATTN: AMSMI-CM Redstone Arsenal, AL 35898-5249

DISTRIBUTION LIST

No. Of Copies	Organization
1	Commander, U.S. Army Missile Command, Research, Development & Engineering Center, ATTN: AMSMI-RD Redstone Arsenal, AL 35898
1	Director, U.S. Army Missile & Intelligence Center ATTN: AIAMS-YDL Redstone Arsenal, AL 35898-5500
1	Commandant US Army Aviation School ATTN: Aviation Agency Fort Rucker, AL 36360
1	Commander US Army Tank Automotive Command ATTN: AMSTA-TSL Warren, MI 48092-2498
1	Commander US Army Tank Automotive Command ATTN: AMSTA-CG Warren, MI 48092-2498
1	Project Manager Improved TOW Vehicle ATTN: AMCPM-ITV US Army Tank Automotive Command Warren, MI 48092-2498
2	Program Manager M1 Abrams Tank System ATTN: AMCPM-GMC-SA, T. Dean Warren, MI 48092-2498
1	Project Manager Fighting Vehicle Systems ATTN: AMCPM-FVS Warren, MI 48092-2498
1	President US Army Armor & Engineer Board ATTN: ATZK-AD-S Fort Knox, KY 40121-5200
1	Project Manager M-60 Tank Development ATTN: AMCPM-M60TD Warren, MI 48092-2498
1	Director US Army TRADOC Systems Analysis Activity ATTN: ATAA-SL White Sands Missile Range, NM 88002
1	Commander US Army Training & Doctrine Command ATTN: ATCD-MA/ MAJ Williams Fort Monroe, VA 23651
2	Commander US Army Materials and Mechanics Research Center ATTN: AMXMR-ATL Tech Library Watertown, MA 02172
1	Commander US Army Research Office ATTN: Tech Library P. O. Box 12211 Research Triangle Park, NC 27709-2211
1	Commander US Army Belvoir Research & Development Center ATTN: STRBE-WC Fort Belvoir, VA 22060-5606

DISTRIBUTION LIST

No. Of Copies	Organization
1	Commander US Army Logistics Mgmt Ctr Defense Logistics Studies Fort Lee, VA 23801
1	Commandant US Army Infantry School ATTN: ATSH-CD-CSO-OR Fort Benning, GA 31905
1	President US Army Artillery Board Ft. Sill, OK 73503-5600
1	Commandant US Army Command and General Staff College Fort Leavenworth, KS 66027
1	Commandant US Army Special Warfare School ATTN: Rev & Tng Lit Div Fort Bragg, NC 28307
3	Commander Radford Army Ammunition Plant ATTN: SMCRA-QA/HI LIB Radford, VA 24141-0298
1	Commander US Army Foreign Science & Technology Center ATTN: AMXST-MO-3 220 Seventh Street, NE Charlottesville, VA 22901-5396
2	Commandant US Army Field Artillery Center & School ATTN: ATSF-CO-MW, B. Willis Ft. Sill, OK 73503-5600
1	Commander US Army Development and Employment Agency ATTN: MODE-TED-SAB Fort Lewis, WA 98433-5099
1	Office of Naval Research ATTN: Code 473, R. S. Miller 800 N. Quincy Street Arlington, VA 22217-9999
3	Commandant US Army Armor School ATTN: ATZK-CD-MS M. Falkovitch Armor Agency Fort Knox, KY 40121-5215
2	Commander Naval Sea Systems Command ATTN: SEA 62R SEA 64 Washington, DC 20362-5101
1	Commander Naval Air Systems Command ATTN: AIR-954-Tech Lib Washington, DC 20360
1	Assistant Secretary of the Navy (R, E, and S) ATTN: R. Reichenbach Room 5E787 Pentagon Bldg. Washington, DC 20350
1	Naval Research Lab Tech Library Washington, DC 20375
5	Commander Naval Surface Weapons Center ATTN: Code G33, J. L. East W. Burrell J. Johndrow Code G23, D. McClure Code DX-21 Tech Lib Dahlgren, VA 22448-5000

DISTRIBUTION LIST

No. Of Copies	Organization
2	Comander US Naval Surface Weapons Center ATTN: J. P. Consaga C. Gotzmer Indian Head, MD 20640-5000
4	Commander Naval Surface Weapons Center ATTN: S. Jacobs/Code 240 Code 730 K. Kim/Code R-13 R. Bernecker Silver Spring, MD 20903-5000
2	Commanding Officer Naval Underwater Systems Center Energy Conversion Dept. ATTN: CODE 5B331, R. S. Lazar Tech Lib Newport, RI 02840
4	Commander Naval Weapons Center ATTN: Code 388, R. L. Derr C. F. Price T. Boggs Info. Sci. Div. China Lake, CA 93555-6001
2	Superintendent Naval Postgraduate School Dept. of Mechanical Engineering Monterey, CA 93943-5100
1	Program Manager AFOSR Directorate of Aerospace Sciences ATTN: L. H. Caveny Bolling AFB, DC 20332-0001
10	Central Intelligence Agency Office of Central Reference Dissemination Branch Room GE-47 HQS Washington, D.C. 20502
6	Commander Naval Ordnance Station ATTN: P. L. Stang J. Birkett L Torreyson T. C. Smith D. Brooks Tech Library Indian Head, MD 20640-5000
1	AFSC/SDOA Andrews AFB, MD 20334
3	AFRPL/DY, Stop 24 ATTN: J. Levine/DYCR R. Corley/DYC D. Williams/DYCC Edwards AFB, CA 93523-5000
1	AFFDL ATTN: TST-Lib Wright-Patterson AFB, OH 45433
1	AFRPL/TSTL (Tech Library) Stop 24 Edwards AFB, CA 93523-5000
1	AFATL/DLYV Eglin AFB, FL 32542-5000
1	AFATL/DLXP Eglin AFB, FL 32542-5000
1	AFATL/DLJE Eglin AFB, FL 32542-5000
1	AFATL/DLODL ATTN: Tech Lib Eglin AFB, FL 32542-5000
1	AFWL/SUL Kirtland AFB, NM 87117

DISTRIBUTION LIST

No. Of Copies	Organization
1	NASA/Lyndon B. Johnson Space Center ATTN: NHS-22, Library Sectin Houston, TX 77054
1	AFELM, The Rand Corporation ATTN: Library Dr 1700 Main Street Santa Monica CA 90401-3297
1	General Applied Sciences Lab ATTN: J. Erdos Merrick & Stewart Avenues Westbury Long Isld, NY 11590
1	AAI Corporation ATTN: J. Hebert J. Frankle P. O. Box 6767 Baltimore, MD 21204
1	Aerodyne Research, Inc. Bedford Research Park ATTN: V. Yousefian Bedford, MA 01730-1497
1	Aerojet Ordnance Company ATTN: D. Thatcher 2521 Michelle Drive Tustin, CA 92680-7014
1	Aerojet Solid Propulsion Co. ATTN: P. Micheli Sacramento, CA 95813
1	Atlantic Research Corporation ATTN: M. K. King 5390 Cheorokee Avenue Alexandria, VA 22312-2302
1	AVCO Everett Rsch Lab ATTN: D. Stickler 2385 Revere Beach Parkway Everett, MA 02149-5936
2	Calspan Corporation ATTN: C. Morphy P. O. Box 400 Buffalo, NY 14225-0400
1	Foster Miller Associates ATTN: A. Erickson 135 Second Avenue Waltham, MA 02154
1	General Electric Company Armament Systems Dept. ATTN: M. J. Bulman, Room 1311 128 Lakeside Avenue Burlington, VT 05401-4985
1	IITRI ATTN: M. J. Klein 10 W. 35th Street Chicago, IL 60616-3799
1	Hercules Inc. Allegheny Ballistics Laboratory ATTN: R. B. Miller P. O. Box 210 Cumberland, MD 21501-0210
1	Hercules, Inc. Bacchus Works ATTN: K. P. McCarty P. O. Box 98 Magna, UT 84044-0098
1	Hercules, Inc. Radford Army Ammunition Plant ATTN: J. Pierce Radford, VA 24141-0299
1	Honeywell, Inc. Defense Systems Division ATTN: C. Hargreaves 5901 So. City Road 18 Edina, MN 55436

DISTRIBUTION LIST

No. Of Copies	Organization
1	Honeywell, Inc. Defense Systems Division ATTN: P. Williamson 23100 Sugar Bush Road Elk River, MN 55330
1	Lawrence Livermore National Laboratory ATTN: L-355, A. Buckingham M. Finger P. O. Box 808 Livermore, CA 94550-0622
1	Lawrence Livermore National Laboratory ATTN: L-324 M. Constantino P. O. Box 808 Livermore, CA 94550-0622
1	Olin Corporation Badger Army Ammunition Plant ATTN: R. J. Thiede Baraboo, WI 53913
1	Olin Corporation Smokeless Powder Operations ATTN: D. C. Mann P.O. Box 222 St. Marks, FL 32355-0222
1	Paul Gough Associates, Inc. ATTN: P. S. Gough P. O. Box 1614, 1048 South St. Portsmouth, NH 03801-1614
1	Physics International Company ATTN: Library H. Wayne Wampler 2700 Merced Street San Leandro, CA 94577-5602
1	Princeton Combustion Research Lab., Inc. ATTN: M. Summerfield 475 US Highway One Monmouth Junction, NJ 08852-9650
2	Rockwell International Rocketdyne Division ATTN: BA08 J. E. Flanagan J. Gray 6633 Canoga Avenue Canoga Park, CA 91303-2703
4	Sandia National Laboratories ATTN: N. Lapetina, 8152 R. Peterson, 8173 G. Bendetti, 8241 D. Stoner, 8173 P. O. Box 969 Livermore, CA 94550
1	Science Applications, Inc. ATTN: R. B. Edelman 23146 Cumorah Crest Drive Woodland Hills, CA 91364-3710
3	Thiokol Corporation Huntsville Division ATTN: D. Flanigan R. Glick Tech Library Huntsville, AL 35807
1	Scientific Research Assoc., Inc. ATTN: H. McDonald P.O. Box 498 Glastonbury, CT 06033-0498
1	Thiokol Corporation Wasatch Division ATTN: J. A. Peterson P. O. Box 524 Brigham City, UT 84302-0524

DISTRIBUTION LIST

No. Of Copies	Organization
2	Thiokol Corporation Elkton Division ATTN: R. Biddle Tech Lib. P. O. Box 241 Elkton, MD 21921-0241
2	United Technologies Chemical Systems Division ATTN: R. Brown Tech Library P. O. Box 358 Sunnyvale, CA 94086-9998
1	Veritay Technology, Inc. ATTN: E. Fisher 4845 Millersport Hwy. P. O. Box 305 East Amherst, NY 14051-0305
1	Universal Propulsion Company ATTN: H. J. McSpadden Black Canyon Stage 1 Box 1140 Phoenix, AZ 85029
1	Battelle Memorial Institute ATTN: Tech Library 505 King Avenue Columbus, OH 43201-2693
1	Brigham Young University Dept. of Chemical Engineering ATTN: M. Beckstead Provo, UT 84601
1	California Institute of Tech 204 Karman Lab Main Stop 301-46 ATTN: F. E. C. Culick 1201 E. California Street Pasadena, CA 91109
1	California Institute of Tech Jet Propulsion Laboratory ATTN: L. D. Strand 4800 Oak Grove Drive Pasadena, CA 91109-8099
1	University of Illinois Dept of Mech/Indust Engr ATTN: H. Krier 144 MEB; 1206 N. Green St. Urbana, IL 61801-2978
1	University of Massachusetts Dept. of Mechanical Engineering ATTN: K. Jakus Amherst, MA 01002-0014
1	University of Minnesota Dept. of Mechanical Engineering ATTN: E. Fletcher Minneapolis, MN 55414-3368
1	Case Western Reserve University Division of Aerospace Sciences ATTN: J. Tien Cleveland, OH 44135
3	Georgia Institute of Tech School of Aerospace Eng. ATTN: B. T. Zinn E. Price W. C. Strahle Atlanta, GA 30332
1	Institute of Gas Technology ATTN: D. Gidaspow 3424 S. State Street Chicago, IL 60616-3896
1	Johns Hopkins University Applied Physics Laboratory Chemical Propulsion Information Agency ATTN: T. Christian Johns Hopkins Road Laurel, MD 20707-0690

DISTRIBUTION LIST

No. Of Copies	Organization
1	Massachusetts Institute of Technology Dept of Mechanical Engineering ATTN: T. Toong 77 Massachetts Avenue Cambridge, MA 02139-4307
1	University of Michigan Gas Dynamics Laboratory Aerospace Engineering Bldg. ATTN: G. M. Faeth Ann Arbor, MI 48109-2140
1	Pennsylvania State University Dept. Of Mech. Engineering ATTN: K. Kuo University Park, PA 16802-7501
1	Purdue University School of Mechanical Engineering ATTN: J. R. Osborn TSPC Chaffee Hall West Lafayette, IN 47907-1199
1	SRI International Propulsion Sciences Division ATTN: Tech Library 333 Ravenswood Avenue Menlo Park, CA 94025-3493
1	Rensselaer Polytechnic Inst. Department of Mathematics Troy, NY 12181
2	Director Los Alamos Scientific Lab ATTN: T3, D. Butler M. Division, B. Craig P. O. Box 1663 Los Alamos, NM 87544
1	Stevens Institute of Technology Davidson Laboratory ATTN: R. McAlevy, III Castle Point Station Hoboken, NJ 07030-5907
1	Rutgers University Dept. of Mechanical and Aerospace Engineering ATTN: S. Temkin University Heights Campus New Brunswick, NJ 08903
1	University of Southern California Mechanical Engineering Dept. ATTN: OHE200, M. Gerstein Los Angeles, CA 90089-5199
2	University of Utah Dept. of Chemical Engineering ATTN: A. Baer G. Flandro Salt Lake City, UT 84112-1194
1	Washington State University Dept. of Mechanical Engineering ATTN: C. T. Crowe Pullman, WA 99163-5201

Aberdeen Proving Ground

Dir, USAMSAA
ATTN: AMXSY-D
AMXSY-MP, H. Cohen
Cdr, USATECOM
ATTN: AMSTE-TO-F
AMSTE-CM-F, L. Nealley
Cdr, CSTA
ATTN: STECS-AS-H, R. Hendricksen
ATTN: STECS-DA-J, S. Walton
L. Francis
ATTN: STECS-EN-BM, V. Betzold
Cdr, CRDC, AMCCOM
ATTN: SMCCR-RSP-A
SMCCR-MU
SMCCR-SPS-IL

USER EVALUATION SHEET/CHANGE OF ADDRESS

This Laboratory undertakes a continuing effort to improve the quality of the reports it publishes. Your comments/answers to the items/questions below will aid us in our efforts.

1. BRL Report Number_____ Date of Report_____

2. Date Report Received_____

3. Does this report satisfy a need? (Comment on purpose, related project, or other area of interest for which the report will be used.)_____

4. How specifically, is the report being used? (Information source, design data, procedure, source of ideas, etc.)_____

5. Has the information in this report led to any quantitative savings as far as man-hours or dollars saved, operating costs avoided or efficiencies achieved, etc? If so, please elaborate._____

6. General Comments. What do you think should be changed to improve future reports? (Indicate changes to organization, technical content, format, etc.)

CURRENT ADDRESS

Name

Organization

Address

City, State, Zip

7. If indicating a Change of Address or Address Correction, please provide the New or Correct Address in Block 6 above and the Old or Incorrect address below.

OLD ADDRESS

Name

Organization

Address

City, State, Zip

(Remove this sheet along the perforation, fold as indicated, staple or tape closed, and mail.)

— — — — — — — — — — FOLD HERE — — — — — — — — — —

Director
U.S. Army Ballistic Research Laboratory
ATTN: SLCBR-DD-T
Aberdeen Proving Ground, MD 21005-5066

OFFICIAL BUSINESS
PENALTY FOR PRIVATE USE, $300

NO POSTAGE
NECESSARY
IF MAILED
IN THE
UNITED STATES

BUSINESS REPLY MAIL
FIRST CLASS PERMIT NO 12062 WASHINGTON, DC
POSTAGE WILL BE PAID BY DEPARTMENT OF THE ARMY

Director
U.S. Army Ballistic Research Laboratory
ATTN: SLCBR-DD-T
Aberdeen Proving Ground, MD 21005-9989

— — — — — — — — — — FOLD HERE — — — — — — — — — —

END